Attachment 5

Modeling Protocol for
Duke Energy Progress, INC – Asheville
Steam Electric Plant

Environment

Submitted to:
Duke Energy
Asheville Generating Station

Submitted by:
AECOM
Chelmsford, MA
60493296
June 2016

Modeling Protocol for Characterization of 1-Hour SO_2 Concentrations for the Asheville Generating Station

AECOM Environment

Submitted to:
Duke Energy
Asheville Generating Station

Submitted by:
AECOM
Chelmsford, MA
60493296
June 2016

Modeling Protocol for Characterization of 1-Hour SO_2 Concentrations of the Asheville Generating Station

Prepared By: Laura L. Warren

Reviewed By: Robert Paine

Contents

List of Tables

List of Figures

1.0 Introduction

The United States Environmental Protection Agency (EPA) is implementing the 2010 1-hour SO_2 National Ambient Air Quality Standard (NAAQS)[1] in an approach that involves either a dispersion modeling or monitoring approach to characterize local SO_2 concentrations near isolated emission sources. In August 2015, the EPA issued the SO_2 Data Requirements Rule[2] (DRR), which directs state and tribal air agencies in "an orderly process" to identify maximum ambient air 1-hour SO_2 concentrations in areas with large sources of SO_2 emissions.

The purposes of the DRR is to identify large SO_2-emitting sources, generally those with annual emissions > 2000 tons for the most recent year for which emissions data are available and to characterize SO_2 concentrations in the vicinity of these sources. The affected sources are those that have not been previously captured as part of the initial SO_2 NAAQS non-attainment designations in August 2013, or with the sources identified by the March 2015 Consent Decree between the EPA and the Sierra Club and National Resources Defense Council.

North Carolina Division of Air Quality (NCDAQ) is consulting with the owners or operators of such sources to identify the means for determining whether the area surrounding the source is in attainment with the SO_2 NAAQS for attainment designations purposes. According to the DRR, the method of characterizing the SO_2 concentrations around each source can be done by either:

- Installing and operating an ambient air monitoring network; or
- Performing an air dispersion modeling study to characterize ambient air impacts

Alternatively, instead of a characterization, each source can modify its air operating permit prior to January 13, 2017 such that the source either:

- Limits annual SO_2 emissions < 2000 tons; or
- Limits short-term (1-hour) and/or longer-term (up to 30-day average) SO_2 emissions that, based on the results of an air dispersion modeling study conducted in 2015-2016, demonstrate that the area surrounding the source is in attainment with the SO_2 NAAQS, allowing the state air agency to provide a recommendation for a designation of attainment with the NAAQS. The emission limits determined from this analysis must be in place as of January 2017.

The Asheville Generating Station ("Asheville") is owned and operated by Duke Energy, and is a DRR-affected source. Based on discussions and communications among NCDAQ, Duke Energy and AECOM (Duke Energy's contract air dispersion modeler), Duke Energy informed NCDAQ of its interest to follow the modeling path by performing an air dispersion modeling study to characterize ambient air impacts.

---

[1] 75 FR 35571 is the final rule for the 2010 SO_2 NAAQS.

[2] Docket ID No. EPA–HQ–OAR–2013–0711, August 10, 2015. http://www.epa.gov/oaqps001/sulfurdioxide/pdfs/so2_drr__final_081215.pdf.

This modeling protocol describes the proposed procedures for conducting a dispersion modeling analysis for the 2013-2015 period. In general, the proposed modeling procedures are consistent with applicable guidance, including the February 2016 "SO_2 NAAQS Designations Modeling Technical Assistance Document" (TAD)[3] issued by the EPA. In addition, this protocol requests the use of the "ADJ_U*" beta model option, an option EPA has proposed for inclusion as a preferred modeling approach. Furthermore, a source characterization technique called AERMOIST is also described and proposed for use as a technique that more accurately models the plume rise effect caused by moisture in a stack's plume, currently unaccounted for in AERMOD.

1.1 Report Organization

Section 2 of this report describes the emission sources of SO_2 at the Asheville Generating Station and provides actual emissions levels along with planned operational changes.

Section 3 describes the proposed dispersion model approaches to be used in the characterization of 1-hour SO_2 concentrations. This section also describes the proposed source of regional monitoring data that will represent impacts from sources that were not explicitly included in the modeling effort.

Section 4 presents the proposed procedure for representing the modeling results.

Documentation for the use of the low wind options as a non-default model is provided in **Appendices A - C**. Documentation for the use of a source characterization technique, AERMOIST, and EPA comments on the use of a similar source characterization technique in a recent modeling application are provided in **Appendices D - E**.

[3] https://www.epa.gov/airquality/sulfurdioxide/pdfs/SO2ModelingTAD.pdf.

2.0 Asheville Emission Sources

2.1 Description of Facility Emission Sources

The Asheville Generating Station is a 376-megawatt coal-fired power plant located in Skyland, North Carolinas, about 12 km south of the city of Asheville. The station operates two coal-fired dry bottom wall-fired boilers (Units 1 and 2). Two other sources are combustion turbines that operate on natural gas or oil (Units 3 and 4). The area surrounding Asheville, shown in **Figures 2-1 and 2-2**, is considered rural with complex terrain features that are higher in elevation than Asheville's stack top. Terrain features of particular significance are located approximately 3 to 5 km away called Brown Mountain and Busbee Mountain.

Historic SO_2 emissions from the Units 3 and 4 combustion turbines are negligible and thus, per EPA's guidance, can be excluded from the compliance modeling study. These units generally operate on a limited basis. In fact, during 2013-2015, these units operated only very infrequently and emitted less than 0.4 tons/year. The exclusion of these infrequently-utilized and low SO_2-emitting sources is consistent with EPA's SO_2 Modeling TAD. The SO_2 Modeling TAD includes guidance that addresses intermittent emission sources in the modeling effort (see Section 5.5 of that document). This guidance document referred to a previous EPA guidance document from March 2011, which in turn included more detailed guidance on the "treatment of intermittent emissions." The March 2011 guidance document noted the following:

> *"Given the implications of the probabilistic form of the 1-hour NO_2 NAAQS discussed above, we are concerned that assuming continuous operations for intermittent emissions would effectively impose an additional level of stringency beyond that intended by the level of the standard itself. As a result, we feel that it would be inappropriate to implement the 1-hour NO_2 standard in such a manner and recommend that compliance demonstrations for the 1-hour NO_2 NAAQS be based on emission scenarios that can logically be assumed to be relatively continuous or which occur frequently enough to contribute significantly to the annual distribution of daily maximum 1-hour concentrations."*

The March 2011 guidance document also applies to modeling studies in support of the SO_2 NAAQS.

2.2 Emissions and Stack Parameters

Units 1 and 2 are currently configured to exhaust through individual flues in a shared 327-foot stack. For more accurate representation of these units, these sources will be characterized as a merged stack when both units operate simultaneously, while individual stacks will be modeled when a unit operates alone. For the merged stack, an equivalent merged stack diameter will be modeled. The use of a merged stack is consistent with EPA precedent established with Model Clearinghouse Memo 91-II-01[4] and 96-V-10[5]. Individual stack diameters will be used when a unit operates alone.

Hourly SO_2 emissions, exit temperatures, and flow rates for the Asheville facility will be provided by Duke Energy for the latest three years (2013-2015). Exit velocities will be determined based on the

[4] https://cfpub.epa.gov/oarweb/MCHISRS/index.cfm?fuseaction=main.resultdetails&recnum=91-II -01.

[5] https://cfpub.epa.gov/oarweb/MCHISRS/index.cfm?fuseaction=main.resultdetails&recnum=96-V -10.

flow rates. **Table 2-1** provides the stack locations and exhaust parameters used in this modeling analysis.

Table 2-1: Stack Locations and Exhaust Parameters

Unit	X (UTM83)	Y (UTM83)	Base Elevation (m)	Stack Height (m)	Stack Diameter (m)	Emissions (g/s)	Exit Velocity (m/s)	Exit Temp. (K)
Unit 1	359955.6	3926330.0	661.5	99.7	5.03	Varying	Varying	Varying
Unit 2	359961.3	3926330.0	661.5	99.7	5.03	Varying	Varying	Varying
Units 1 & 2, Merged	359958.5	3926330.0	661.5	99.7	7.11	Varying	Varying	Varying

Figure 2-1: Aerial Imagery of SO_2 Sources and Property Boundary for Inclusion in the Modeling Analysis

Figure 2-2: Location of the Asheville Generating Station with Topography

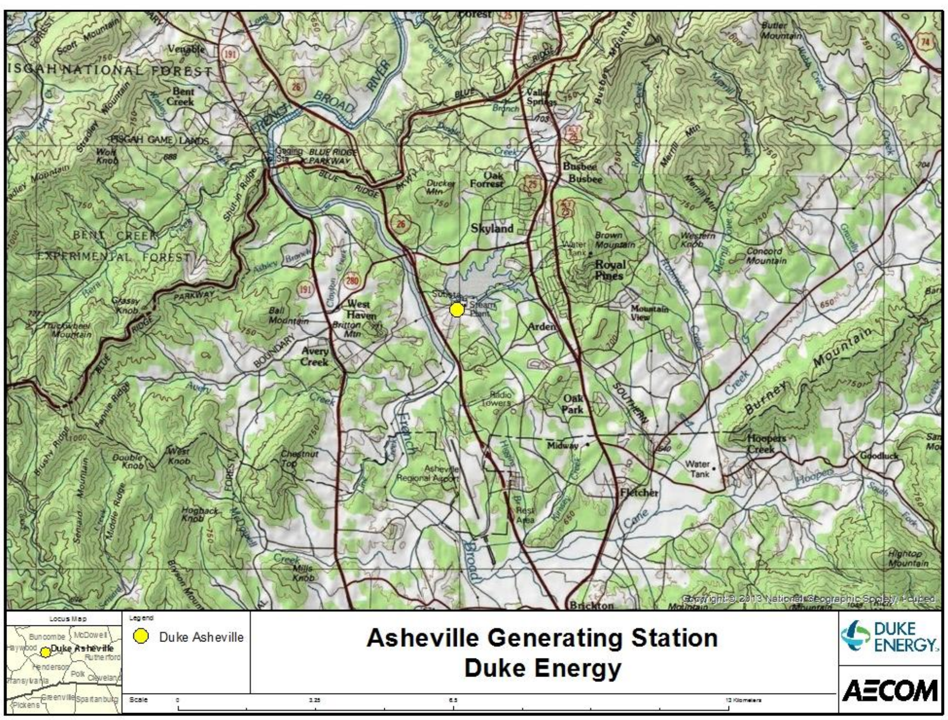

3.0 Dispersion Modeling Approach

The suitability of an air quality dispersion model for a particular application is dependent upon several factors. The following selection criteria will be evaluated:

- dispersion environment;
- stack height relative to nearby structures;
- local terrain; and
- representative meteorological data.

The EPA Guideline on Air Quality Models (Appendix W[6]) prescribes a set of approved models for regulatory applications for a wide range of source types and dispersion environments. Based on a review of the factors discussed below, the latest version of AERMOD (version 15181) will be used to assess air quality impacts for the Asheville facility. The AERMOD modeling system consists of two preprocessors and the dispersion model. AERMET is the meteorological preprocessor component and AERMAP is the terrain pre-processor component that characterizes the terrain and generates receptor elevations along with critical hill heights for those receptors.

The dispersion modeling analysis will be conducted using EPA's currently-approved AERMOD model with the AERMET low wind speed adjustment, "ADJ_U*". In a proposed rulemaking published in the July 29, 2015 Federal Register (80 FR 45340), EPA proposed refinements to its preferred short-range model, AERMOD, involving low wind conditions. One of these refinements involves an adjustment to the computation of the friction velocity ("ADJ_U*") in the AERMET meteorological pre-processor. This adjustment improves model performance by adjusting frictional velocity (u*) in stable, low wind conditions, consistent with Qian and Venkatram (2011).[7] Furthermore, EPA's February 10, 2016 and April 29, 2016 releases of the Model Clearinghouse Review of the Use of ADJ_U* Beta Option[8, 9] support the use of this non-guideline beta option. In particular, the April 29, 2016 concurrence memo discusses a facility (Schiller Station) with a tall stack located near complex terrain, where high modeled concentrations were likely to occur under low wind, stable conditions. The tall stack at the Asheville facility with surrounding terrain features is similar to this environment. As previously shown in **Figure 2-2**, a topographic map depicting the terrain within the modeling domain indicates the closest complex terrain (terrain above the stack top of 761.1 meters) is about 2.5 kilometers to the

---

[6] http://www.epa.gov/ttn/scram/guidance/guide/appw_05.pdf.

[7] Qian, W., and A. Venkatram, 2011: "Performance of Steady-State Dispersion Models Under Low Wind-Speed Conditions", Boundary Layer Meteorology, 138, 475-491.

[8] http://www3.epa.gov/ttn/scram/guidance/mch/new_mch/16-X-01_MCResponse_Region10_Donlin-02102016.pdf

[9] https://www3.epa.gov/ttn/scram/guidance/mch/new_mch/16-I-01_MCResponse_Region1_Schiller-04292016.pdf

north of the Asheville stack. Brown Mountain and Busbee Mountain are also considered complex terrain features at about 3 km to 5 km away, respectively. Alternative model justification consistent with Appendix W, Section 3.2.2 for the use of ADJ_U* is provided in the **Appendix A**, with supporting documentation provided in **Appendix B - C**.

3.1 Dispersion Environment

The application of AERMOD requires characterization of the local (within 3 kilometers) dispersion environment as either urban or rural, based on an EPA-recommended procedure that characterizes an area by prevalent land use. This land use approach classifies an area according to 12 land use types. In this scheme, areas of industrial, commercial, and compact residential land use are designated urban. According to EPA modeling guidelines, if more than 50% of an area within a 3-km radius of the facility is classified as rural, then rural dispersion coefficients are to be used in the dispersion modeling analysis. Conversely, if more than 50% of the area is urban, urban dispersion coefficients are used. Based on this procedure, the 3-km area surrounding Asheville is rural. Therefore, rural dispersion will be used.

3.2 Good Engineering Practice Stack Height Analysis

Good engineering practice (GEP) stack height is defined as the stack height necessary to ensure that emissions from the stack do not result in excessive concentrations of any air pollutant as a result of atmospheric downwash, wakes, or eddy effects created by the source, nearby structures, or terrain features. In this modeling exercise, actual stack heights will be used, consistent with the EPA SO_2 Modeling TAD. BPIP downwash parameters will be developed for Asheville using Duke Energy-provided building information processed using BPIPPRIME (version 04274). **Figure 3-1** shows the Asheville building layout.

3.3 Model Receptor Grid and Terrain

AERMAP (version 11103) will be used to generate receptor input to AERMOD. The receptor placement at the plant fence line will be at 50-m intervals. Beyond the property fence line, the receptors will be placed in nested Cartesian grids with the following spacing:

- Every 50 meters out to a distance of 0.5 km
- Every 100 meters between 0.5 and 1 km
- Every 150 meters between 1 and 2.5 km
- Every 250 meters between 2.5 and 4 km
- Every 300 meters between 4 and 6 km
- Every 500 meters between 6 and 8 km
- Every 1,000 meters between 8 and 11.5 km
- Every 1,500 meters between 11.5 and 20 km
- Every 2,000 meters between 20 and 35 km.

Additionally, 100-m grid spacing is proposed for Brown and Busbee Mountains as these mountains are among the highest terrain features near the facility. The proposed receptor grid is shown in **Figure 3-2** with the near-field view of receptors in **Figure 3-3**. If necessary, additional 100-meter spaced receptors will be placed at the location of the maximum concentrations should it not already be in an area covered by 100-meter grid spacing. This receptor grid excludes receptors within the property boundary as well as excludes locations where an SO_2 monitor could not physically be placed (e.g., over water), consistent with the SO_2 Modeling TAD. In particular, receptors were removed over the Lake Julian.

Receptor height scales at each receptor location will be developed by AERMAP, the terrain preprocessor for AERMOD, which requires processing of terrain data files. Terrain elevations from 1-arc second, or 30-meter, National Elevation Data (NED) from USGS using the NAD83 coordinate system will be used to develop the receptor terrain elevations required by AERMOD.

3.4 Meteorological Data Processing

Three years (2013-2015) of the Asheville Regional Airport National Weather Service (NWS) surface station and the Greensboro upper air meteorological data are proposed for use in this modeling analysis. The proximity of the airport to the Asheville facility makes this meteorological data appropriate for use in the proposed dispersion modeling analysis. Location of these stations relative to the Asheville facility is shown in **Figure 3-4** and a wind rose is shown in **Figure 3-5**.

The meteorological data required for input to AERMOD will utilize hourly surface observations from Asheville Regional Airport, NC along with concurrent upper air data from Greensboro, NC airport that will be processed by AERMET using the ADJ_U* option as previously noted. One-minute wind data will be processed using an AERMET preprocessor, AERMINUTE (version 15272, or an update if available), to generate hourly average winds to reduce instances of calm winds.

The surface data (wind direction, wind speed, temperature, sky cover, and relative humidity) is measured 10 m above ground level. AERMET creates two output files for input to AERMOD:

- SURFACE: a file with boundary layer parameters such as sensible heat flux, surface friction velocity, convective velocity scale, vertical potential temperature gradient in the 500-meter layer above the planetary boundary layer, and convective and mechanical mixing heights. Also provided are values of Monin-Obukhov length, surface roughness, albedo, Bowen ratio, wind speed, wind direction, temperature, and heights at which measurements were taken.
- PROFILE: a file containing multi-level meteorological data with wind speed, wind direction, temperature, sigma-theta (σ_θ) and sigma-w (σ_w) when such data are available. For this application involving representative data from the nearest NWS station, the profile file contained a single level of wind data and the temperature data.

AERMET requires specification of site characteristics including surface roughness (z_o), albedo (r), and Bowen ratio (B_o). These parameters were developed according to the guidance provided by EPA in the recently revised AERMOD Implementation Guide (AIG; EPA, 2015[10]).

The revised AIG provides the following recommendations for determining the site characteristics:

1. The determination of the surface roughness length should be based on an inverse distance weighted geometric mean for a default upwind distance of 1 kilometer relative to the measurement site. Surface roughness length may be varied by sector to account for

[10] U.S. EPA 2015. AERMOD Implementation Guide (Revised). U.S. Environmental Protection Agency, Research Triangle Park, NC. August 3, 2015.

variations in land cover near the measurement site; however, the sector widths should be no smaller than 30 degrees. As discussed below, 12 sectors will be used in this application.

2. The determination of the Bowen ratio should be based on a simple un-weighted geometric mean (i.e., no direction or distance dependency) for a representative domain, with a default domain defined by a 10-km by 10-km region centered on the measurement site.

3. The determination of the albedo should be based on a simple un-weighted arithmetic mean (i.e., no direction or distance dependency) for the same representative domain as defined for Bowen ratio, with a default domain defined by a 10-km by 10-km region centered on the measurement site.

The AIG recommends that the surface characteristics be determined based on digitized land cover data. AERSURFACE will be used to determine the site characteristics based on digitized land cover data in accordance with the recommendations from the AIG discussed above. AERSURFACE incorporates look-up tables of representative surface characteristic values by land cover category and seasonal category. AERSURFACE will be applied with the instructions provided in the AERSURFACE User's Guide (EPA, 2013[11]).

The current version of AERSURFACE (version 13016) supports the use of land cover data from the USGS National Land Cover Data 1992 archives[12] (NLCD92). The NLCD92 archive provides data at a spatial resolution of 30 meters based upon a 21-category classification scheme applied over the continental U.S. The AIG recommends that the surface characteristics be determined based on the land use surrounding the site where the surface meteorological data were collected. For this analysis, AERSURFACE version 13016 will be used.

As recommended in the AIG for surface roughness, the 1-km radius circular area centered at the meteorological station site was created. The default 12 sectors of 30˚ are proposed for use in this modeling analysis.

In AERSURFACE, the various land cover categories are linked to a set of seasonal surface characteristics. As such, AERSURFACE requires specification of the seasonal category for each month of the year. The following five seasonal categories are supported by AERSURFACE, with the applicable months of the year specified for this site.

1. Midsummer with lush vegetation (June-August).
2. Autumn with un-harvested cropland (September-November).
3. Late autumn after frost and harvest, or winter with no snow (December-February).
4. Winter with continuous snow on ground (not applicable).
5. Transitional spring with partial green coverage or short annuals (March-May).

For Bowen ratio, the land use values are linked to three categories of surface moisture corresponding to average, wet, and dry conditions. The surface moisture condition for the site may vary depending on the meteorological data period for which the surface characteristics will be applied. AERSURFACE applies the surface moisture condition for the entire data period. Therefore, if the

[11] U.S.EPA 2013. AERSURFACE User's Guide. EPA-454/B-08-001. U.S. Environmental Protection Agency, Research Triangle Park, NC. . January, 2013.

[12] http://www.mrlc.gov/viewerjs/.

surface moisture condition varies significantly across the data period, then AERSURFACE can be applied multiple times to account for those variations. As recommended in the AERSURFACE User's Guide, the surface moisture condition for each year was determined by comparing precipitation for the period of data to be processed to the 30-year climatological record, selecting "wet" conditions if precipitation is in the upper 30^{th} percentile, "dry" conditions if precipitation is in the lower 30^{th} percentile, and "average" conditions if precipitation is in the middle 40^{th} percentile. The 30-year precipitation data set used in this modeling was taken from the NOAA. The annual designations of surface moisture input to AERSURFACE are "wet" for 2013 and 2015, and "average" for 2014.

3.5 Regional Background

According to the EPA March 1, 2011 Memorandum[13] and the analysis presented at the 2011 EPA modeling workshop,[14] selection of regional background sources should be limited to 10 kilometers from the source location. According to the EPA 2011 National Emissions Inventory (NEI), there are no nearby SO_2 sources within 10 km of the Asheville plant. In fact, there are no nearby SO_2 sources out 20 km as well. As a result, no background sources will be modeled in this analysis.

The background concentrations for this modeling application will be represented by using season and hour-of-day based on 3-year (2013-2015) average of the 99^{th} percentile of the distribution of hourly SO_2 concentrations from the Greenville, SC (AQS ID 45-045-0015) operated by South Carolina Department Health and Environmental Control. This monitor is in a suburban setting similar to the Asheville facility and is located about 75 km away from Asheville as shown in **Figure 3-6**. Background concentrations will be developed using data obtained from the EPA AirData website and the EPA methodology discussed in the March 1, 2011 Memorandum. The resulting season and hour-of-day 3-year average background concentrations are listed in **Table 3-1** and shown in **Figure 3-7**.

[13] http://www.epa.gov/scram001/guidance/clarification/Additional_Clarifications_AppendixW_Hourly-NO2-NAAQS_FINAL_03-01-2011.pdf

[14] http://www.cleanairinfo.com/regionalstatelocalmodelingworkshop/archive/2011/Presentations/6-Thursday_AM/6-3_AB-3_Presentation_at_EPA_Modeling_Workshop.pdf, Page 5

Table 3-1: 2013-2015 Average 99th Percentile Concentration at the Greenville, SC SO_2 Monitor

Hour (Local)	Winter (µg/m³)	Spring (µg/m³)	Summer (µg/m³)	Fall (µg/m³)
00	4.4	2.6	2.8	2.4
01	4.4	3.5	1.7	2.3
02	4.4	3.5	1.7	2.2
03	4.4	3.8	1.7	2.1
04	5.2	4.4	1.7	2.2
05	5.2	3.5	2.1	2.3
06	3.5	3.5	2.0	2.2
07	4.4	3.5	2.9	2.3
08	6.1	3.5	2.8	2.4
09	5.2	4.4	3.8	2.4
10	6.1	4.4	2.7	3.4
11	5.3	6.1	2.6	2.4
12	7.0	4.4	2.5	3.3
13	4.4	5.2	1.7	3.1
14	4.4	3.5	1.7	3.1
15	4.4	2.6	2.4	3.1
16	5.2	3.5	2.5	3.1
17	5.2	2.6	2.4	2.3
18	6.1	2.6	3.4	3.1
19	6.1	2.6	1.8	2.6
20	6.1	2.6	3.0	2.6
21	6.1	2.7	2.4	2.5
22	6.1	4.5	2.4	2.4
23	6.1	2.6	2.0	2.4

3.6 Source Characterization using the AERMOIST Technique

The proposed modeling analysis described in this report will use the ADJ_U* AERMET model option. In addition, we propose to use a more accurate characterization of SO_2 concentrations in the vicinity of the Asheville facility using a source characterization technique called AERMOIST.

Units 1 and 2 have operated wet lime flue gas desulfurization (FGD) SO_2 control devices since 2005-2006. These control devices result in an average stack moisture content of 11.5% for each plume. Stacks with substantially moist plumes can lead to latent heat release of condensation after the plume exits the stack, providing additional plume rise relative to a “dry” plume scenario. Although some of the initial added buoyancy is later lost due to partial evaporation, a net gain in plume rise occurs. The AERMOD plume rise formulation is based on the assumption of a dry plume, in that the chimney plume is considered to be far from being saturated and carries essentially no moisture. A procedure to incorporate the moist plume effect can be performed by adjusting the input exit temperature data prior to an AERMOD model analysis using a pre-processor called “AERMOIST”. AERMOIST makes use of a European validated plume rise model called “IBJpluris” that already incorporates moist plume effects and has been found to accurately predict the final rise of a moist plume (Janicke and Janicke, 2001; Janicke Consulting, 2015)[15,16]. IBJpluris has been evaluated by Presotto et al. (2005)[17], which indicated that despite a number of entrainment formulas available, IBJpluris possessed the physical capability of representing the impacts of heat of condensation on symmetric chimney plume rise. Presotto et al. (2005) also reported field evaluation results for the IBJpluris model involving aircraft measurements through moist plumes emitted by stacks and cooling towers.

Plume rise adjustments using IBJpluris with and without moist plume effects are transferred to AERMOD through AERMOIST by adjusting the input stack temperature to calculate the equivalent dry plume temperature on an hourly basis, as a function of ambient temperature and relative humidity. Ambient temperature and relative humidity are obtained from the AERMET surface file. These equivalent dry plume temperatures are used in AERMOD as an hourly emission and stack exhaust parameter file.

This source characterization technique is not a modification to AERMOD, and has been included in numerous SO_2 DRR modeling protocols submitted nationwide in 2016. The AERMOIST formulation has been peer-reviewed and published in open access scientific literature and is provided in **Appendix D**. A similar technique for combining plume rise from stacks in a line was accepted by EPA Region 4 for Eastman Chemical (see **Appendix E**).

AERMOIST uses constant stack parameters. However, hourly-varying stack parameters can also be processed with the AERMOIST technique if AERMOIST is first run for multiple load conditions over the range[18] of each source's operations. Then, an interpolation procedure determines on an hourly basis an appropriate value for the equivalent dry plume hourly stack temperature.

[15] Janicke, U., Janicke, L., 2001. A three-dimensional plume rise model for dry and wet plumes. *Atmos. Environ*. 35, 877-890.

[16] Janicke Consulting, Environmental Physics, 2015. Plume Rise Model IBJpluris. http://www.janicke.de/en/download-programs.html.

[17] Presotto, L., Bellasia, R., Bianconi, R., 2005. Assessment of the visibility impact of a plume emitted by a desulphuration plant. *Atmos. Environ*. 39 (4), 719-737.

[18] The load-dependent stack temperature and exit velocity data are either provided through engineering considerations, or through a review of historical unit operations.

Figure 3-1: Building Layout for the Asheville Generating Station Modeling Analysis

Figure 3-2: Far Field View of the Modeling Receptor Grid

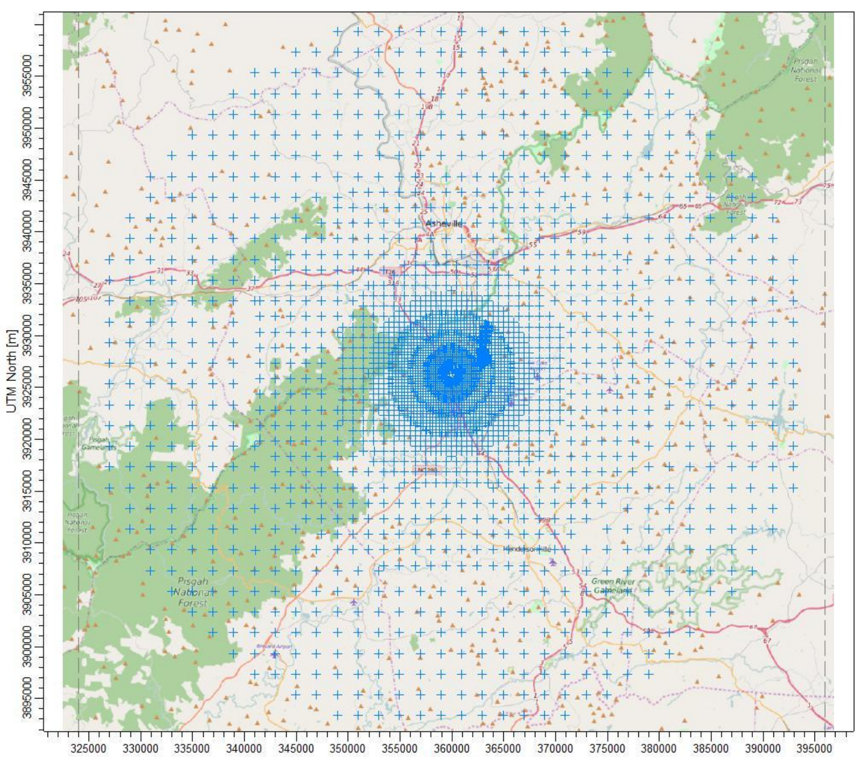

Figure 3-3: Near Field View of the Modeling Receptor Grid

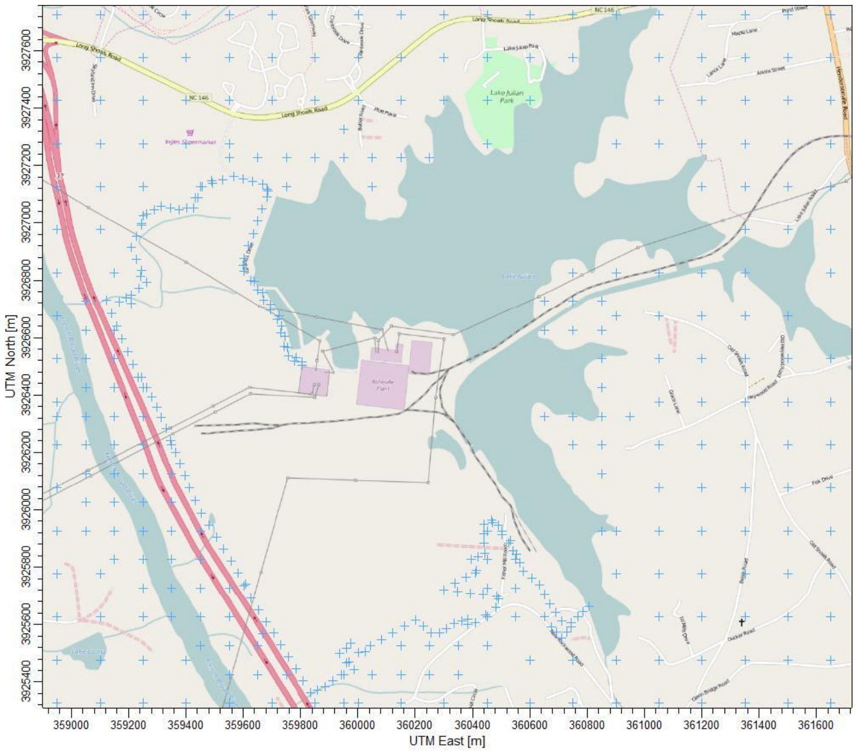

Figure 3-4: Asheville Regional Airport Location Relative to the Asheville Generating Station

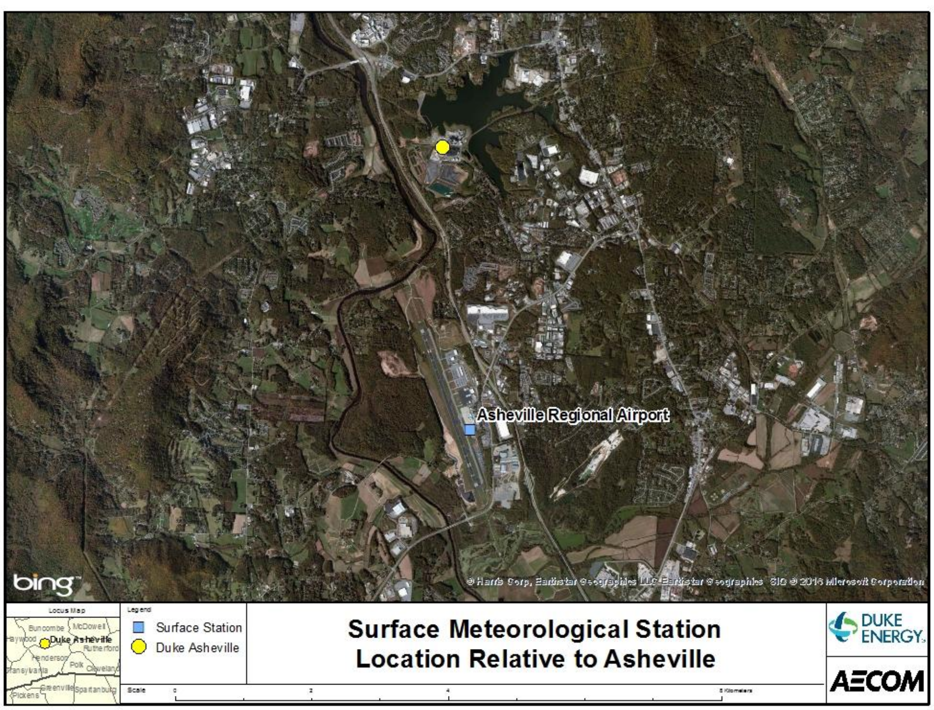

Figure 3-5: Asheville Regional Airport Wind Rose (2013-2015)

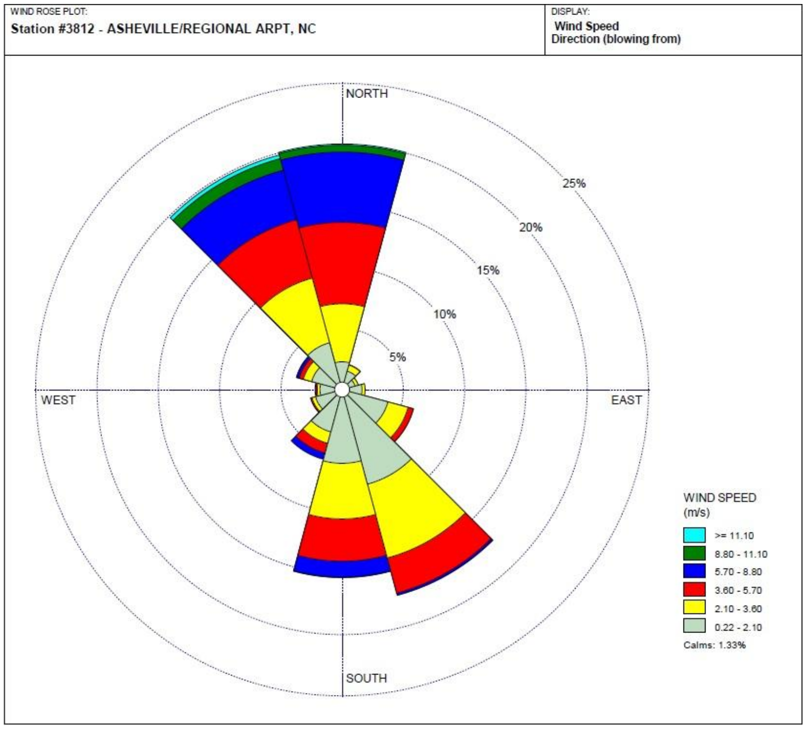

Figure 3-6: Greenville, SC SO_2 Monitor Location Relative to the Asheville Generating Station

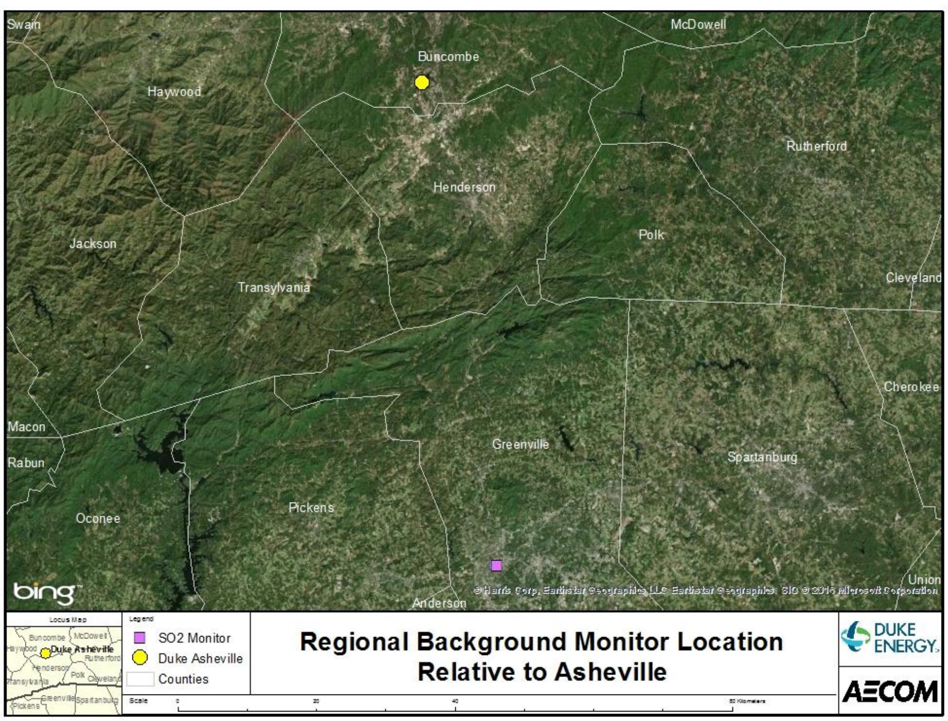

Figure 3-7: 2013-2015 Average 99th Percentile Concentration at the Greenville, SC SO_2 Monitor

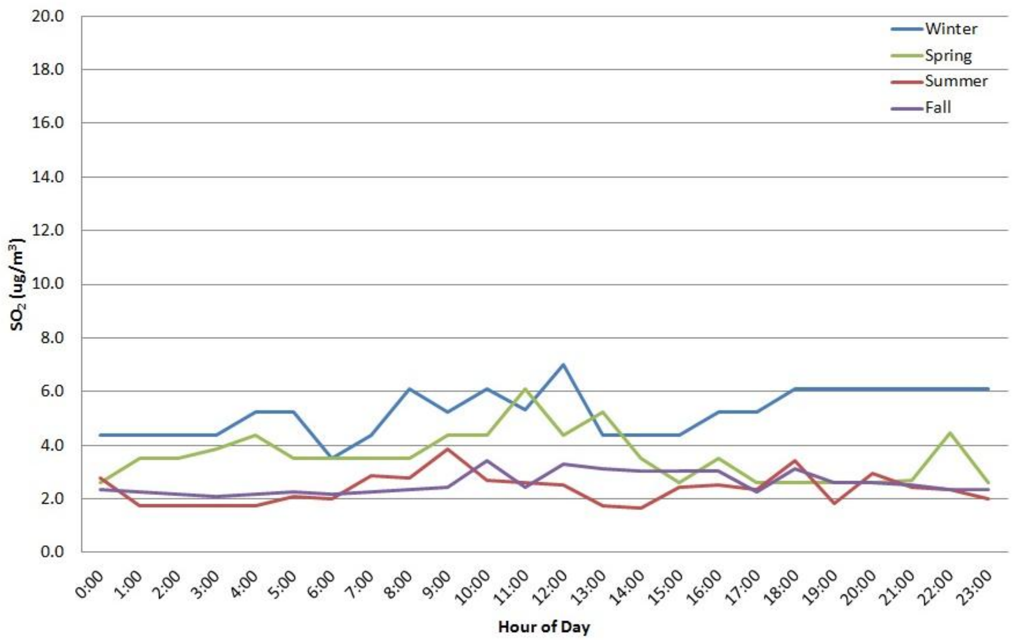

4.0 Presentation of Modeling Results

AERMOD modeling will be conducted to characterize 1-hour SO_2 concentrations in the vicinity of the Asheville plant relative to the 1-hour SO_2 NAAQS.

A modeling report will be provided that documents the 1-hour SO_2 air quality impact analysis with a description of the input data, the modeling procedures, and the results in tabular and graphical form. Much of the information regarding locations, plot plans, etc., associated with the project that is included in this modeling protocol will be included in the air quality impact analysis report.

The computer files associated with the air quality analysis will be submitted on computer-readable media. All meteorological and monitoring data will be presented so that a reviewer can completely reconstruct the entire modeling demonstration on Window-based PC. Descriptions of files will be included in the computer documentation to promote portability of the files to other computer systems.

Appendix A

Alternative Model Justification for Low Wind Speed Beta ADJ_U* Option in AERMET

Alternative Model Justification for Low Wind Speed Beta ADJ_U* Option in AERMET

Appendix W, Section 3.2.2 provides an approach for approval of an alternative model to determine whether it is more appropriate for this modeling application. The principle sources involve tall stack buoyant releases.

EPA indicates that for this purpose, an alternative refined model may be used provided that:

1. The model has received a scientific peer review;
2. The model can be demonstrated to be applicable to the problem on a theoretical basis;
3. The data bases which are necessary to perform the analysis are available and adequate;
4. Appropriate performance evaluations of the model have shown that the model is not biased toward underestimates; and
5. A protocol on methods and procedures to be followed has been established.

These five points are discussed below.

The model selected for this modeling application is the EPA-proposed updates to the AERMOD modeling system version 15181, including the AERMET ADJ_U* option. EPA has indicated support for these changes in the Appendix W proposal and in the Roger Brode presentation made at the 11th Modeling Conference on August 12, 2015 (see presentation at http://www.epa.gov/ttn/scram/11thmodconf/presentations/1-5_Proposed_Updates_AERMOD_System.pdf).

1. The model has received a scientific peer review

The AERMET changes reference a Boundary-Layer Meteorology peer-reviewed paper[19] that is the source of the AERMET formulation for changes in the friction velocity computation for low wind speeds. The combination of the AERMET changes and the AERMOD changes (version 14134 LOWWIND2, similar to version 15181 LOWWIND3) has been evaluated and the study[20] has been published in the Journal of the Air & Waste Management Association (JAWMA). The manuscript associated with the JAWMA article is provided in Appendix B. The evaluation database from the JAWMA article that is most relevant for the Asheville application is the Mercer County, North Dakota database, for which model over-predictions for default options are clearly evident for the monitor at the elevated terrain feature. For both the North Dakota and the Asheville applications, the key meteorological conditions for the default modeling option are low wind speed, stable cases.

In addition, Appendix F of the AERMOD User's Guide (provided here as Appendix C) presents results of a model evaluation study performed by EPA for several AERMOD evaluation databases. This additional evaluation further supports use of the ADJ_U* option. For this

---

[19] Qian, W., and A. Venkatram. Performance of Steady-State Dispersion Models Under Low Wind-Speed Conditions. Boundary-Layer Meteorology 138:475–491. (2011)

[20] Paine, R., O. Samani, M. Kaplan, E. Knipping and N. Kumar (2015) Evaluation of low wind modeling approaches for two tall-stack databases, *Journal of the Air & Waste Management Association*, 65:11, 1341-1353, DOI: 10.1080/10962247.2015.1085924.

application, we are not including observed turbulence measurements as input to the modeling (they are not available for ASOS data observing stations).

2. The model can be demonstrated to be applicable to the problem on a theoretical basis.

There is no theoretical limitation to the application of the AERMET ADJ_U* option – it is generally applicable. The current default algorithm in AERMET has been demonstrated to be faulty and needs to be replaced by the ADJ_U* approach. The improvements are demonstrated with the low wind model evaluations reported by the presentations[21] at the 11th EPA modeling conference. It is noteworthy that the critical conditions for the North Dakota evaluation study and the Asheville application are low wind, stable cases. Therefore, the conditions for which AERMOD over-predictions were demonstrated for the North Dakota database are also the controlling ones for the Asheville application.

3. The databases which are necessary to perform the analysis are available and adequate.

Routine meteorological databases that are already available are sufficient for exercising this low wind options. There are no special database requirements for the use of these options.

4. Appropriate performance evaluations of the model have shown that the model is not biased toward underestimates.

The studies cited above by EPA and AECOM provide this demonstration.

5. A protocol on methods and procedures to be followed has been established.

The protocol associated with case-specific applications for the non-guideline application of this approach documents the methods and procedures to be followed.

---

[21] http://www.epa.gov/ttn/scram/11thmodconf/presentations/1-5_Proposed_Updates_AERMOD_System.pdf and http://www.epa.gov/ttn/scram/11thmodconf/presentations/2-3_Low_Wind_Speed_Evaluation_Study.pdf.

Appendix B

Evaluation of Low Wind Modeling Approaches for Two Tall-Stack Databases

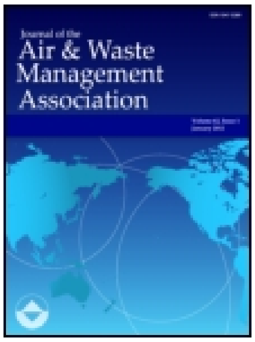

Taylor & Francis
Taylor & Francis Group

Journal of the Air & Waste Management Association

ISSN: 1096-2247 (Print) 2162-2906 (Online) Journal homepage: http://www.tandfonline.com/loi/uawm20

Evaluation of low wind modeling approaches for two tall-stack databases

Robert Paine, Olga Samani, Mary Kaplan, Eladio Knipping & Naresh Kumar

To cite this article: Robert Paine, Olga Samani, Mary Kaplan, Eladio Knipping & Naresh Kumar (2015) Evaluation of low wind modeling approaches for two tall-stack databases, Journal of the Air & Waste Management Association, 65:11, 1341-1353, DOI: 10.1080/10962247.2015.1085924

To link to this article: http://dx.doi.org/10.1080/10962247.2015.1085924

TECHNICAL PAPER

Evaluation of low wind modeling approaches for two tall-stack databases

Robert Paine,[1,*] Olga Samani,[1] Mary Kaplan,[1] Eladio Knipping,[2] and Naresh Kumar[2]
[1]*AECOM, Chelmsford, MA, USA*
[2]*Electric Power Research Institute, Palo Alto, CA, USA*
[*]*Please address correspondence to: Robert Paine, AECOM, 250 Apollo Drive, Chelmsford, MA 01824, USA; e-mail:* bob.paine@aecom.com

The performance of the AERMOD air dispersion model under low wind speed conditions, especially for applications with only one level of meteorological data and no direct turbulence measurements or vertical temperature gradient observations, is the focus of this study. The analysis documented in this paper addresses evaluations for low wind conditions involving tall stack releases for which multiple years of concurrent emissions, meteorological data, and monitoring data are available. AERMOD was tested on two field-study databases involving several SO_2 monitors and hourly emissions data that had sub-hourly meteorological data (e.g., 10-min averages) available using several technical options: default mode, with various low wind speed beta options, and using the available sub-hourly meteorological data. These field study databases included (1) Mercer County, a North Dakota database featuring five SO_2 monitors within 10 km of the Dakota Gasification Company's plant and the Antelope Valley Station power plant in an area of both flat and elevated terrain, and (2) a flat-terrain setting database with four SO_2 monitors within 6 km of the Gibson Generating Station in southwest Indiana. Both sites featured regionally representative 10-m meteorological databases, with no significant terrain obstacles between the meteorological site and the emission sources. The low wind beta options show improvement in model performance helping to reduce some of the overprediction biases currently present in AERMOD when run with regulatory default options. The overall findings with the low wind speed testing on these tall stack field-study databases indicate that AERMOD low wind speed options have a minor effect for flat terrain locations, but can have a significant effect for elevated terrain locations. The performance of AERMOD using low wind speed options leads to improved consistency of meteorological conditions associated with the highest observed and predicted concentration events. The available sub-hourly modeling results using the Sub-Hourly AERMOD Run Procedure (SHARP) are relatively unbiased and show that this alternative approach should be seriously considered to address situations dominated by low-wind meander conditions.

Implications: AERMOD was evaluated with two tall stack databases (in North Dakota and Indiana) in areas of both flat and elevated terrain. AERMOD cases included the regulatory default mode, low wind speed beta options, and use of the Sub-Hourly AERMOD Run Procedure (SHARP). The low wind beta options show improvement in model performance (especially in higher terrain areas), helping to reduce some of the overprediction biases currently present in regulatory default AERMOD. The SHARP results are relatively unbiased and show that this approach should be seriously considered to address situations dominated by low-wind meander conditions.

Introduction

During low wind speed (LWS) conditions, the dispersion of pollutants is limited by diminished fresh air dilution. Both monitoring observations and dispersion modeling results of this study indicate that high ground-level concentrations can occur in these conditions. Wind speeds less than 2 m/sec are generally considered to be "low," with steady-state modeling assumptions compromised at these low speeds (Pasquill et al., 1983). Pasquill and Van der Hoven (1976) recognized that for such low wind speeds, a plume is unlikely to have any definable travel. Wilson et al. (1976) considered this wind speed (2 m/sec) as the upper limit for conducting tracer experiments in low wind speed conditions.

Anfossi et al. (2005) noted that in LWS conditions, dispersion is characterized by meandering horizontal wind oscillations. They reported that as the wind speed decreases, the standard deviation of the wind direction increases, making it more difficult to define a mean plume direction. Sagendorf and Dickson (1974) and Wilson et al. (1976) found that under LWS conditions, horizontal diffusion was enhanced because of this meander and the resulting ground-level concentrations could be much lower than that predicted by steady-state Gaussian plume models that did not account for the meander effect.

A parameter that is used as part of the computation of the horizontal plume spreading in the U.S. Environmental Protection Agency (EPA) preferred model, AERMOD (Cimorelli et al., 2005), is the standard deviation of the crosswind component, σ_v, which can be parameterized as being proportional to the friction velocity, u_* (Smedman, 1988; Mahrt, 1998). These investigators

Journal of the Air & Waste Management Association, 65(11):1341–1353, 2015. Copyright © 2015 A&WMA. ISSN: 1096-2247 print
DOI: 10.1080/10962247.2015.1085924. Submitted March 17, 2015; final version submitted July 20, 2015; accepted August 11, 2015.
Color versions of one or more of the figures in the article can be found online at www.tandfonline.com/uawm.

found that there was an elevated minimum value of σ_v that was attributed to meandering. While at higher wind speeds small-scale turbulence is the main source of variance, lateral meandering motions appear to exist in all conditions. Hanna (1990) found that σ_v maintains a minimum value of about 0.5 m/sec even as the wind speed approaches zero. Chowdhury et al. (2014) noted that a minimum σ_v of 0.5 m/s is a part of the formulation for the SCICHEM model. Anfossi (2005) noted that meandering exists under all meteorological conditions regardless of the stability or wind speed, and this phenomenon sets a lower limit for the horizontal wind component variances as noted by Hanna (1990) over all types of terrain.

An alternative method to address wind meander was attempted by Sagendorf and Dickson (1974), who used a Gaussian model, but divided each computation period into sub-hourly (2-min) time intervals and then combined the results to determine the total hourly concentration. This approach directly addresses the wind meander during the course of an hour by using the sub-hourly wind direction for each period modeled. As we discuss later, this approach has some appeal because it attempts to use direct wind measurements to account for sub-hourly wind meander. However, the sub-hourly time interval must not be so small as to distort the basis of the horizontal plume dispersion formulation in the dispersion model (e.g., AERMOD). Since the horizontal dispersion shape function for stable conditions in AERMOD is formulated with parameterizations derived from the 10-min release and sampling times of the Prairie Grass experiment (Barad, 1958), it is appropriate to consider a minimum sub-hourly duration of 10 minutes for such modeling using AERMOD. The Prairie Grass formulation that is part of AERMOD may also result in an underestimate of the lateral plume spread shape function in some cases, as reported by Irwin (2014) for Kincaid SF_6 releases. From analyses of hourly samples of SF_6 taken at Kincaid (a tall stack source), Irwin determined that the lateral dispersion simulated by AERMOD could underestimate the lateral dispersion (by 60%) for near-stable conditions (conditions for which the lateral dispersion formulation that was fitted to the Project Prairie Grass data could affect results).

It is clear from the preceding discussion that the simulation of pollutant dispersion in LWS conditions is challenging. In the United States, the use of steady-state plume models before the introduction of AERMOD in 2005 was done with the following rule implemented by EPA: "When used in steady-state Gaussian plume models, measured site-specific wind speeds of less than 1 m/sec but higher than the response threshold of the instrument should be input as 1 m/sec" (EPA, 2004).

With EPA's implementation of a new model, AERMOD, in 2005 (EPA, 2005), input wind speeds lower than 1 m/sec were allowed due to the use of a meander algorithm that was designed to account for the LWS effects. As noted in the AERMOD formulation document (EPA, 2004), "AERMOD accounts for meander by interpolating between two concentration limits: the coherent plume limit (which assumes that the wind direction is distributed about a well-defined mean direction with variations due solely to lateral turbulence) and the random plume limit (which assumes an equal probability of any wind direction)."

A key aspect of this interpolation is the assignment of a time scale (= 24 hr) at which mean wind information at the source is no longer correlated with the location of plume material at a downwind receptor (EPA, 2004). The assumption of a full diurnal cycle relating to this time scale tends to minimize the weighting of the random plume component relative to the coherent plume component for 1-hr time travel. The resulting weighting preference for the coherent plume can lead to a heavy reliance on the coherent plume, ineffective consideration of plume meander, and a total concentration overprediction.

For conditions in which the plume is emitted aloft into a stable layer or in areas of inhomogeneous terrain, it would be expected that the decoupling of the stable boundary layer relative to the surface layer could significantly shorten this time scale. These effects are discussed by Brett and Tuller (1991), where they note that lower wind autocorrelations occur in areas with a variety of roughness and terrain effects. Perez et al. (2004) noted that the autocorrelation is reduced in areas with terrain and in any terrain setting with increasing height in stable conditions when decoupling of vertical motions would result in a "loss of memory" of surface conditions. Therefore, the study reported in this paper has reviewed the treatment of AERMOD in low wind conditions for field data involving terrain effects in stable conditions, as well as for flat terrain conditions, for which convective (daytime) conditions are typically associated with peak modeled predictions.

The computation of the AERMOD coherent plume dispersion and the relative weighting of the coherent and random plumes in stable conditions are strongly related to the magnitude of σ_v, which is directly proportional to the magnitude of the friction velocity. Therefore, the formulation of the friction velocity calculation and the specification of a minimum σ_v value are also considered in this paper. The friction velocity also affects the internally calculated vertical temperature gradient, which affects plume rise and plume–terrain interactions, which are especially important in elevated terrain situations.

Qian and Venkatram (2011) discuss the challenges of LWS conditions in which the time scale of wind meandering is large and the horizontal concentration distribution can be non-Gaussian. It is also quite possible that wind instrumentation cannot adequately detect the turbulence levels that would be useful for modeling dispersion. They also noted that an analysis of data from the Cardington tower indicates that Monin–Obukhov similarity theory underestimates the surface friction velocity at low wind speeds. This finding was also noted by Paine et al. (2010) in an independent investigation of Cardington data as well as data from two other research-grade databases. Both Qian and Venkatram and Paine et al. proposed similar adjustments to the calculation of the surface friction velocity by AERMET, the meteorological processor for AERMOD. EPA incorporated the Qian and Venkatram suggested approach as a "beta option" in AERMOD in late 2012 (EPA, 2012). The same version of AERMOD also introduced low wind modeling options affecting the minimum value of σ_v and the weighting of the meander component that were used in the Test Cases 2–4 described in the following.

AERMOD's handling of low wind speed conditions, especially for applications with only one level of meteorological data and no direct turbulence measurements or vertical temperature gradient observations, is the focus of this study. Previous evaluations of AERMOD for low wind speed conditions (e.g., Paine et al., 2010) have emphasized low-level tracer release studies conducted in the 1970s and have utilized results of researchers such as Luhar and Rayner (2009). The focus of the study reported here is a further evaluation of AERMOD, but focusing upon tall-stack field databases. One of these databases was previously evaluated (Kaplan et al., 2012) with AERMOD Version 12345, featuring a database in Mercer County, North Dakota. This database features five SO_2 monitors in the vicinity of the Dakota Gasification Company plant and the Antelope Valley Station power plant in an area of both flat and elevated terrain. In addition to the Mercer County, ND, database, this study considers an additional field database for the Gibson Generating Station tall stack in flat terrain in southwest Indiana.

EPA released AERMOD version 14134 with enhanced low wind model features that can be applied in more than one combination. There is one low wind option (beta u_*) applicable to the meteorological preprocessor, AERMET, affecting the friction velocity calculation, and a variety of options available for the dispersion model, AERMOD, that focus upon the minimum σ_v specification. These beta options have the potential to reduce the overprediction biases currently present in AERMOD when run for neutral to stable conditions with regulatory default options (EPA, 2014a, 2014b). These new low wind options in AERMET and AERMOD currently require additional justification for each application in order to be considered for use in the United States. While EPA has conducted evaluations on low-level, nonbuoyant studies with the AERMET and AERMOD low wind speed beta options, it has not conducted any new evaluations on tall stack releases (U.S. EPA, 2014a, 2014b). One of the purposes of this study was to augment the evaluation experiences for the low wind model approaches for a variety of settings for tall stack releases.

This study also made use of the availability of sub-hourly meteorological observations to evaluate another modeling approach. This approach employs AERMOD with sub-hourly meteorological data and is known as the Sub-Hourly AERMOD Run Procedure or SHARP (Electric Power Research Institute [EPRI], 2013). Like the procedure developed by Sagendorf and Dickson as described earlier, SHARP merely subdivides each hour's meteorology (e.g., into six 10-min periods) and AERMOD is run multiple times with the meteorological input data (e.g., minutes 1–10, 11–20, etc.) treated as "hourly" averages for each run. Then the results of these runs are combined (averaged). In our SHARP runs, we did not employ any observed turbulence data as input. This alternative modeling approach (our Test Case 5 as discussed later) has been compared to the standard hourly AERMOD modeling approach for default and low wind modeling options (Test Cases 1–4 described later, using hourly averaged meteorological data) to determine whether it should be further considered as a viable technique. This study provides a discussion of the various low wind speed modeling options and the field study databases that were tested, as well as the modeling results.

Modeling Options and Databases for Testing

Five AERMET/AERMOD model configurations were tested for the two field study databases, as listed in the following. All model applications used one wind level, a minimum wind speed of 0.5 m/sec, and also used hourly average meteorological data with the exception of SHARP applications. As already noted, Test Cases 1–4 used options available in the current AERMOD code. The selections for Test Cases 1–4 exercised these low wind speed options over a range of reasonable choices that extended from no low wind enhancements to a full treatment that incorporates the Qian and Venkatram (2011) u_* recommendations as well as the Hanna (1990) and Chowdhury (2014) minimum σ_v recommendations (0.5 m/sec). Test Case 5 used sub-hourly meteorological data processed with AERMET using the beta u_* option for SHARP applications. We discuss later in this document our recommendations for SHARP modeling without the AERMOD meander component included.

Test Case 1: AERMET and AERMOD in default mode.

Test Case 2: Low wind beta option for AERMET and default options for AERMOD (minimum σ_v value of 0.2 m/sec).

Test Case 3: Low wind beta option for AERMET and the LOWWIND2 option for AERMOD (minimum σ_v value of 0.3 m/sec).

Test Case 4: Low wind beta option for AERMET and the LOWWIND2 option for AERMOD (minimum σ_v value of 0.5 m/sec).

Test Case 5: Low wind beta option for AERMET and AERMOD run in sub-hourly mode (SHARP) with beta u*option.

The databases that were selected for the low wind model evaluation are listed in Table 1 and described next. They were selected due to the following attributes:

- They feature multiple years of hourly SO_2 monitoring at several sites.
- Emissions are dominated by tall stack sources that are available from continuous emission monitors.
- They include sub-hourly meteorological data so that the SHARP modeling approach could be tested as well.
- There are representative meteorological data from a single-level station typical of (or obtained from) airport-type data.

Mercer County, North Dakota. An available 4-year period of 2007–2010 was used for the Mercer County, ND, database with five SO_2 monitors within 10 km of two nearby emission facilities (Antelope Valley and Dakota Gasification Company), site-specific meteorological data at the DGC#12 site (10-m level data in a low-cut grassy field in the location shown in Figure 1), and hourly emissions data from 15 point sources. The terrain in the area is rolling and features three of the monitors (Beulah, DGC#16, and especially DGC#17) being above or close to stack top for some of the nearby emission sources; see Figure 2 for more close-up terrain details. Figure 1 shows a layout of the sources, monitors, and the meteorological station. Tables 2 and 3 provide details about the emission sources and the monitors. Although this modeling application employed sources as far away as 50 km, the proximity of the monitors to the two nearby emission facilities meant that emissions from those facilities dominated the impacts. However, to avoid criticism from reviewers that other regional sources that

Table 1. Databases selected for the model evaluation.

	Mercer County, North Dakota	Gibson Generating Station, Indiana
Number of emission sources modeled	15	5
Number of SO_2 monitors	5 (one above stack top for several sources)	4 (all below stack top)
Type of terrain	Rolling	Flat
Meteorological years and data source	2007–2010 Local 10-m tower data	2008–2010 Evansville airport
Meteorological data time step	Hourly and sub-hourly	Hourly and sub-hourly
Emissions and exhaust data	Actual hourly variable emissions and velocity, fixed temperature	Actual hourly variable emissions and velocity, fixed temperature

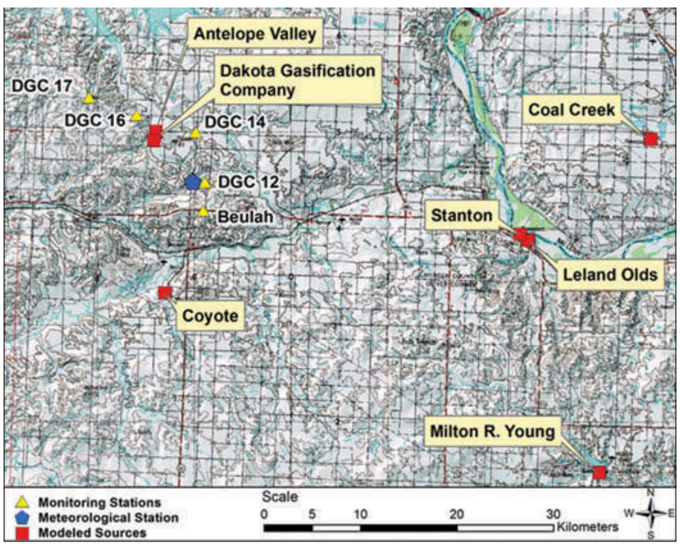

Figure 1. Map of North Dakota model evaluation layout.

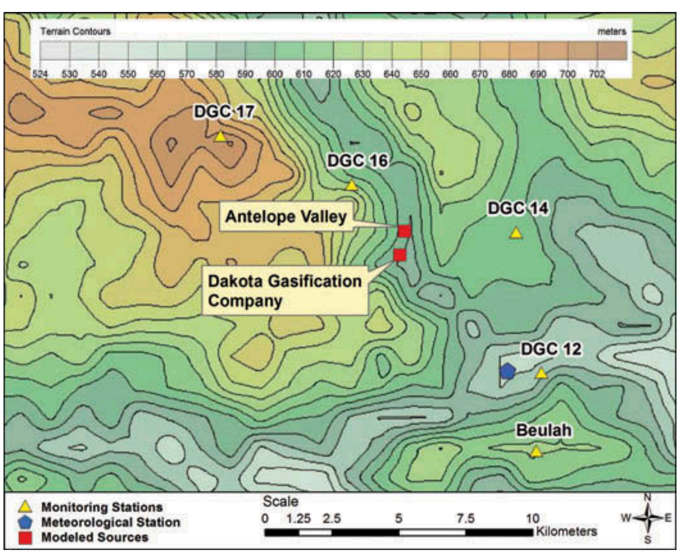

Figure 2. Terrain around the North Dakota monitors.

should have been modeled were omitted, other regional lignite-fired power plants were included in the modeling.

Gibson Generating Station, Indiana. An available 3-year period of 2008–2010 was used for the Gibson Generating Station in southwest Indiana with four SO_2 monitors within 6 km of the plant, airport hourly meteorological data (from Evansville, IN, 1-min data, located about 40 km SSE of the plant), and hourly emissions data from one electrical generating station (Gibson). The terrain in the area is quite flat and the stacks are tall. Figure 3 depicts the locations of the emission source and the four SO_2 monitors. Although the plant had an on-site meteorological tower, EPA (2013a) noted that the tower's location next to a large lake resulted in nonrepresentative boundary-layer conditions for the area, and that the use of airport data would be preferred. Tables 2 and 3 provide details about the emission sources and the monitors. Due to the fact that there are no major SO_2 sources within at least 30 km of Gibson, we modeled emissions from only that plant.

Meteorological Data Processing

For the North Dakota and Gibson database evaluations, the hourly surface meteorological data were processed with AERMET, the meteorological preprocessor for AERMOD. The boundary layer parameters were developed according to the guidance provided by EPA in the current AERMOD Implementation Guide (EPA, 2009). For the first modeling evaluation option, Test Case 1, AERMET was run using the default options. For the other four model evaluation options, Test Cases 2 to 5, AERMET was run with the beta u_* low wind speed option.

North Dakota meteorological processing

Four years (2007–2010) of the 10-m meteorological data collected at the DGC#12 monitoring station (located about 7 km SSE of the central emission sources) were processed with AERMET. The data measured at this monitoring station were wind direction, wind speed, and temperature. Hourly cloud

Table 2. Source information.

Database	Source ID	UTM X (m)	UTM Y (m)	Base elevation (m)	Stack height (m)	Exit temperature (K)	Stack diameter (m)
ND	Antelope Valley	285920	5250189	588.3	182.9	Vary	7.0
ND	Antelope Valley	285924	5250293	588.3	182.9	Vary	7.0
ND	Leland Olds	324461	5239045	518.3	106.7	Vary	5.3
ND	Leland Olds	324557	5238972	518.3	152.4	Vary	6.7
ND	Milton R Young	331870	5214952	597.4	171.9	Vary	6.2
ND	Milton R Young	331833	5214891	600.5	167.6	Vary	9.1
ND	Coyote	286875	5233589	556.9	151.8	Vary	6.4
ND	Stanton	323642	5239607	518.2	77.7	Vary	4.6
ND	Coal Creek	337120	5249480	602.0	201.2	Vary	6.7
ND	Coal Creek	337220	5249490	602.0	201.2	Vary	6.7
ND	Dakota Gasification Company	285552	5249268	588.3	119.8	Vary	7.0
ND	Dakota Gasification Company	285648	5249553	588.3	68.6	Vary	0.5
ND	Dakota Gasification Company	285850	5248600	588.3	76.2	Vary	1.0
ND	Dakota Gasification Company	285653	5249502	588.3	30.5	Vary	0.5
Gibson	Gibson 1	432999	4247189	119.0	189.0	327.2	7.6
Gibson	Gibson 2	432999	4247189	119.0	189.0	327.2	7.6
Gibson	Gibson 3	432923	4247251	118.5	189.0	327.2	7.6
Gibson	Gibson 4	432886	4247340	117.9	152.4	327.2	7.2
Gibson	Gibson 5	432831	4247423	116.3	152.4	327.2	7.2

Notes: SO_2 emission rate and exit velocity vary on hourly basis for each modeled source. Exit temperature varies by hour for the ND sources. UTM zones are 14 for North Dakota and 16 for Gibson.

Table 3. Monitor locations.

Database	Monitor	UTM X (m)	UTM Y (m)	Monitor elevation (m)
ND	DGC#12	291011	5244991	593.2
ND	DGC#14	290063	5250217	604.0
ND	DGC#16	283924	5252004	629.1
ND	DGC#17[a]	279025	5253844	709.8
ND	Beulah	290823	5242062	627.1
Gibson	Mt. Carmel	432424	4250202	119.0
Gibson	East Mt. Carmel	434654	4249666	119.3
Gibson	Shrodt	427175	4247182	138.0
Gibson	Gibson Tower	434792	4246296	119.0

Note: [a]This monitor's elevation is above stack top for several of the ND sources.

cover data from the Dickinson Theodore Roosevelt Regional Airport, North Dakota (KDIK) ASOS station (85 km to the SW), were used in conjunction with the monitoring station data. Upper air data were obtained from the Bismarck Airport, North Dakota (KBIS; about 100 km to the SE), twice-daily soundings.

In addition, the sub-hourly (10-min average) 10-m meteorological data collected at the DGC#12 monitoring station were also processed with AERMET. AERMET was set up to read six 10-min average files with the tower data and output six 10-min average surface and profile files for use in SHARP. SHARP then used the sub-hourly output of AERMET to calculate hourly modeled concentrations, without changing the internal computations of AERMOD. The SHARP user's manual (EPRI, 2013) provides detailed instructions on processing sub-hourly meteorological data and executing SHARP.

Gibson meteorological processing

Three years (2008–2010) of hourly surface data from the Evansville Airport, Indiana (KEVV), ASOS station (about 40 km SSE of Gibson) were used in conjunction with the

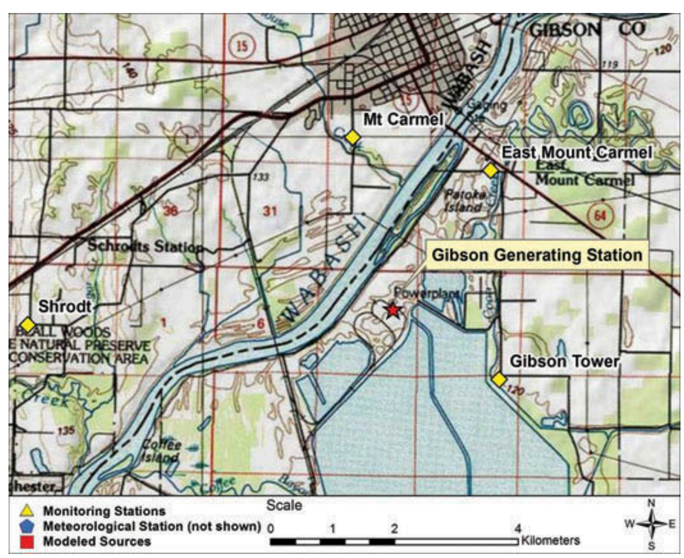

Figure 3. Map of Gibson model evaluation layout.

twice-daily soundings upper air data from the Lincoln Airport, Illinois (KILX, about 240 km NW of Gibson). The 10-min sub-hourly data for SHARP were generated from the 1-min meteorological data collected at Evansville Airport.

Emission Source Characteristics

Table 2 summarizes the stack parameters and locations of the modeled sources for the North Dakota and Gibson databases. Actual hourly emission rates, stack temperatures, and stack gas exit velocities were used for both databases.

Model Runs and Processing

For each evaluation database, the candidate model configurations were run with hourly emission rates provided by the plant operators. In the case of rapidly varying emissions (startup and shutdown), the hourly averages may average intermittent conditions occurring during the course of the hour. Actual stack heights were used, along with building dimensions used as input to the models tested. Receptors were placed only at the location of each monitor to match the number of observed and predicted concentrations.

The monitor (receptor) locations and elevations are listed in Table 3. For the North Dakota database, the DGC#17 monitor is located in the most elevated terrain of all monitors. The monitors for the Gibson database were located at elevations at or near stack base, with stack heights ranging from 152 to 189 m.

Tolerance Range for Modeling Results

One issue to be aware of regarding SO_2 monitored observations is that they can exhibit over- or underprediction tendencies up to 10% and still be acceptable. This is related to the tolerance in the EPA procedures (EPA, 2013b) associated with quality control checks and span checks of ambient measurements. Therefore, even ignoring uncertainties in model input parameters and other contributions (e.g., model science errors and random variations) that can also lead to modeling uncertainties, just the uncertainty in measurements indicates that modeled-to-monitored ratios between 0.9 and 1.1 can be considered "unbiased." In the discussion that follows, we consider model performance to be "relatively unbiased" if its predicted model to monitor ratio is between 0.75 and 1.25.

Model Evaluation Metrics

The model evaluation employed metrics that address three basic areas, as described next.

The 1-hr SO_2 NAAQS design concentration

An operational metric that is tied to the form of the 1-hour SO_2 National Ambient Air Quality Standards (NAAQS) is the "design concentration" (99th percentile of the peak daily 1-hr maximum values). This tabulated statistic was developed for each modeled case and for each individual monitor for each database evaluated.

Quantile–quantile plots

Operational performance of models for predicting compliance with air quality regulations, especially those involving a peak or near-peak value at some unspecified time and location, can be assessed with quantile–quantile (Q-Q) plots (Chambers et al., 1983), which are widely used in AERMOD evaluations. Q-Q plots are created by independently ranking (from largest to smallest) the predicted and the observed concentrations from a set of predictions initially paired in time and space. A robust model would have all points on the diagonal (45-degree) line. Such plots are useful for answering the question, "Over a period of time evaluated, does the distribution of the model predictions match those of observations?" Therefore, the Q-Q plot instead of the scatterplot is a pragmatic procedure for demonstrating model performance of applied models, and it is widely used by EPA (e.g., Perry et al. 2005). Venkatram et al. (2001) support the use of Q-Q plots for evaluating regulatory models. Several Q-Q plots are included in this paper in the discussion provided in the following.

Meteorological conditions associated with peak observed versus modeled concentrations

Lists of the meteorological conditions and hours/dates of the top several predictions and observations provide an indication as to whether these conditions are consistent between the model and monitoring data. For example, if the peak observed concentrations generally occur during daytime hours, we would expect that a well-performing model would indicate that the peak predictions are during the daytime as well. Another meteorological variable of interest is the wind speed magnitudes associated with observations and predictions. It would be expected, for example, that if the wind speeds associated with peak observations are low, then the modeled peak predicted hours would have the same characteristics. A brief qualitative summary of this analysis is included in this paper, and supplemental files contain the tables of the top 25 (unpaired) predictions and observations for all monitors and cases tested.

North Dakota Database Model Evaluation Procedures and Results

AERMOD was run for five test cases to compute the 1-hr daily maximum 99th percentile averaged over 4 years at the five ambient monitoring locations listed in Table 3. A regional background of 10 μg/m^3 was added to the AERMOD modeled predictions. The 1-hr 99th percentile background concentration was computed from the 2007–2010 lowest hourly monitored concentration among the five monitors so as to avoid double-counting impacts from sources already being modeled.

The ratios of the modeled (including the background of 10μg/m^3) to monitored design concentrations are summarized in

Table 4. North Dakota ratio of monitored to modeled design concentrations.

Test case	Monitor	Observed	Predicted	Ratio
Test Case 1	DGC#12	91.52	109.96	1.20
(Default AERMET, Default	DGC#14	95.00	116.84	1.23
AERMOD)	DGC#16	79.58	119.94	1.51
	DGC#17	83.76	184.48	2.20
	Beulah	93.37	119.23	1.28
Test Case 2	DGC#12	91.52	109.96	1.20
(Beta AERMET, Default	DGC#14	95.00	116.84	1.23
AERMOD)	DGC#16	79.58	119.94	1.51
	DGC#17	83.76	127.93	1.53
	Beulah	93.37	119.23	1.28
Test Case 3	DGC#12	91.52	103.14	1.13
(Beta AERMET, AERMOD with	DGC#14	95.00	110.17	1.16
LOWWIND2 σ_v = 0.3 m/sec)	DGC#16	79.58	111.74	1.40
	DGC#17	83.76	108.69	1.30
	Beulah	93.37	106.05	1.14
Test Case 4	DGC#12	91.52	95.86	1.05
(Beta AERMET, AERMOD with	DGC#14	95.00	100.50	1.06
LOWWIND2 σ_v = 0.5 m/sec)	DGC#16	79.58	106.65	1.34
	DGC#17	83.76	101.84	1.22
	Beulah	93.37	92.32	0.99
Test Case 5	DGC#12	91.52	82.18	0.90
(SHARP)	DGC#14	95.00	84.24	0.89
	DGC#16	79.58	95.47	1.20
	DGC#17	83.76	88.60	1.06
	Beulah	93.37	86.98	0.93

Notes: *Design concentration: 99th percentile peak daily 1-hr maximum, averaged over the years modeled and monitored.

Table 4 and graphically plotted in Figure 4 and are generally greater than 1. (Note that the background concentration is a small fraction of the total concentration, as shown in Table 4.) For the monitors in simple terrain (DGC#12, DGC#14, and Beulah), the evaluation results are similar for both the default and beta options and are within 5–30% of the monitored concentrations depending on the model option. The evaluation result for the monitor in the highest terrain (DGC#17) shows that the ratio of modeled to monitored concentration is more than 2, but when this location is modeled with the AERMET and AERMOD low wind beta options, the ratio is significantly better, at less than 1.3. It is noteworthy that the modeling results for inclusion of just the beta u_* option are virtually identical to the default AERMET run for the simple terrain monitors, but the differences are significant for the higher terrain monitor (DGC#17). For all of the monitors, it is evident that further reductions of AERMOD's overpredictions occur as the minimum σ_v in AERMOD is increased from 0.3 to 0.5 m/sec. For a minimum σ_v of 0.5 m/sec at all the monitors, AERMOD is shown to be conservative with respect to the design concentration.

The Q-Q plots of the ranked top fifty daily maximum 1-hr SO_2 concentrations for predictions and observations are shown in Figure 5. For the convenience of the reader, a vertical dashed line is included in each Q-Q plot to indicate the observed design concentration. In general, the Q-Q plots indicate the following:

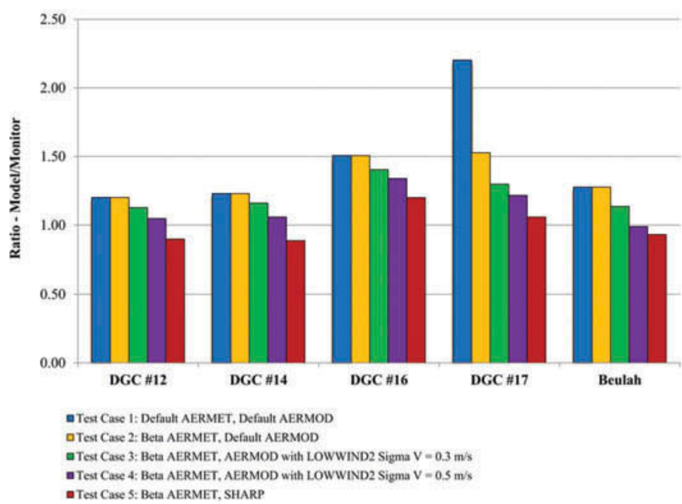

Figure 4. North Dakota ratio of monitored to modeled design concentration values at specific monitors.

- For all of the monitors, to the left of the design concentration line, the AERMOD hourly runs all show ranked predictions at or higher than observations. To the right of the design concentration line, the ranked modeled values for specific

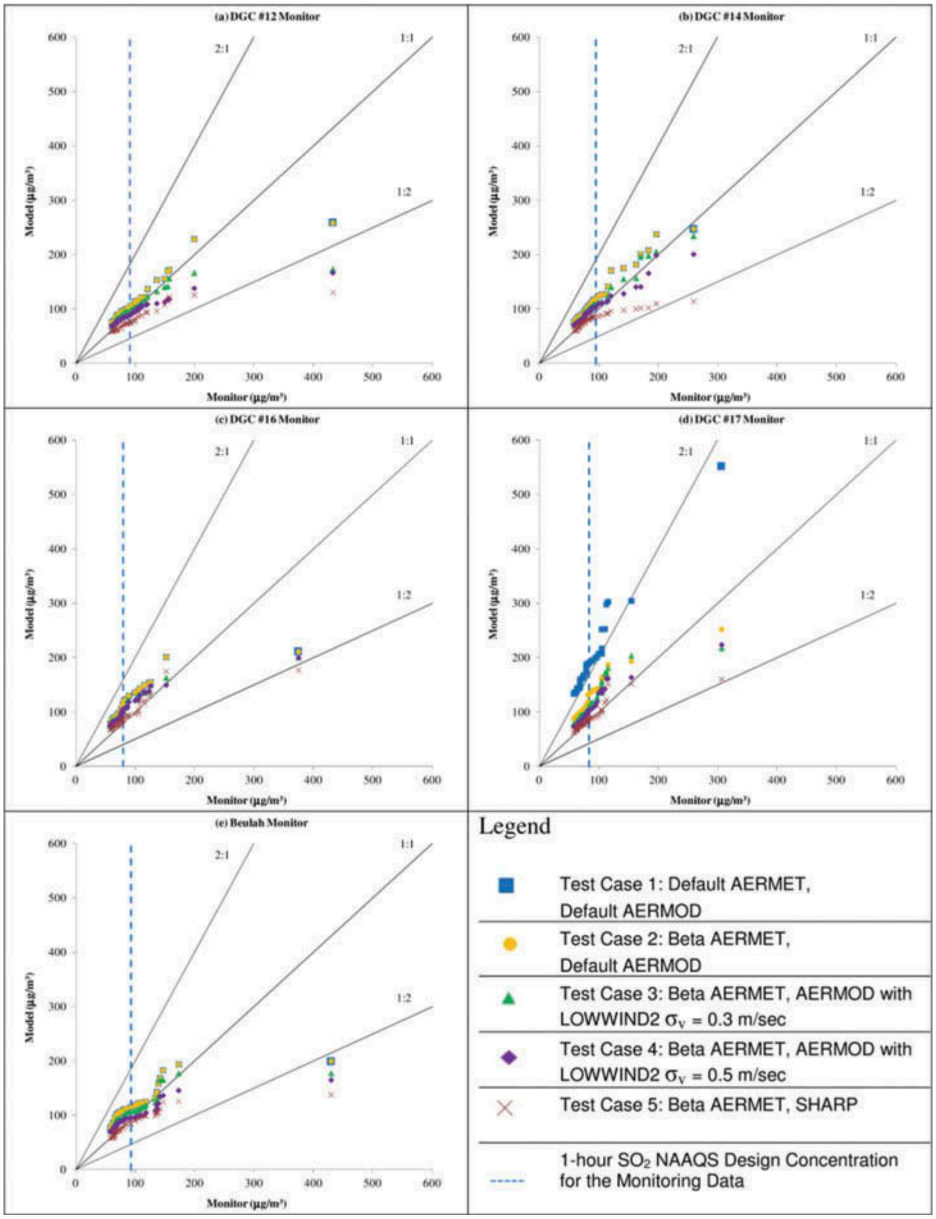

Figure 5. North Dakota Q-Q plots: top 50 daily maximum 1-hr SO_2 concentrations: (a) DGC #12 Monitor. (b) DGC#14 monitor. (c) DGC#16 monitor. (d) DGC#17 monitor. (e) Beulah monitor.

test cases and monitors are lower than the ranked observed levels, and the slope of the line formed by the plotted points is less than the slope of the 1:1 line. For model performance goals that would need to predict well for the peak concentrations (rather than the 99th percentile statistic), this area of the Q-Q plots would be of greater importance.

- The very highest observed value (if indeed valid) is not matched by any of the models for all of the monitors, but since the focus is on the 99th percentile form of the United States ambient standard for SO_2, this area of model performance is not important for this application.
- The ranked SHARP modeling results are lower than all of the hourly AERMOD runs, but at the design concentration level, they are, on average, relatively unbiased over all of the monitors. The AERMOD runs for SHARP included the meander component, which probably contributed to the small underpredictions noted for SHARP. In future modeling, we would advise users of SHARP to employ the AERMOD LOWWIND1 option to disable the meander component.

Gibson Generating Station Database Model Evaluation Procedures and Results

AERMOD was run for five test cases for this database as well in order to compute the 1-hr daily maximum 99th percentile averaged over three years at the four ambient monitoring locations listed in Table 3. A regional background of 18 μg/m^3 was added to the AERMOD modeled predictions. The 1-hr 99th percentile background concentration was computed from the 2008–2010 lowest hourly monitored concentration among the four monitors so as to avoid impacts from sources being modeled.

The ratio of the modeled (including the background of 18 μg/m^3) to monitored concentrations is summarized in Table 5 and graphically plotted in Figure 6 and are generally greater than 1.0. (Note that the background concentration is a small fraction of the total concentration, as shown in Table 5.) Figure 6 shows that AERMOD with hourly averaged meteorological data overpredicts by about 40–50% at Mt. Carmel and Gibson Tower monitors and by about 9–31% at East Mt. Carmel and Shrodt monitors. As expected (due to dominance of impacts with convective conditions), the AERMOD results do not vary much with the various low wind speed options in this flat terrain setting. AERMOD with sub-hourly meteorological data (SHARP) has the best (least biased predicted-to-observed ratio of design concentrations) performance among the five cases modeled. Over the four monitors, the range of predicted-to-observed ratios for SHARP is a narrow one, ranging from a slight underprediction by 2% to an overprediction by 14%.

The Q-Q plots of the ranked top fifty daily maximum 1-hr SO_2 concentrations for predictions and observations are shown in Figure 7. It is clear from these plots that the SHARP results parallel and are closer to the 1:1 line for a larger portion of the concentration range than any other model tested. In general, AERMOD modeling with hourly data exhibits an overprediction tendency at all of the monitors for the peak ranked concentrations at most of the monitors. The AERMOD/SHARP models predicted lower relative to observations at the East Mt. Carmel monitor for the very highest values, but match well for the 99th percentile peak daily 1-hr maximum statistic.

Evaluation Results Discussion

The modeling results for these tall stack releases are sensitive to the source local setting and proximity to complex terrain. In general, for tall stacks in simple terrain, the peak ground-level impacts mostly occur in daytime convective conditions. For settings with a mixture of simple and complex terrain, the peak impacts for the higher terrain are observed to occur during both daytime and nighttime conditions, while AERMOD tends to favor stable conditions only without low wind speed enhancements. Exceptions to this “rule of thumb” can occur for stacks with aerodynamic building downwash effects. In that case, high observed and modeled predictions are likely to occur during high wind events during all times of day.

The significance of the changes in model performance for tall stacks (using a 90th percentile confidence interval) was independently tested for a similar model evaluation conducted for Eastman Chemical Company (Paine et al., 2013; Szembek et al., 2013), using a modification of the Model Evaluation Methodology (MEM) software that computed estimates of the hourly stability class (Strimaitis et al., 1993). That study indicated that relative to a perfect model, a model that

Table 5. Gibson ratio of monitored to modeled design concentrations*.

Test case	Monitor	Observed	Predicted	Ratio
Test Case 1 (Default AERMET, Default AERMOD)	Mt. Carmel	197.25	278.45	1.41
	East Mt. Carmel	206.89	230.74	1.12
	Shrodt	148.16	189.63	1.28
	Gibson Tower	127.12	193.71	1.52
Test Case 2 (Beta AERMET, Default AERMOD)	Mt. Carmel	197.25	287.16	1.46
	East Mt. Carmel	206.89	229.22	1.11
	Shrodt	148.16	189.63	1.28
	Gibson Tower	127.12	193.71	1.52
Test Case 3 (Beta AERMET, AERMOD with LOWWIND2 σ_v = 0.3 m/sec)	Mt. Carmel	197.25	280.32	1.42
	East Mt. Carmel	206.89	224.65	1.09
	Shrodt	148.16	184.82	1.25
	Gibson Tower	127.12	192.22	1.51
Test Case 4 (Beta AERMET, AERMOD with LOWWIND2 σ_v = 0.5 m/sec)	Mt. Carmel	197.25	277.57	1.41
	East Mt. Carmel	206.89	224.65	1.09
	Shrodt	148.16	176.81	1.19
	Gibson Tower	127.12	192.22	1.51
Test Case 5 (SHARP)	Mt. Carmel	197.25	225.05	1.14
	East Mt. Carmel	206.89	202.82	0.98
	Shrodt	148.16	136.41	0.92
	Gibson Tower	127.12	148.64	1.17

Notes: *Design Concentration: 99th percentile peak daily 1-hr maximum, averaged over the years modeled and monitored.

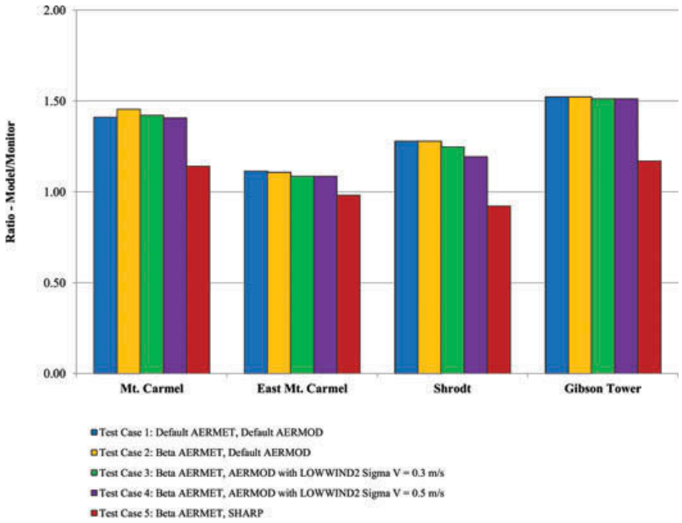

Figure 6. Gibson ratio of monitored to modeled design concentration values at specific monitors.

overpredicted or underpredicted by less than about 50% would likely show a performance level that was not significantly different. For a larger difference in bias, one could expect a statistically significant difference in model performance. This finding has been adopted as an indicator of the significance of different modeling results for this study.

A review of the North Dakota ratios of monitored to modeled values in Figure 4 generally indicates that for DGC#12, DGC#14, and Beulah, the model differences were not significantly different. For DGC#16, it could be concluded that the SHARP results were significantly better than the default AERMOD results, but other AERMOD variations were not significantly better. For the high terrain monitor, DGC#17, it is evident that all of the model options departing from default were significantly better than the default option, especially the SHARP approach.

For the Gibson monitors (see Figure 6), the model variations did not result in significantly different performance except for the Gibson Tower (SHARP vs. the hourly modes of running AERMOD).

General conclusions from the review of meteorological conditions associated with the top observed concentrations at the North Dakota monitors, provided in the supplemental file called "North Dakota Meteorological Conditions Resulting in Top 25 Concentrations," are as follows:

- A few peak observed concentrations occur at night with light winds. The majority of observations for the DGC#12 monitor are mostly daytime conditions with moderate to strong winds.
- Peak observations for the DGC#14 and Beulah monitors are mostly daytime conditions with a large range of wind speeds. Once again, a minority of the peak concentrations occur at night with a large range of wind speeds.

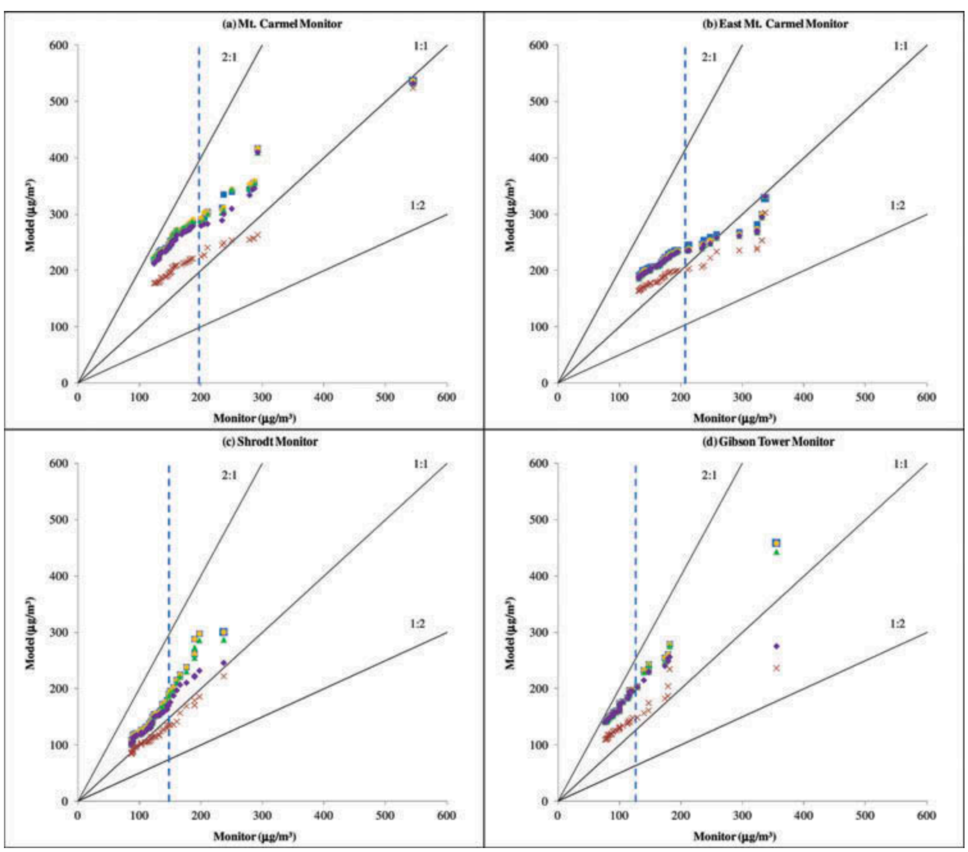

Figure 7. Gibson Q-Q plots: top 50 daily maximum 1-hour SO_2 concentrations. (a) Mt. Carmel monitor. (b) East Mt. Carmel monitor. (c) Shrodt monitor. (d) Gibson tower monitor. For the legend, see Figure 5.

- Peak observed concentrations for the DGC#16 and DGC#17 monitors occur at night with light winds. Majority of observations are mixed between daytime and nighttime conditions with a large range of wind speeds for both. The DGC#17 monitor is located in elevated terrain.

The conclusions from the review of the meteorological conditions associated with peak AERMOD or SHARP predictions are as follows:

- AERMOD hourly peak predictions for the DGC#12 and Beulah monitors are consistently during the daytime with light to moderate wind speeds and limited mixing heights. This is a commonly observed situation that is further discussed later.
- There are similar AERMOD results for DGC#14, except that there are more periods with high winds and higher mixing heights.
- The AERMOD results for DGC#16 still feature mostly daytime hours, but with more high wind conditions.
- The default AERMOD results for DGC#17 are distinctly different from the other monitors, with most hours featuring stable, light winds. There are also a few daytime hours of high predictions with low winds and low mixing heights. This pattern changes substantially with the beta u_* options employed, when the majority of the peak prediction hours are daytime periods with light to moderate wind speeds. This pattern is more consistent with the peak observed concentration conditions.
- The SHARP peak predictions at the North Dakota monitors were also mostly associated with daytime hours with a large range of wind speeds for all of the monitors.

The North Dakota site has some similarities due to a mixture of flat and elevated terrain to the Eastman Chemical Company model evaluation study in Kingsport, TN (this site features three coal-fired boiler houses with tall stacks). In that study (Paine et al. 2013; Szembek et al., 2013), there was one monitor in elevated terrain and two monitors in flat terrain with a full year of data. Both the North Dakota and Eastman sites featured observations of the design concentration being within about 10% of the mean design concentration over all monitors. Modeling results using default options in AERMOD for both of these sites indicated a large spread of the predictions, with predictions in high terrain exceeding observations by more than a factor of 2. In contrast, the predictions in flat terrain, while higher than observations, showed a lower overprediction bias. The use of low wind speed improvements in AERMOD (beta u_* in AERMET and an elevated minimum σ_v value) did improve model predictions for both databases.

The conclusions from the review of the meteorological conditions associated with peak observations, provided in the supplemental file called "Gibson Meteorological Conditions Resulting in Top 25 Concentrations," are as follows:

- Peak observations for the Mt. Carmel and East Mt. Carmel monitors occur during both light wind convective conditions and strong wind conditions (near neutral, both daytime and nighttime).
- Nighttime peaks that are noted at Mt. Carmel and East Mt. Carmel could be due to downwash effects with southerly winds.
- Gibson Tower and Shrodt monitors were in directions with minimal downwash effects; therefore, the peak impacts at these monitors occur with convective conditions.
- The Gibson Tower and Shrodt monitor peak observation conditions were similarly mixed for wind speeds, but they were consistently occurring during the daytime only.

AERMOD (hourly) modeling runs and SHARP runs are generally consistent with the patterns of observed conditions for Shrodt and Gibson Tower monitors. Except for downwash effects, the peak concentrations were all observed and predicted during daytime hours. There are similar AERMOD results for Mt. Carmel and East Mt. Carmel, except that there are more nighttime periods and periods with strong wind conditions.

As noted earlier, AERMOD tends to focus its peak predictions for tall stacks in simple terrain (those not affected by building downwash) for conditions with low mixing heights in the morning. However, a more detailed review of these conditions indicates that the high predictions are not simply due to plumes trapped within the convective mixed layer, but instead due to plumes that initially penetrate the mixing layer, but then emerge (after a short travel time) into the convective boundary layer in concentrated form with a larger-than-expected vertical spread. Tests of this condition were undertaken by Dr. Ken Rayner of the Western Australia Department of Environmental Regulation (2013), who found the same condition occurring for tall stacks in simple terrain for a field study database in his province. Rayner found that AERMOD tended to overpredict peak concentrations by a factor of about 50% at a key monitor, while with the penetrated plume removed from consideration, AERMOD would underpredict by about 30%. Therefore, the correct treatment might be a more delayed entrainment of the penetrated plume into the convective mixed layer. Rayner's basic conclusions were:

- A plume penetrates and disperses within a 1-hr time step in AERMOD, while in the real world, dispersion of a penetrated puff may occur an hour or more later, after substantial travel time.
- A penetrated plume initially disperses via a vertical Gaussian formula, not a convective probability density function. Because penetrated puffs typically have a very small vertical dispersion, they are typically fully entrained (in AERMOD) in a single hour by a growing mixed layer, and dispersion of a fully entrained puff is via convective mixing, with relatively rapid vertical dispersion, and high ground-level concentrations.

Conclusions and Recommendations for Further Research

This study has addressed additional evaluations for low wind conditions involving tall stack releases for which multiple years of concurrent emissions, meteorological data, and monitoring data were available. The modeling cases that were the focus of this study involved applications with only one level of meteorological data and no direct turbulence measurements or vertical temperature gradient observations.

For the North Dakota evaluation, the AERMOD model overpredicted, using the design concentration as the metric for each monitor. For the relatively low elevation monitors, the results were similar for both the default and beta options and are within 5–30% of the monitored concentrations depending on the model option. The modeling result for the elevated DGC#17 monitor showed that this location is sensitive to terrain, as the ratio of modeled to monitored concentration is over 2. However, when this location was modeled with the low wind beta option, the ratio was notably better, at less than 1.3. Furthermore, the low wind speed beta option changed the AERMOD's focus on peak predictions conditions from mostly nighttime to mostly daytime periods, somewhat more in line with observations. Even for a minimum σ_v as high as 0.5 m/sec, all of the AERMOD modeling results were conservative or relatively unbiased (for the design concentration). The North Dakota evaluation results for the sub-hourly (SHARP) modeling were, on average, relatively unbiased, with a predicted-to-observed design concentration ratio ranging from 0.89 to 1.2. With a 10% tolerance in the SO_2 monitored values, we find that the SHARP performance is quite good. Slightly higher SHARP predictions would be expected if AERMOD were run with the LOWWIND1 option deployed.

For the Gibson flat terrain evaluation, AERMOD with hourly averaged meteorological data overpredicted at three of the four monitors between 30 and 50%, and about 10% at the fourth monitor. The AERMOD results did not vary much with the various low wind speed options in this flat terrain setting. AERMOD with sub-hourly meteorological data (SHARP) had the best (least biased predicted-to-observed ratio of design concentrations) performance among the five cases modeled. Over the four monitors, the range of predicted-to-observed ratios for SHARP was a narrow one, ranging from a slight underprediction by 2% to an overprediction by 14%. All other modeling options had a larger range of results.

The overall findings with the low wind speed testing on these tall stack databases indicate that:

- The AERMOD low wind speed options have a minor effect for flat terrain locations.
- The AERMOD low wind speed options have a more significant effect with AERMOD modeling for elevated terrain locations, and the use of the LOWWIND2 option with a minimum σ_v on the order of 0.5 m/sec is appropriate.
- The AERMOD sub-hourly modeling (SHARP) results are mostly in the unbiased range (modeled to observed design concentration ratios between 0.9 and 1.1) for the two databases tested with that option.
- The AERMOD low wind speed options improve the consistency of meteorological conditions associated with the highest observed and predicted concentration events.

Further analysis of the low wind speed performance of AERMOD with either the SHARP procedure or the use of the minimum σ_v specifications by other investigators is encouraged. However, SHARP can only be used if sub-hourly meteorological data is available. For Automated Surface Observing Stations (ASOS) with 1-min data, this option is a possibility if the 1-min data are obtained and processed.

Although the SHARP results reported in this paper are encouraging, further testing is recommended to determine the optimal sub-hourly averaging time (no less than 10 min is recommended) and whether other adjustments to AERMOD (e.g., total disabling of the meander option) are recommended. Another way to implement the sub-hourly information in AERMOD and to avoid the laborious method of running AERMOD several times for SHARP would be to include a distribution, or range, of the sub-hourly wind directions to AERMOD so that the meander calculations could be refined.

For most modeling applications that use hourly averages of meteorological data with no knowledge of the sub-hourly wind distribution, it appears that the best options with the current AERMOD modeling system are to implement the AERMET beta u_* improvements and to use a minimum σ_v value on the order of 0.5 m/sec/sec.

It is noteworthy that EPA has recently approved (EPA, 2015) as a site-specific model for Eastman Chemical Company the use of the AERMET beta u_* option as well as the LOWWIND2 option in AERMOD with a minimum σ_v of 0.4 m/sec. This model, which was evaluated with site-specific meteorological data and four SO_2 monitors operated for 1 year, performed well in flat terrain, but overpredicted in elevated terrain, where a minimum σ_v value of 0.6 m/sec actually performed better. This would result in an average value of the minimum σ_v of about 0.5 m/sec, consistent with the findings of Hanna (1990).

The concept of a minimum horizontal wind fluctuation speed on the order of about 0.5 m/sec is further supported by the existence of vertical changes (shears) in wind direction (as noted by Etling, 1990) that can result in effective horizontal shearing of a plume that is not accounted for in AERMOD. Although we did not test this concept here, the concept of vertical wind shear effects, which are more prevalent in decoupled stable conditions than in well-mixed convective conditions, suggests that it would be helpful to have a "split minimum σ_v" approach in AERMOD that enables the user to specify separate minimum σ_v values for stable and unstable conditions. This capability would, of course, be backward-compatible to the current minimum σ_v specification that applies for all stability conditions in AERMOD now.

Supplemental Material

Supplemental data for this article can be accessed at the publisher's website

References

Anfossi, D., D. Oettl, G. Degrazia, and A. Goulart. 2005. An analysis of sonic anemometer observations in low wind speed conditions. *Boundary Layer Meteorol*. 114:179–203. doi:10.1007/s10546-004-1984-4

Barad, M.L. 1958. Project Prairie Grass, a field program in diffusion. *Geophys. Res. Pap*. 59. Bedford, MA: Air Force Cambridge Centre.

Brett, A.C., and S.E. Tuller. 1991. The autocorrelation of hourly wind speed observations. *J. Appl. Meteorol*. 30:823–33. doi:10.1175/1520-0450(1991)030%3C0823:TAOHWS%3E2.0.CO;2

Chambers, J.M., W.S. Cleveland, B. Kleiner, and P.A. Tukey. 1983. Comparing data distributions. Graphical methods for data analysis. Pacific Grove, CA: Bell Laboratories. Wadsworth International Group and Duxbury Press.

Chowdhury, B., R.I. Sykes, D. Henn, and P. Karamchandani. 2014. SCICHEM Version 3.0 (Beta 2) technical documentation. http://sourceforge.net/projects/epri-dispersion/files/SCICHEM/SCICHEM3.0b2.zip/download

Cimorelli, A.J., S.G. Perry, A. Venkatram, J.C. Weil, R.J. Paine, R.B. Wilson, R.F. Lee, W.D. Peters, and R.W. Brode. 2005. AERMOD: A dispersion model for industrial source applications. Part I: General model formulation and boundary layer characterization. *J. Appl. Meteorol*. 44:682–93. doi:10.1175/JAM2227.1

Electric Power Research Institute. 2013. Sub Hourly AERMOD Run Procedure (SHARP), version 13011 user's guide. Research project 1025622. http://sourceforge.net/projects/epri-dispersion/files/SHARP (accessed June 10, 2015).

Etling, D. 1990. On plume meandering under stable stratification. *Atmos. Environ*. 8:1979–85. doi:10.1016/0960-1686(90)90232-C

Hanna, S.R. 1990. Lateral dispersion in light-wind stable conditions, *Nuovo Cimento* 13:889–94. doi:10.1007/BF02514777

Irwin, J.S. 2014. A suggested method for dispersion model evaluation. *J. Air Waste Manage. Assoc*. 64(3):255–64. doi:10.1080/10962247.2013.833147

Kaplan, M., and R.J. Paine. 2012. Comparison of AERMOD modeled 1-hour SO_2 concentrations to observations at multiple monitoring stations in North Dakota. Presented at the 105th Annual Conference and Exhibition of the Air & Waste Management Association, June 2012, San Antonio, TX.

Luhar, A.K., and K.N. Rayner. 2009. Methods to estimate surface fluxes of momentum and heat from routine weather observations for dispersion applications under stable stratification. *Boundary Layer Meteorol*. 132:437–54. doi:10.1007/s10546-009-9409-z

Mahrt, L. 1998. Stratified atmospheric boundary layers and breakdown of models. *Theor. Comput. Fluid Dynam*. 11:263–79. doi:10.1007/s001620050093

Paine, R., J.A. Connors, and C.D. Szembek, 2010. AERMOD low wind speed evaluation study: Results and implementation. Paper 2010-A-631-AWMA. Presented at the 103rd Annual Conference, Air & Waste Management Association, June 2012, Calgary, Alberta, Canada.

Paine, R., F. Tringale, and S. Gossett, 2013. Resolution of 1-hour SO_2 non-attainment area in Kingsport, TN: Advanced meteorological and monitoring study. Presented at the Air & Waste Management Association's Specialty Conference. Raleigh, NC, March.

Pasquill, F., and F.B. Smith. 1983. *Atmospheric Diffusion*. Series in Environmental Science. Ellis Horwood. Chichester: John Wiley & Sons.

Perez, I., M. Garcia, M. Sanchez, and B. De Torre. 2004. Autocorrelation analysis of meteorological data from a RASS Sodar. *J. Appl. Meteorol*., 43:1213–23. doi:10.1175/1520-0450(2004)043%3C1213:AAOMDF%3E2.0.CO;2

Perry, S.G., A.J. Cimorelli, R.J. Paine, R.W. Brode, J.C. Weil, A. Venkatram, R. B. Wilson, R.F. Lee, and W.D. Peters. 2005. AERMOD: A dispersion model for industrial source applications. Part II: Model performance against 17 field study databases. *J. Appl. Meteorol*. 44:694–708. doi:10.1175/JAM2228.1

Qian, W., and A. Venkatram. 2011. Performance of steady-state dispersion models under low wind-speed conditions. *Boundary Layer Meteorol*. 138:475–91. doi:10.1007/s10546-010-9565-1

Rayner, K. 2013. Personal communication with Robert Paine, AECOM.

Sagendorf, J.F., and C.R. Dickson. 1974. Diffusion under low windspeed, inversion conditions. *NOAA Technical Memorandum* 52. http://www.arl.noaa.gov/documents/reports/ARL-52.pdf (accessed September 9, 2015).

Smedman, A.S. 1988. Observations of a multi-level turbulence structure in a very stable atmospheric boundary layer. *Boundary Layer Meteorol*. 66:105–26. doi:10.1007/BF00116064

Strimaitis, D., E. Insley, M. Korc, and F. Lurmann. 1993. User's guide for the Model Evaluation Methodology (MEM) system for comparing model performance, Version 1.0. STI-93261-1392-FR. Prepared for U.S. Environmental Protection Agency, Research Triangle Park, NC.

Szembek, C., R. Paine, and S. Gossett. 2013. Resolution of 1-hour SO_2 non-attainment area in Kingsport, TN: Model evaluation analysis results to date. Presented at the Air & Waste Management Association's Specialty Conference, Raleigh, NC, March.

U.S. Environmental Protection Agency. 2004. AERMOD: Description of model formulation. EPA-454/R-03-004. http://www.epa.gov/ttn/scram/7thconf/aermod/aermod_mfd.pdf (accessed June 10, 2015).

U.S. Environmental Protection Agency. 2005. Revision to the guideline on air quality models: Adoption of a preferred general purpose (flat and complex terrain) dispersion model and other revisions. Final rule. *Fed. Reg*. 70 (216). http://www.gpo.gov/fdsys/pkg/FR-2005-11-09/html/05-21627.htm (accessed June 10, 2015).

U.S. Environmental Protection Agency. 2009. AERMOD implementation guide (AIG). http://www.epa.gov/ttn/scram/7thconf/aermod/aermod_implmtn_guide_19March2009.pdf (accessed June 10, 2015).

U.S. Environmental Protection Agency. 2012. AERMET 12345 model change bulletin MCB#3. http://www.epa.gov/ttn/scram/7thconf/aermod/aermet_mcb3.txt (accessed June 10, 2015).

U.S. Environmental Protection Agency. 2013a. Personal communication from Roger Brode, EPA, to Robert Paine, AECOM.

U.S. Environmental Protection Agency. 2013b. *Quality Assurance Handbook for Air Pollution Measurement Systems, Volume II, Ambient Air Quality Monitoring Program*. http://www.epa.gov/ttnamti1/files/ambient/pm25/qa/QA-Handbook-Vol-II.pdf (accessed June 10, 2015).

U.S. Environmental Protection Agency. 2014a. Webinar: AERMOD modeling system update, January 15. http://www.epa.gov/ttn/scram/webinar/AERMOD_13350_Update/AERMOD_System_Update_Webinar_01-14-2014_FINAL.pdf (accessed June 10, 2015).

U.S. Environmental Protection Agency. 2014b. Webinar: AERMOD modeling system update, August 14. http://www.epa.gov/ttn/scram/webinar/AERMOD_14134-NO2_Memo/20140812-Webinar_Slides.pdf (accessed June 10, 2015).

U.S. Environmental Protection Agency. 2015. Approval of alternative model request: Modeling of sulfur dioxide emissions from Eastman Chemical Company, Sullivan County, Tennessee, 2010 Sulfur dioxide National Ambient Air Quality Standards (NAAQS) nonattainment area. Letter to Mr. Barry R. Stephens, Tennessee Department of Environment and Conservation from Beverly H. Bannister, Director of Air, Pesticides and Toxics Management Division (EPA Region 4).

Van der Hoven, I. 1976. A survey of field measurements of atmospheric diffusion under low-wind-speed inversion conditions. *Nuclear Safety* 17:223–30.

Venkatram, A., R.W. Brode, A.J. Cimorelli, J.T. Lee, R.J. Paine, S.G. Perry, W. D. Peters, J.C. Weil, and R.B. Wilson. 2001. A complex terrain dispersion model for regulatory applications. *Atmos. Environ*. 35:4211–21. doi:10.1016/S1352-2310(01)00186-8

Wilson, R.B., G.E. Start, C.R. Dickson, and N.R. Ricks. 1976. Diffusion under low wind speed conditions near Oak Ridge, Tennessee. *NOAA Technical Memorandum* ERL ARL-61, 83 pp. http://www.arl.noaa.gov/documents/reports/ARL-61.pdf (accessed September 9, 2015).

About the Authors

Robert Paine, CCM, QEP, is an associate vice-president and technical director and **Olga Samani** and **Mary Kaplan** are senior air quality meteorologists with AECOM's Air Quality Modeling group in Chelmsford, MA.

Eladio Knipping is a principal technical leader in the Environment Sector at the Electric Power Research Institute office in Washington, DC.

Naresh Kumar is a senior program manager of air quality in the environment sector at the Electric Power Research Institute office in Palo Alto, CA.

Appendix C

AERMOD User's Guide: Appendix F. Evaluation of Low Wind Beta Options

APPENDIX F. EVALUATION OF LOW WIND BETA OPTIONS

Beginning with version 12345, AERMOD includes non-default BETA options to address concerns regarding model performance under low wind speed conditions. This included the LOWWIND1 and LOWWIND2 BETA options on the MODELOPT keyword in AERMOD, and the ADJ_U* option included in Stage 3 of the AERMET meteorological processor. Beginning with version 15181 a new LOWWIND3 BETA option was incorporated into AERMOD. The LOWWIND3 option increases the minimum value of sigma-v from 0.2 to 0.3 m/s, consistent with the LowWind2 option, but eliminates upwind dispersion, consistent with the LowWind1 option. The LowWind3 option uses an "effective" sigma-y value that replicates the centerline concentration accounting for meander, but sets concentrations to zero (0) for receptors that are more than 6*sigma-y off the plume centerline, similar to the FASTALL option.

Updated evaluation results for these BETA options based on version 15181 of AERMOD are presented below for two field studies conducted in 1974 by the Air Resources Laboratory of the National Oceanic and Atmospheric Administration (NOAA) to investigate diffusion under low wind speed conditions at Idaho Falls (NOAA, 1974) and Oak Ridge (NOAA, 1976). These two field studies were used in the API-sponsored evaluations of AERMOD conducted by AECOM (AECOM, 2009), that were subsequently submitted as part of API's public comments on EPA's 10th Conference on Air Quality Models held in March 2012. Each of these studies used tracer releases with three arcs of samplers located at 100m, 200m, and 400m from the release point. Diagrams for each of the study areas are presented below.

In addition, since the ADJ_U* option in AERMET and the LowWind option in AERMOD are focused on improving model performance during periods of stable/low-wind conditions, additional evaluations are presented below for the Lovett evaluation database, a tall stack located in complex terrain where stable/low-wind conditions can also be important.

The evaluation results presented here for the Idaho Falls and Oak Ridge studies were based in part on the information included in the AECOMs 2009 report and data files subsequently provided by AECOM. However, some adjustments to inputs were made based on an independent assessment of the surface roughness for each of the study locations, an adjustment to the effective tracer release height at Idaho Falls from 1.5 to 3m based on information provided on page 24 of the NOAA Technical Memorandum for Idaho Falls (NOAA, 1974), and adjustments to the wind measurement height for Oak Ridge based on the discussion in Section 2.2 and information provided in Table 1 of the NOAA Technical Memorandum for Oak Ridge (NOAA, 1976).

The AECOM evaluation for Oak Ridge assumed a 2m wind measurement height, whereas page 8 of the NOAA report for Oak Ridge indicated that the wind measurements were "accomplished by laser anemometry" because wind speeds were "below the threshold of standard cup anemometers." Footnotes in Table 1 also confirm that wind speeds were "measured by laser anemometers" for all tests, except for Test 11 where the wind speed was measured at the 30.5m level on one of meteorological towers included in the study. Given that the transmitters and receivers for the laser anemometer were located on the hills on either side of the valley where the tracer was released, at elevations between 50 to 100 feet higher than the elevation at the release point (based on Figure 2b of the NOAA report), a 2m wind measurement height may not be appropriate. However, the NOAA report does not indicate an "effective" measurement height above ground for the wind speeds measured by the laser anemometers. Another aspect of the use of laser anemometry that complicates the determination of an appropriate measurement height is that the "measured" wind speeds may represent more of a volume average than a point measurement. Since the wind speeds estimated by laser anemometry are likely to be more representative of vector averaged wind speeds than scalar averages the VECTORWS option in AERMOD was used for the Oak Ridge evaluations.

Based on these considerations, the evaluation results presented here were based on an "effective" wind measurement height of 10m, and the winds were also assumed to represent vector mean wind speeds. In addition to the different assumptions regarding the appropriate measurement height to assign to the observed wind speeds at Oak Ridge, the results presented below are based on a surface roughness length of 0.6m, consistent with the forest covering most of the study area at the time. The AECOM study assumed a much smaller roughness length of 0.2m.

A series of figures is provided below for each site, starting with the Oak Ridge study followed by the Idaho Falls study. For each site a series of Q-Q plots (results paired by rank), plots of concentrations paired in time, and residual plots showing the distribution of predicted/observed concentration ratios versus downwind distance are provided. Results are shown for the following scenarios:

- Current regulatory default options, i.e., no adjustments (No ADJ_U*/No LowWind)
- U* adjustment with no low wind options (ADJ_U*/No_LowWind)
- U* adjustment with LOWWIND1 (ADJ_U*/LowWind1)
- U* adjustment with LOWWIND2 (ADJ_U*/LowWind2)
- U* adjustment with LOWWIND3 (ADJ_U*/LowWind3)

Based on the limited meteorological data available for the Oak Ridge study, a single set of model comparisons is presented. Given the more robust meteorological data available from the Idaho Falls study, including multiple levels of wind speed, direction, temperature, and sigma-theta, several sets of meteorological inputs are evaluated, including the use of delta-T data with the Bulk Richardson Number (BULKRN) option available in AERMET.

Another important difference between these two field studies is that the Oak Ridge site was located in a hilly area on the Oak Ridge peninsula, with terrain elevations varying about 40m across the study area, with the tracer release point located near the center of the valley that cuts across the peninsula. Given the very low wind speeds during the study period, drainage flows and valley channeling may have influenced plume dispersion. The influence of terrain on low-level non-buoyant releases in AERMOD has not been assessed, and neither the AECOM nor EPA results for Oak Ridge have incorporated terrain elevations in their respective evaluations. As a result, the evaluations based on the Idaho Falls are likely to be more robust than the evaluations based on Oak Ridge.

As noted above, the Oak Ridge evaluations are based on a single set of meteorological inputs, whereas the Idaho Falls evaluation are based on a range of options given the more robust data available. These various sets of meteorological inputs for Idaho Falls are referred to in the figure captions as follows:

1. Base 1-level: no delta-T or turbulence (i.e., sigma-theta) data included;

2. Full 1-level: no delta-T data with sigma-theta data;
3. Base 2-level: delta-T data used with BULKRN option without sigma-theta;
4. Full 2-level: delta-T data used with BULKRN option with sigma-theta

Each of these data sets were used with and without the ADJ_U* option in AERMET and also with and without the LowWind options. For purposes of assessing the proposed BETA options, including the ADJ_U* option in AERMET and the LowWind options in AERMOD, the comparisons below are limited to the current default options, i.e., without ADJ_U* and without the LowWind option (labeled as NoADJ and NoLW), and the proposed options of ADJ_U* and LowWind3 (labeled as ADJ and LW3).

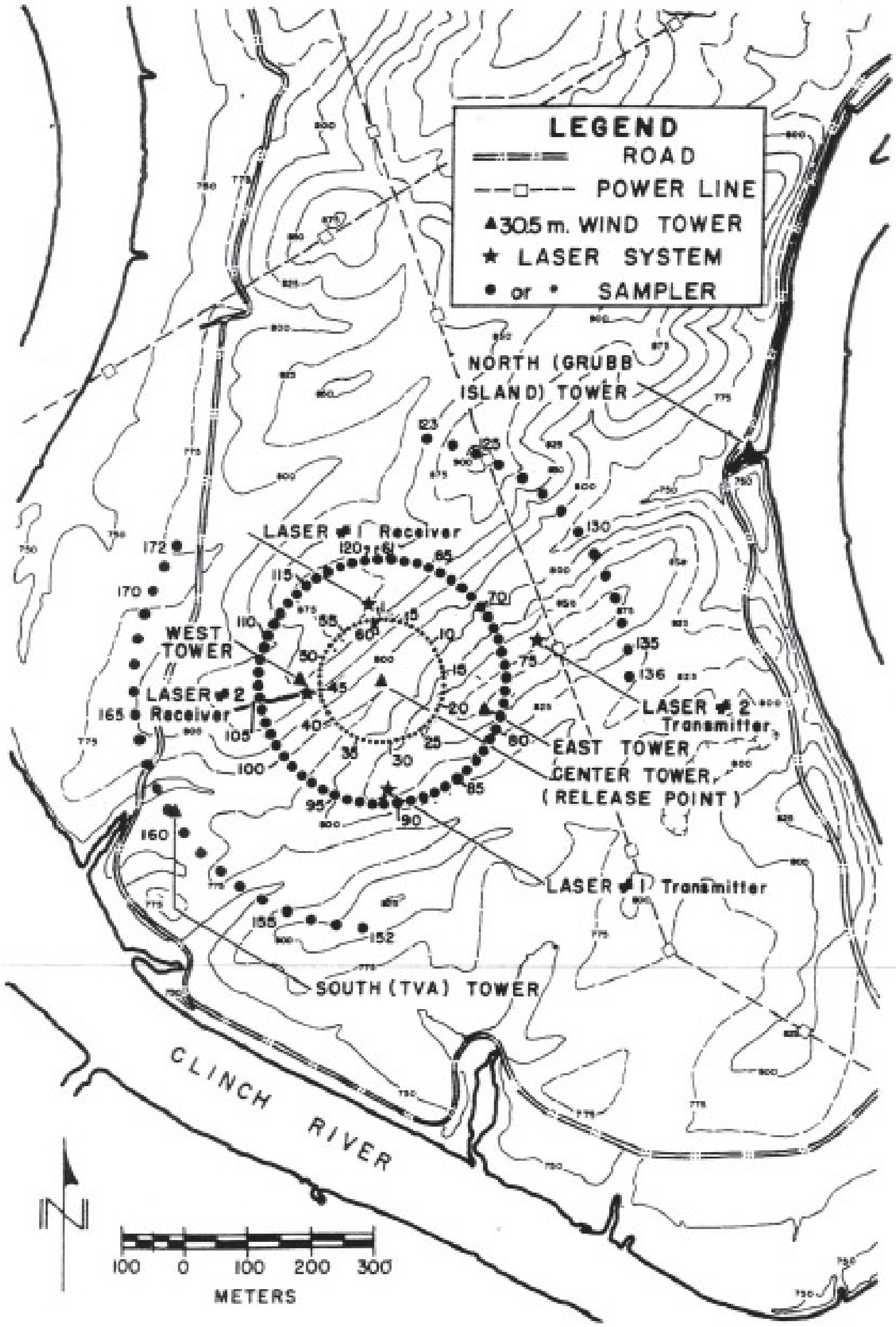

Figure 2b. Detail of inner sampling arcs showing location of meteorological towers and laser transmitters and receivers. (Contour heights are in feet above sea level).

Figure 9-4: Depiction of Sampler Array for Idaho Falls

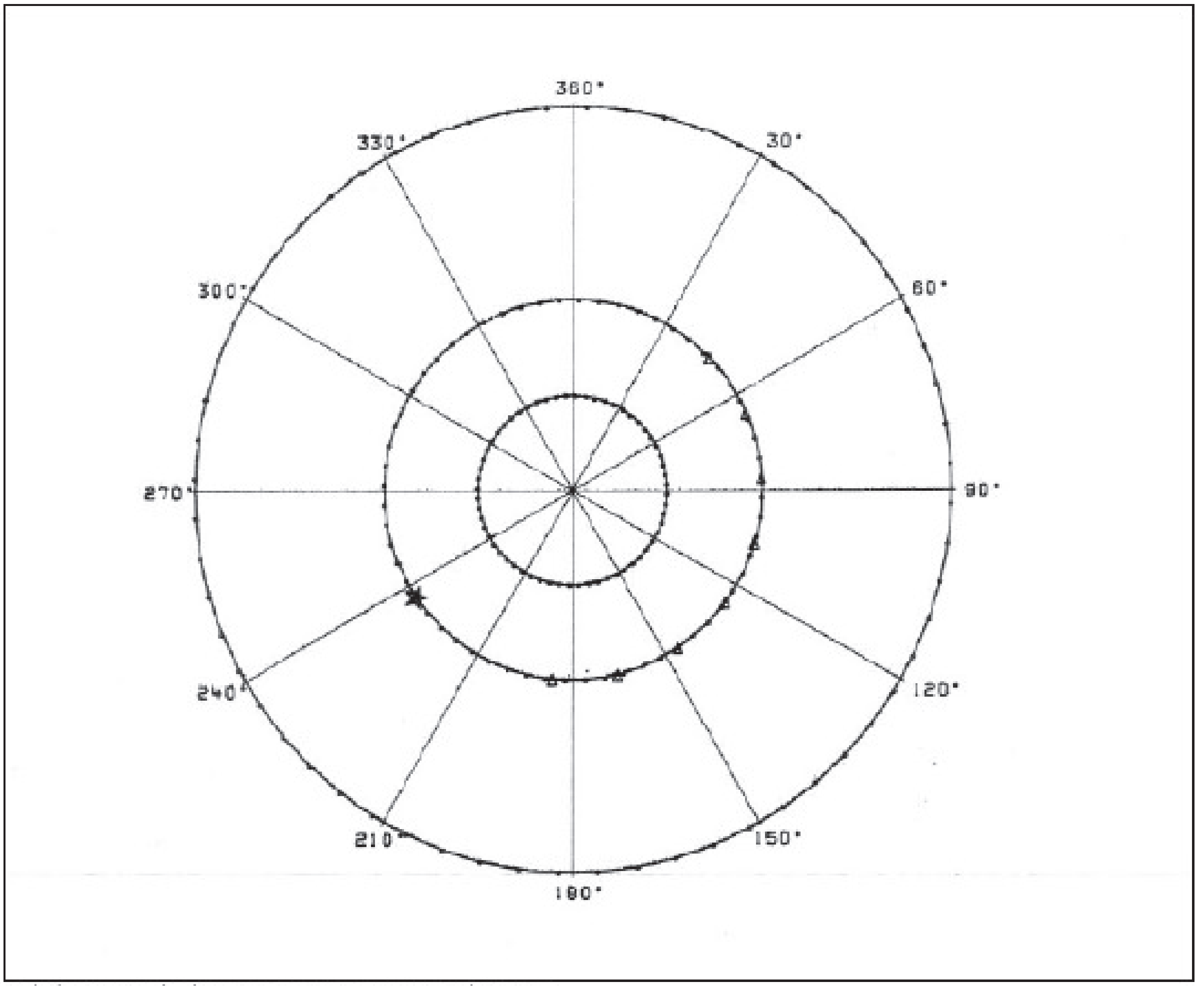

Note: the arcs are at distances of 100, 200, and 400 m from the source.

A series of figures is provided below for each site, starting with the Oak Ridge study followed by the Idaho Falls study. For each site, a series of **Q-Q plots** (i.e., results paired by rank and arc distance), **paired plots** (i.e., results paired in time and arc distance), and **residual plots** (showing the distribution of Pred/Obs ratios by distance) are shown in the following order:

No ADJ_U* / No LowWind Option;
No ADJ_U* / LowWind1 Option;
No ADJ_U* / LowWind2 Option;
No ADJ_U* / LowWind3 Option;
ADJ_U* / No LowWind Option;
ADJ_U* / LowWind1 Option;
ADJ_U* / LowWind2 Option; and
ADJ_U* / LowWind3 Option.

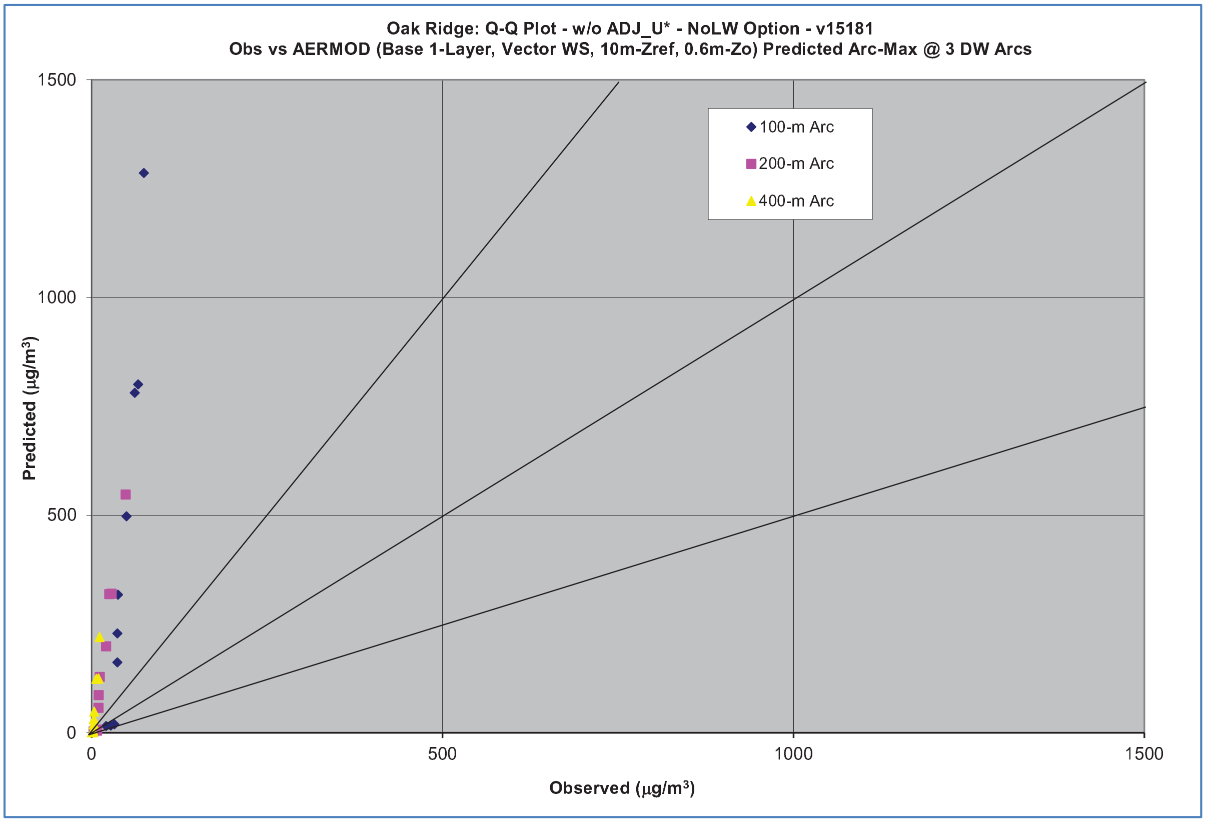
Oak Ridge: Q-Q Plot - w/o ADJ_U* - NoLW Option - v15181
Obs vs AERMOD (Base 1-Layer, Vector WS, 10m-Zref, 0.6m-Zo) Predicted Arc-Max @ 3 DW Arcs
Predicted (µg/m³)
Observed (µg/m³)
0
500
1000
1500
100-m Arc
200-m Arc
400-m Arc

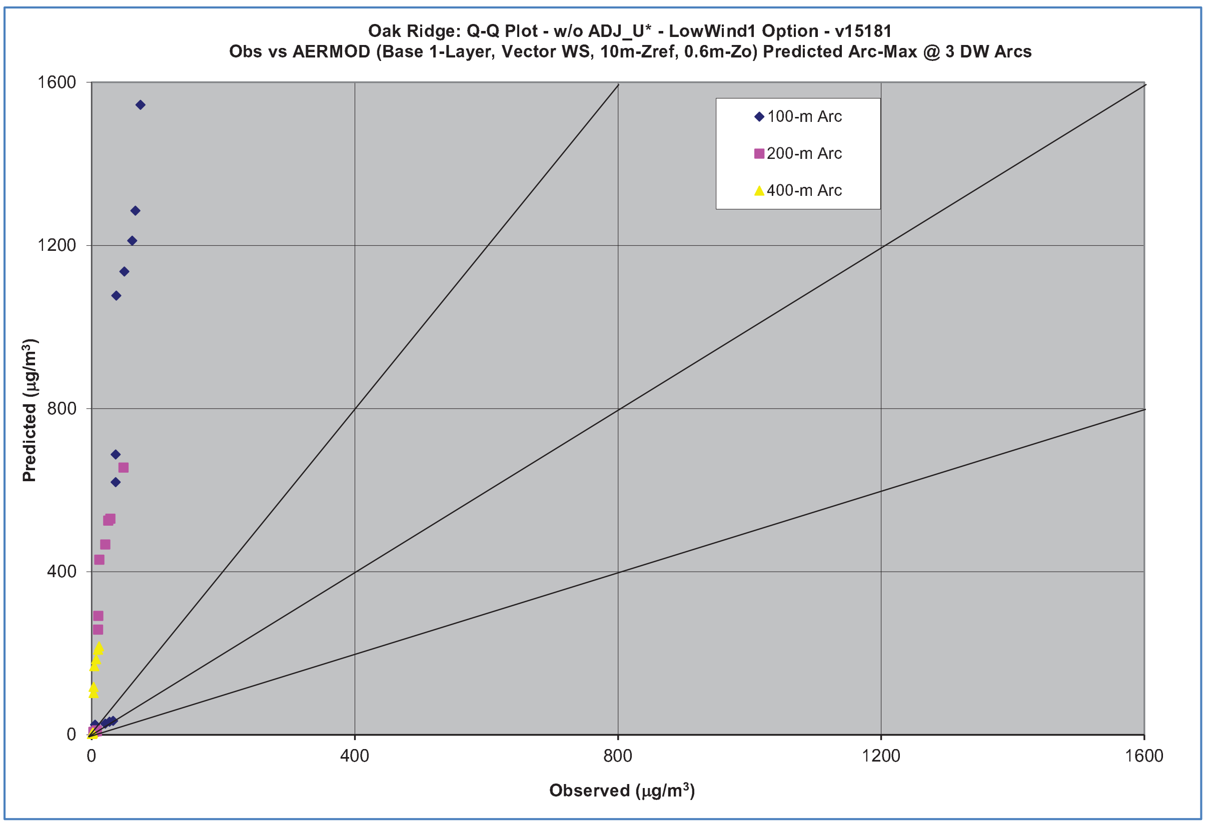
Oak Ridge: Q-Q Plot - w/o ADJ_U* - LowWind1 Option - v15181
Obs vs AERMOD (Base 1-Layer, Vector WS, 10m-Zref, 0.6m-Zo) Predicted Arc-Max @ 3 DW Arcs
Predicted (µg/m³)
Observed (µg/m³)
0
400
800
1200
1600
100-m Arc
200-m Arc
400-m Arc

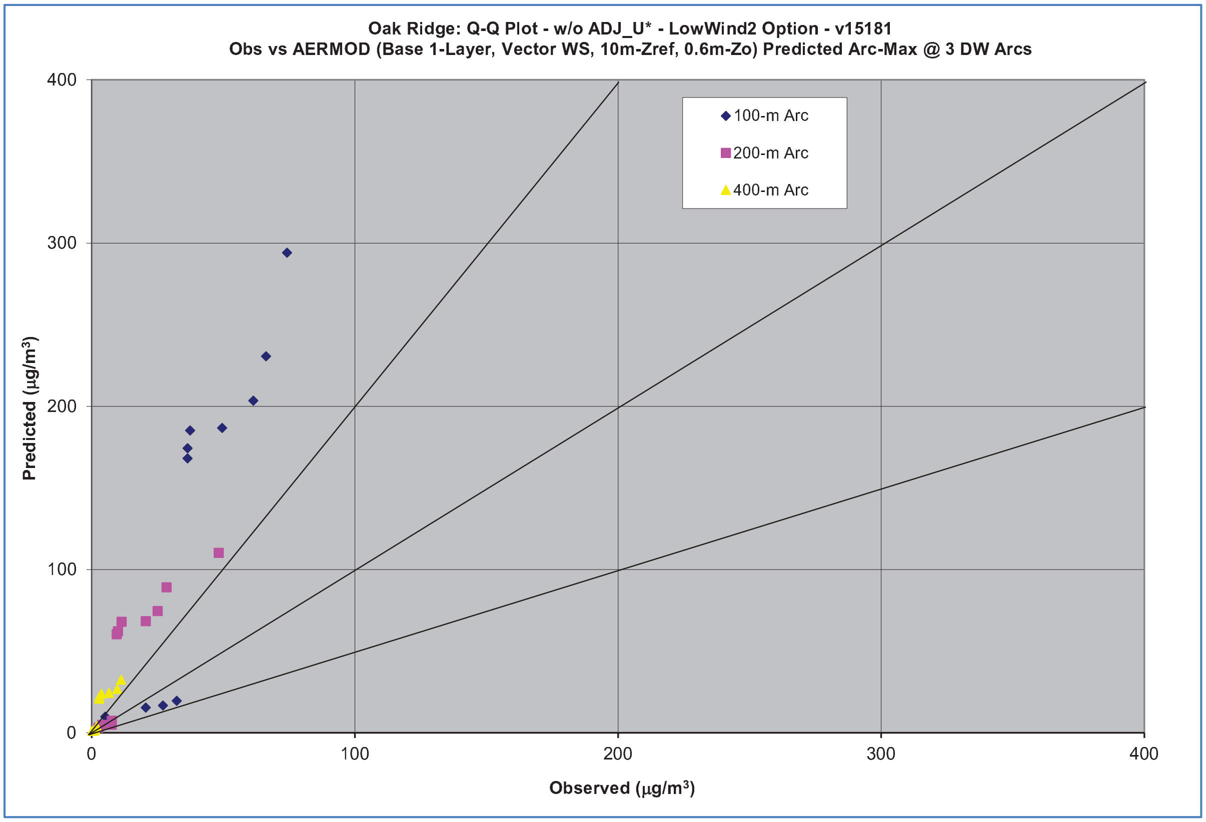
Oak Ridge: Q-Q Plot - w/o ADJ_U* - LowWind2 Option - v15181
Obs vs AERMOD (Base 1-Layer, Vector WS, 10m-Zref, 0.6m-Zo) Predicted Arc-Max @ 3 DW Arcs
100-m Arc
200-m Arc
400-m Arc
Predicted (µg/m³)
Observed (µg/m³)
0
100
200
300
400

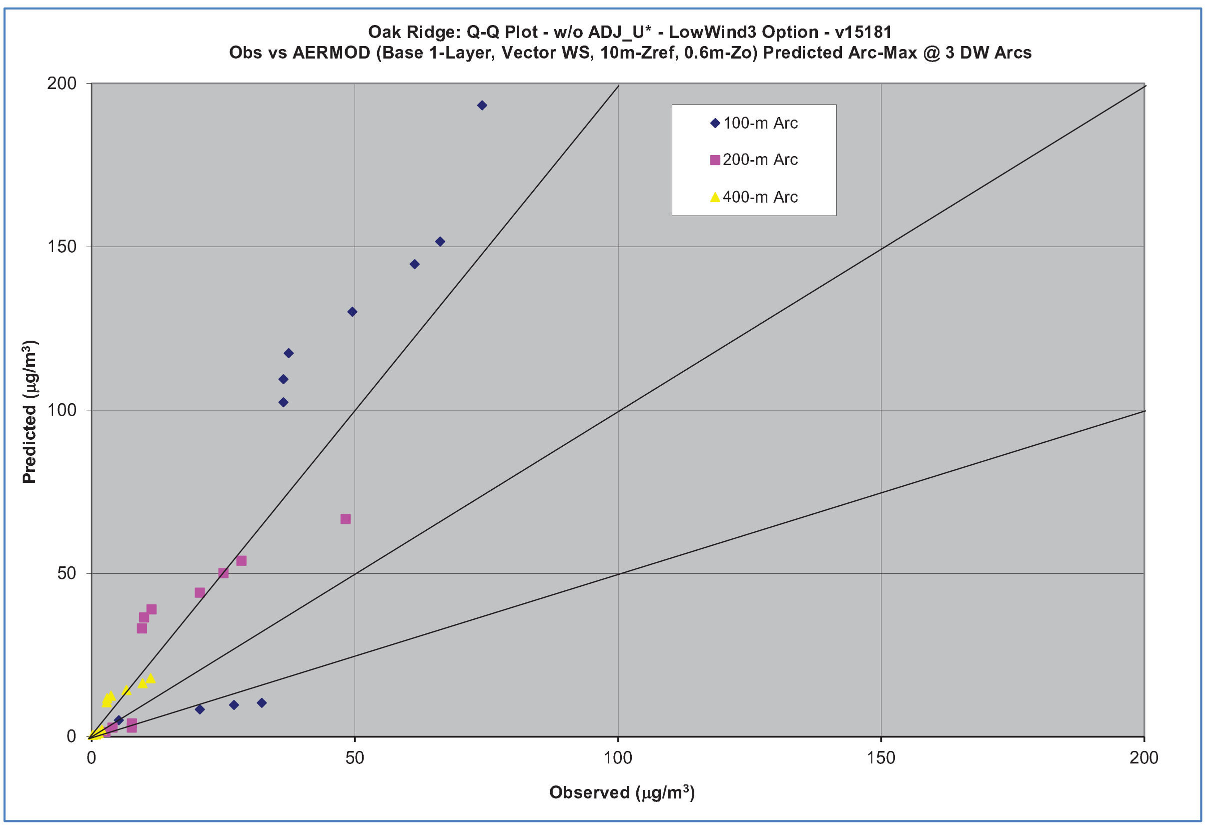
Oak Ridge: Q-Q Plot - w/o ADJ_U* - LowWind3 Option - v15181
Obs vs AERMOD (Base 1-Layer, Vector WS, 10m-Zref, 0.6m-Zo) Predicted Arc-Max @ 3 DW Arcs
100-m Arc
200-m Arc
400-m Arc
Predicted (µg/m³)
Observed (µg/m³)
0
50
100
150
200

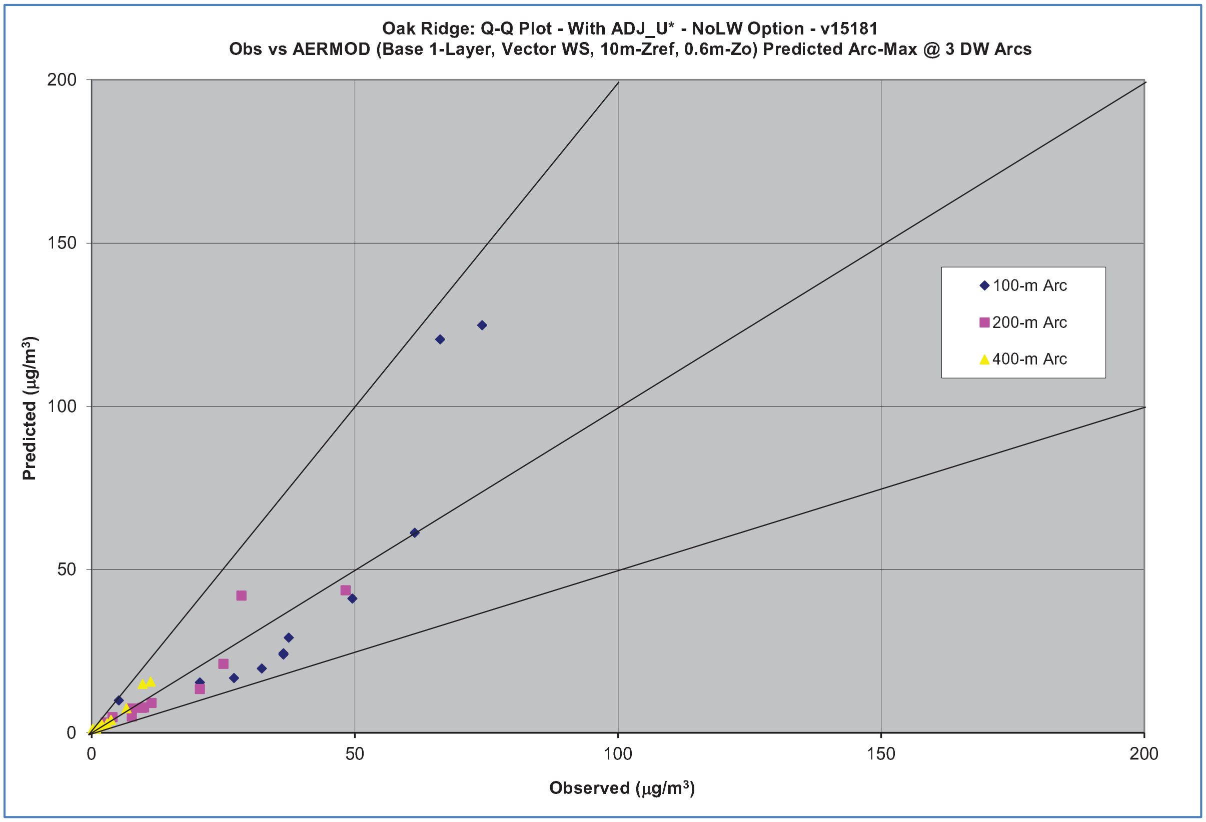
Oak Ridge: Q-Q Plot - With ADJ_U* - NoLW Option - v15181
Obs vs AERMOD (Base 1-Layer, Vector WS, 10m-Zref, 0.6m-Zo) Predicted Arc-Max @ 3 DW Arcs
Predicted (μg/m³)
Observed (μg/m³)
0
50
100
150
200
100-m Arc
200-m Arc
400-m Arc

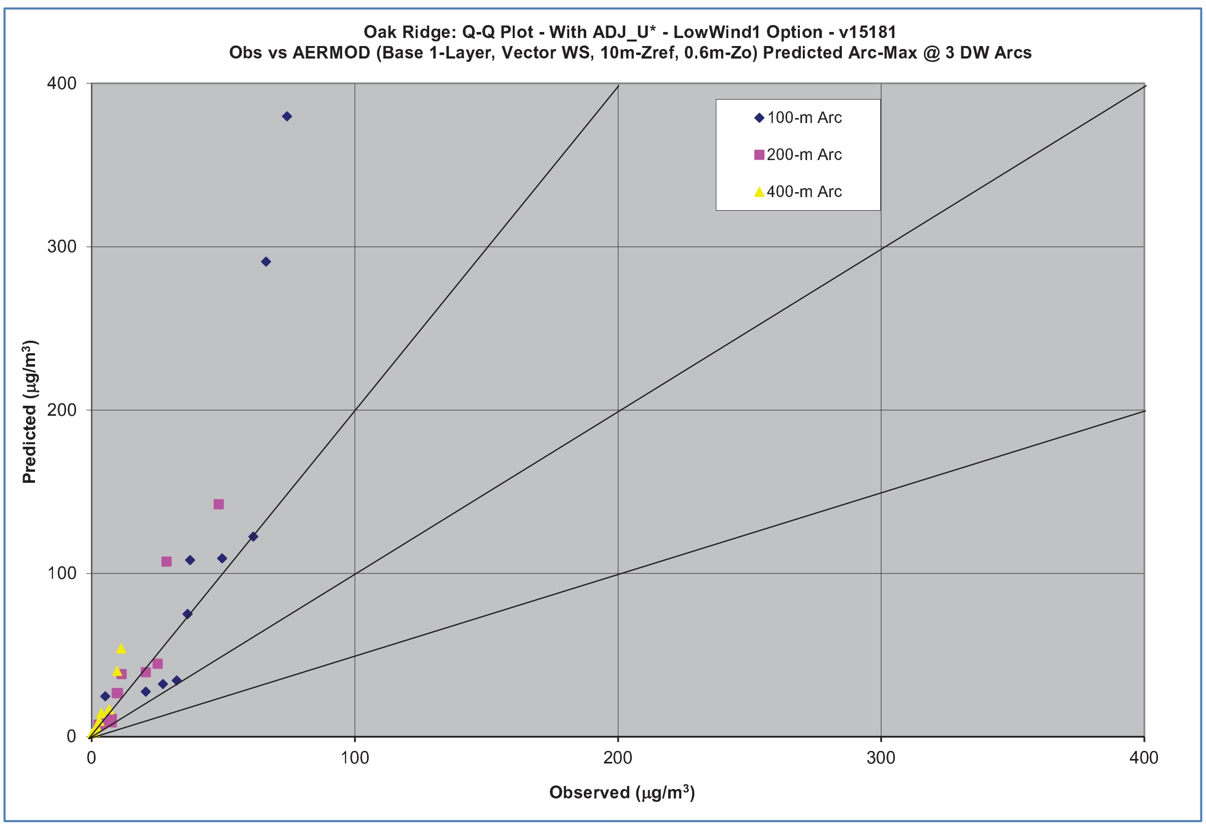
Oak Ridge: Q-Q Plot - With ADJ_U* - LowWind1 Option - v15181
Obs vs AERMOD (Base 1-Layer, Vector WS, 10m-Zref, 0.6m-Zo) Predicted Arc-Max @ 3 DW Arcs
Predicted (μg/m³)
Observed (μg/m³)
0
100
200
300
400
100-m Arc
200-m Arc
400-m Arc

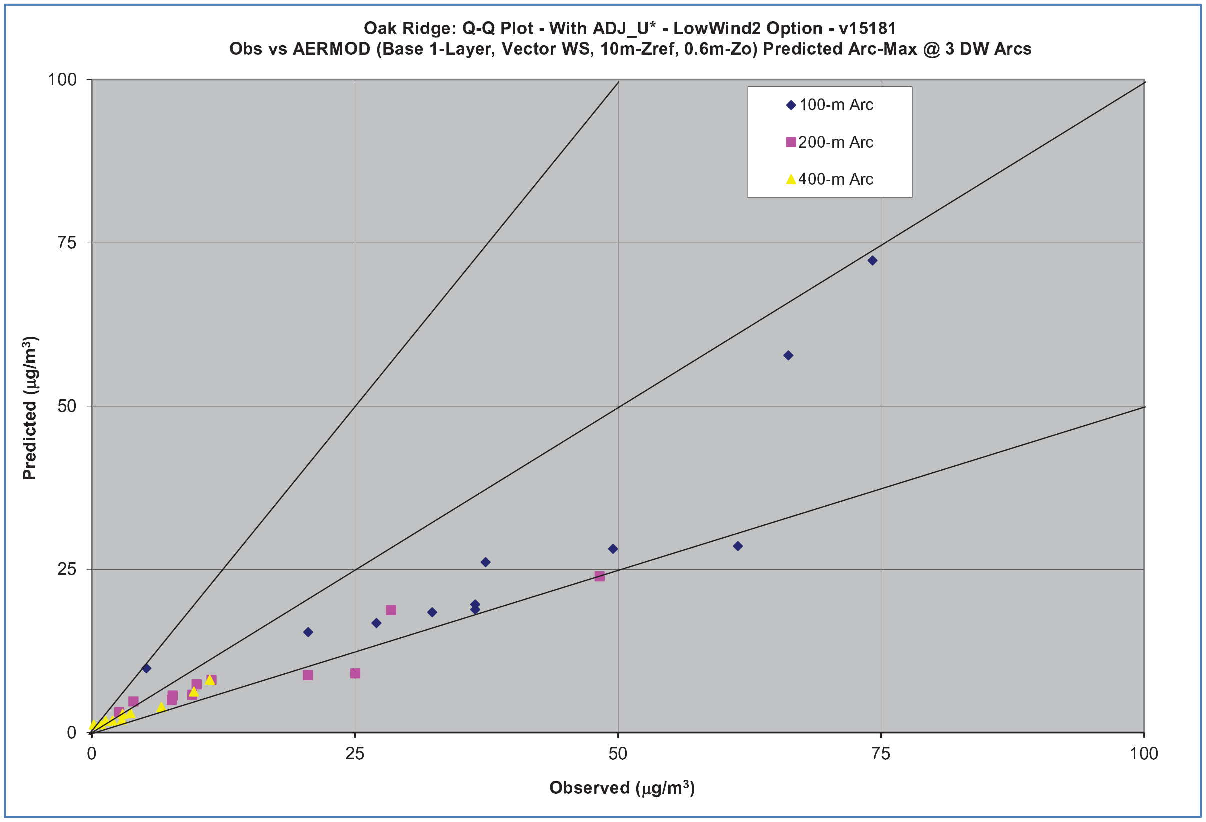
Oak Ridge: Q-Q Plot - With ADJ_U* - LowWind2 Option - v15181
Obs vs AERMOD (Base 1-Layer, Vector WS, 10m-Zref, 0.6m-Zo) Predicted Arc-Max @ 3 DW Arcs
100-m Arc
200-m Arc
400-m Arc
Predicted (µg/m³)
Observed (µg/m³)
0
25
50
75
100

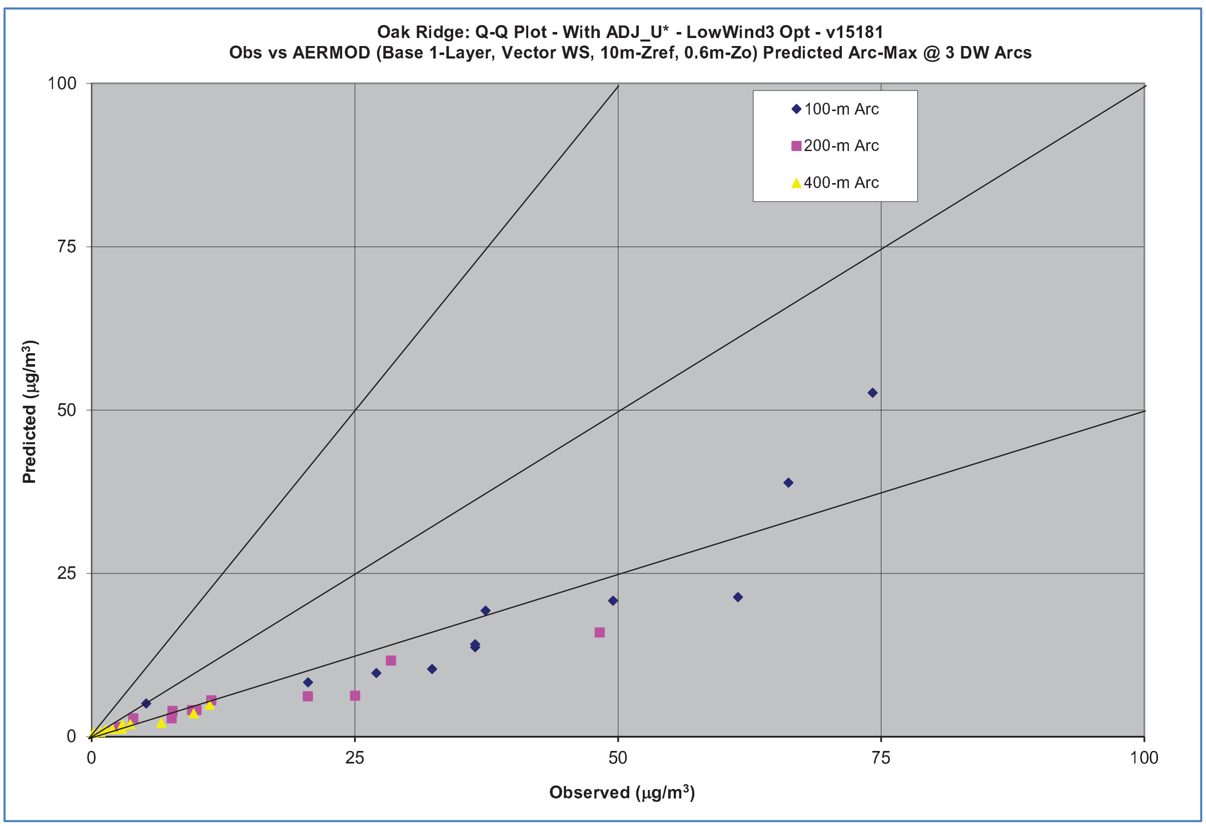
Oak Ridge: Q-Q Plot - With ADJ_U* - LowWind3 Opt - v15181
Obs vs AERMOD (Base 1-Layer, Vector WS, 10m-Zref, 0.6m-Zo) Predicted Arc-Max @ 3 DW Arcs
100-m Arc
200-m Arc
400-m Arc
Predicted (µg/m³)
Observed (µg/m³)
0
25
50
75
100

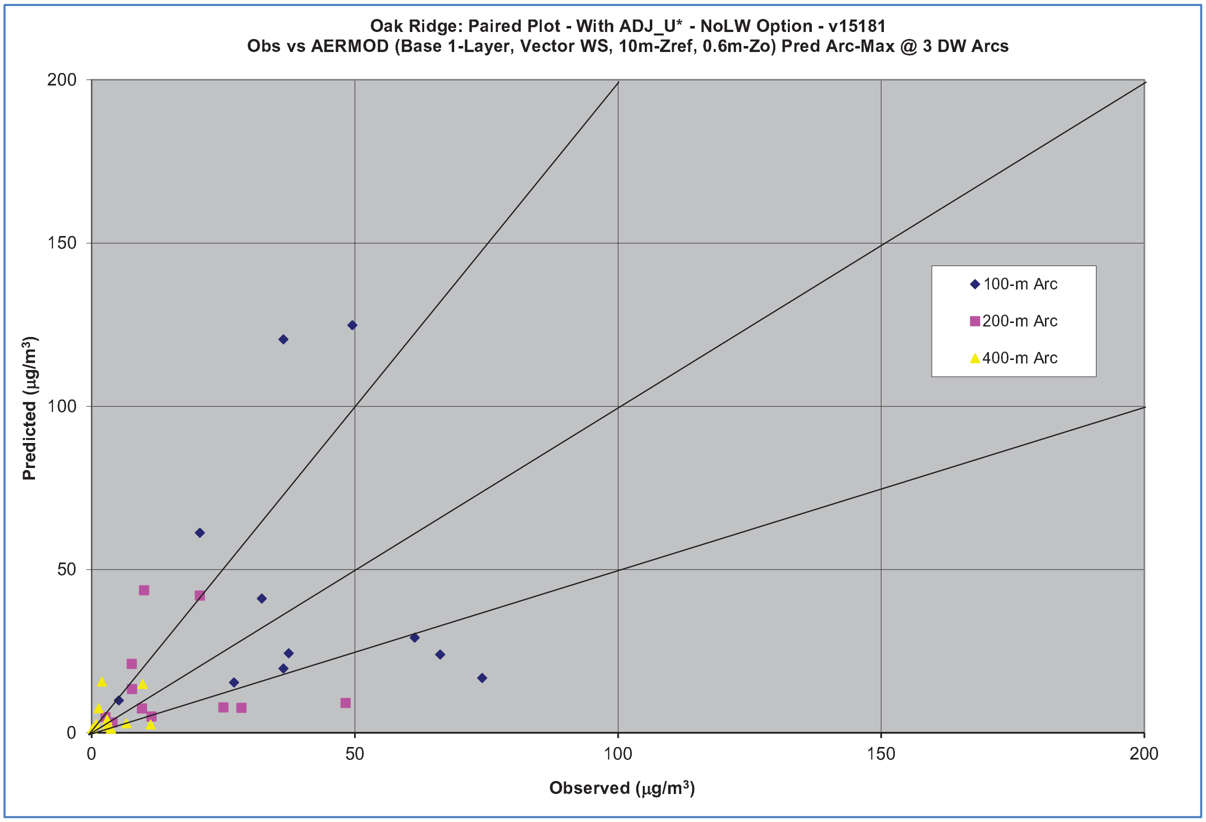
Oak Ridge: Paired Plot - With ADJ_U* - NoLW Option - v15181
Obs vs AERMOD (Base 1-Layer, Vector WS, 10m-Zref, 0.6m-Zo) Pred Arc-Max @ 3 DW Arcs
Predicted (µg/m³)
Observed (µg/m³)
0
50
100
150
200
100-m Arc
200-m Arc
400-m Arc

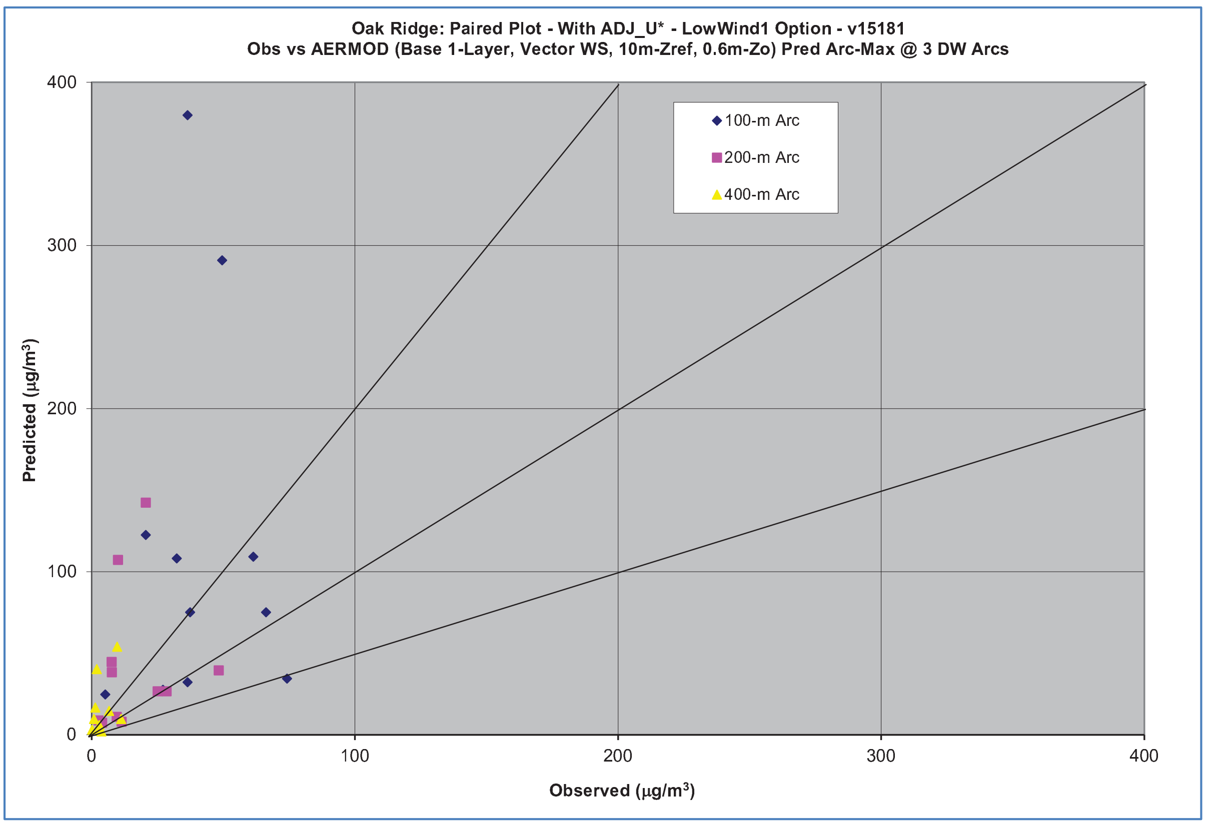
Oak Ridge: Paired Plot - With ADJ_U* - LowWind1 Option - v15181
Obs vs AERMOD (Base 1-Layer, Vector WS, 10m-Zref, 0.6m-Zo) Pred Arc-Max @ 3 DW Arcs
Predicted (µg/m³)
Observed (µg/m³)
0
100
200
300
400
100-m Arc
200-m Arc
400-m Arc

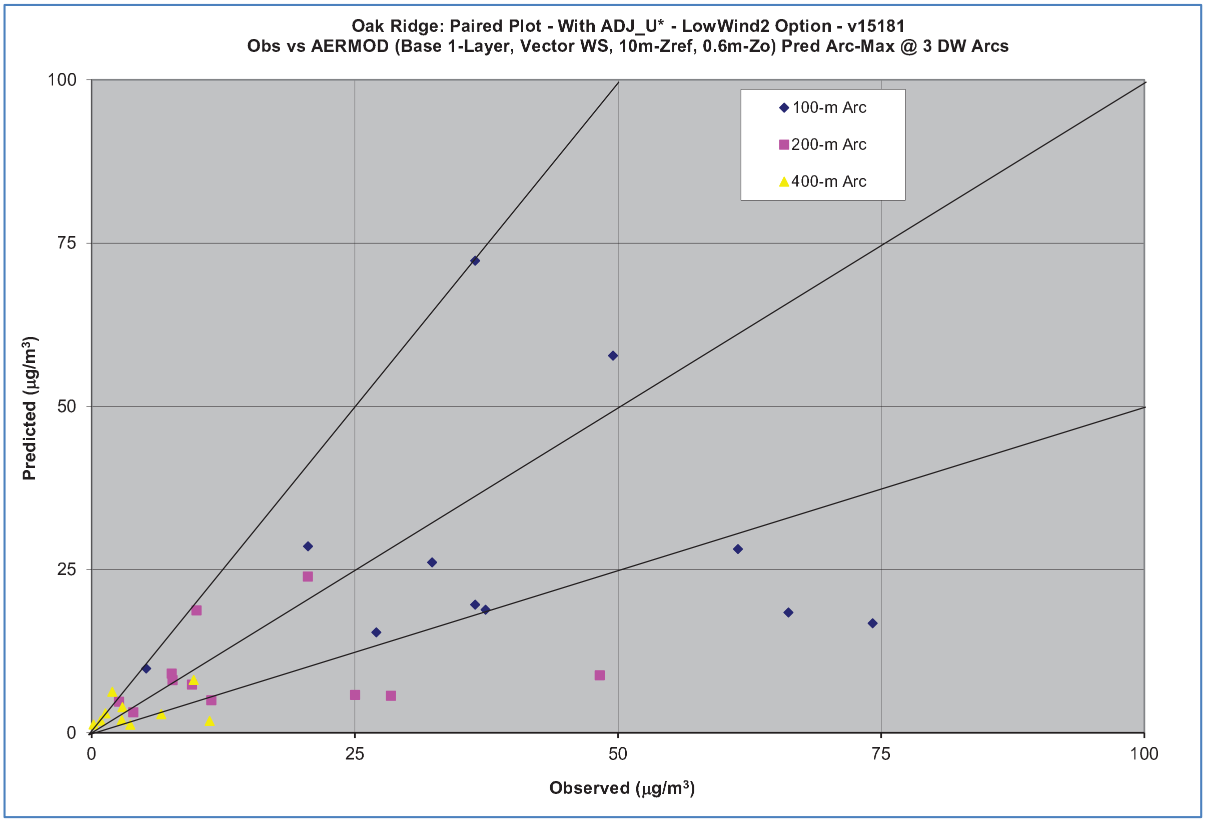
Oak Ridge: Paired Plot - With ADJ_U* - LowWind2 Option - v15181
Obs vs AERMOD (Base 1-Layer, Vector WS, 10m-Zref, 0.6m-Zo) Pred Arc-Max @ 3 DW Arcs
100-m Arc
200-m Arc
400-m Arc
Predicted (µg/m³)
Observed (µg/m³)
0
25
50
75
100

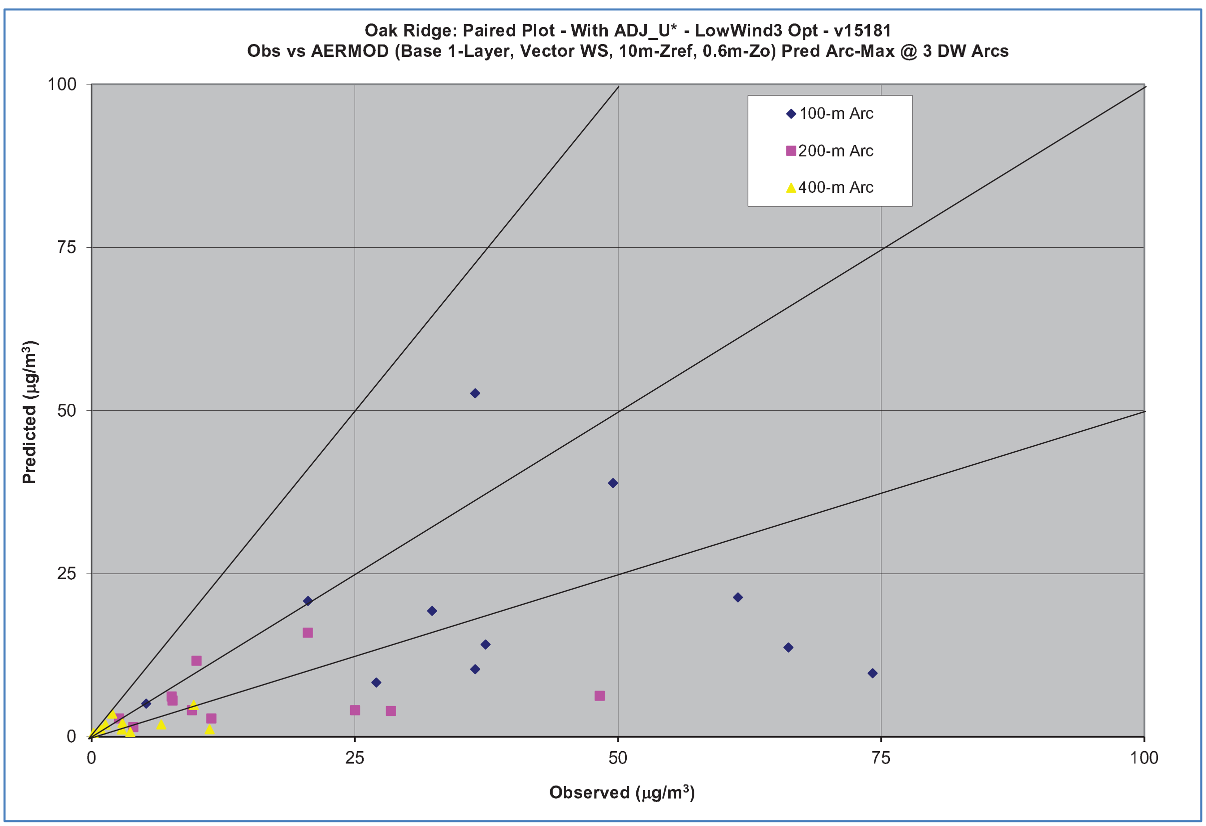
Oak Ridge: Paired Plot - With ADJ_U* - LowWind3 Opt - v15181
Obs vs AERMOD (Base 1-Layer, Vector WS, 10m-Zref, 0.6m-Zo) Pred Arc-Max @ 3 DW Arcs
100-m Arc
200-m Arc
400-m Arc
Predicted (µg/m³)
Observed (µg/m³)
0
25
50
75
100

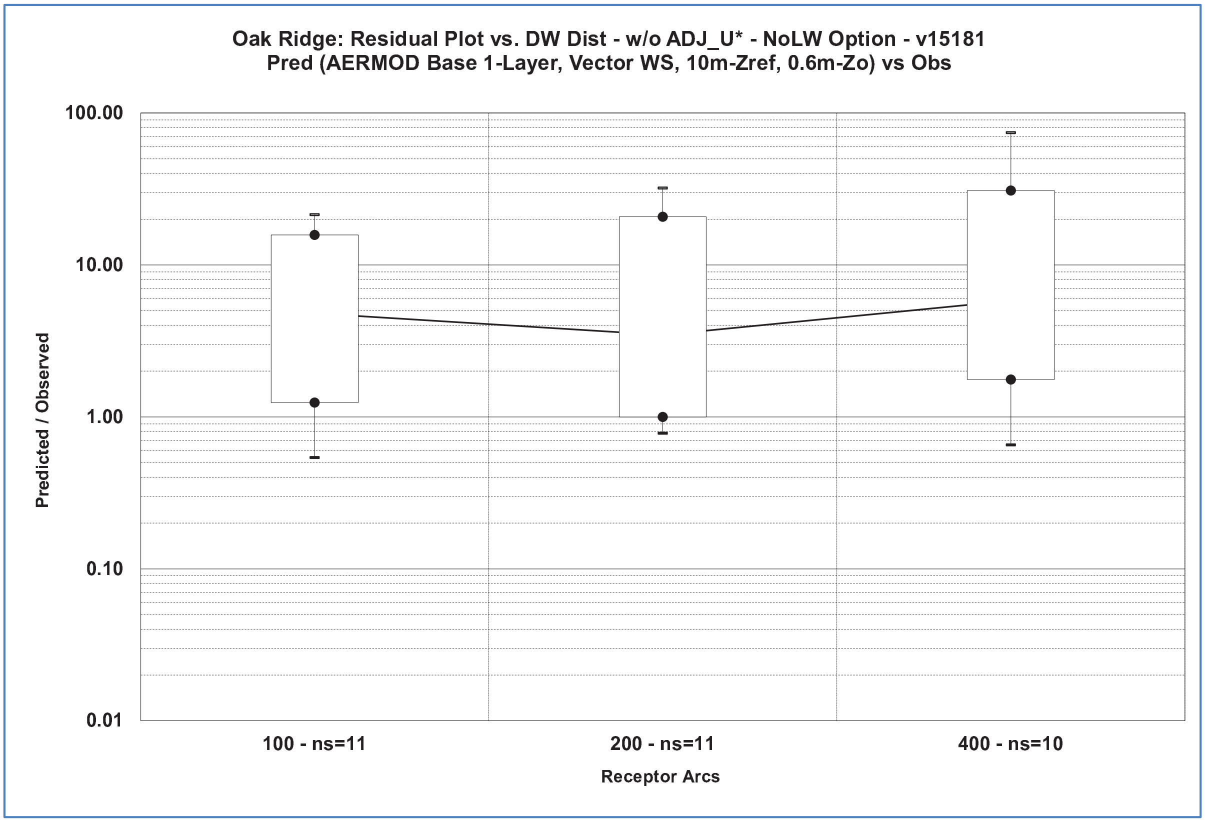
Oak Ridge: Residual Plot vs. DW Dist - w/o ADJ_U* - NoLW Option - v15181
Pred (AERMOD Base 1-Layer, Vector WS, 10m-Zref, 0.6m-Zo) vs Obs
Predicted / Observed
100.00
10.00
1.00
0.10
0.01
100 - ns=11
200 - ns=11
400 - ns=10
Receptor Arcs

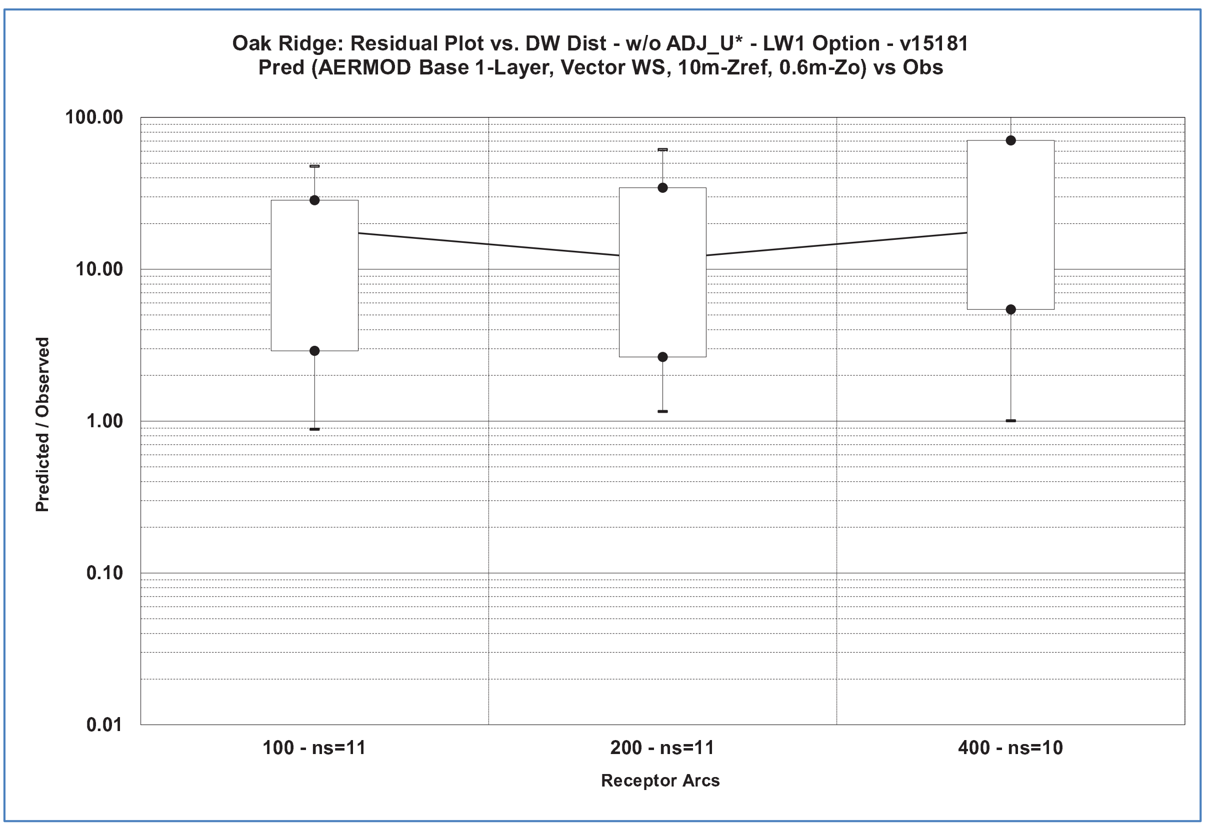
Oak Ridge: Residual Plot vs. DW Dist - w/o ADJ_U* - LW1 Option - v15181
Pred (AERMOD Base 1-Layer, Vector WS, 10m-Zref, 0.6m-Zo) vs Obs
Predicted / Observed
100.00
10.00
1.00
0.10
0.01
100 - ns=11
200 - ns=11
400 - ns=10
Receptor Arcs

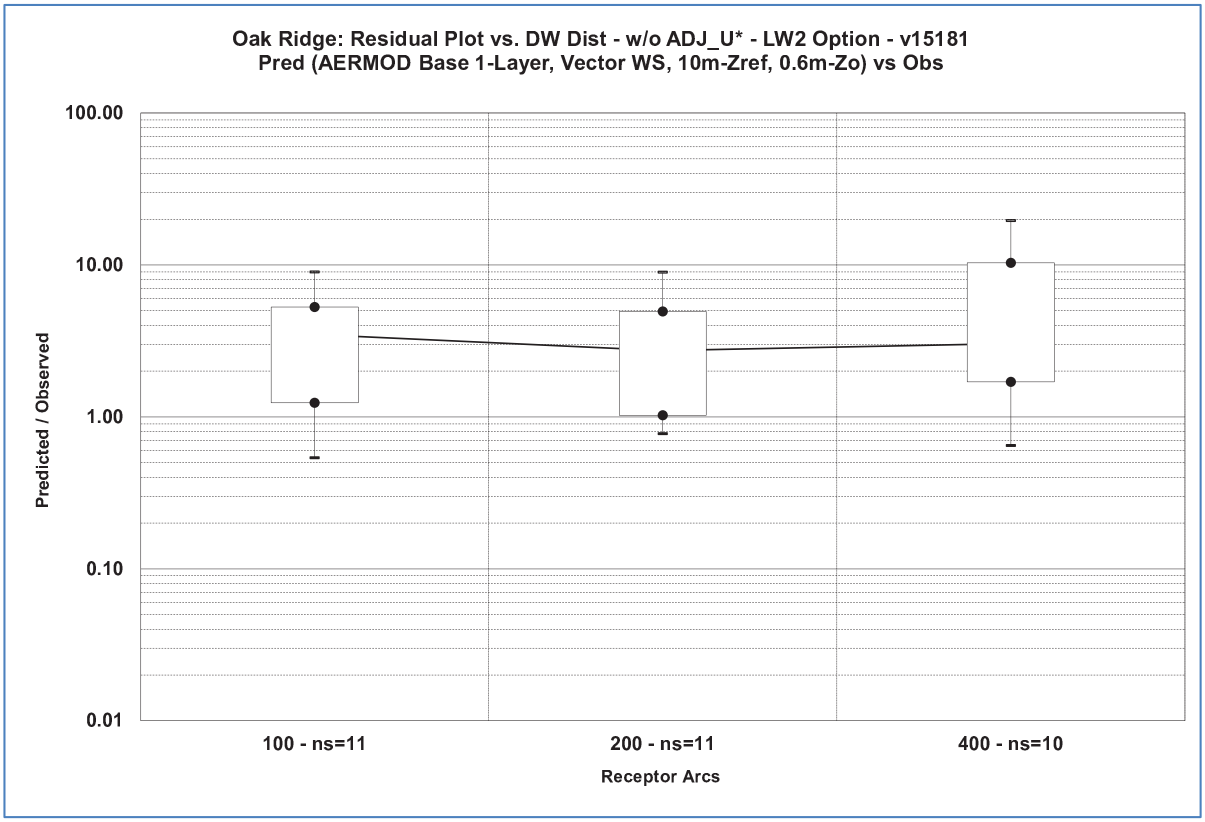
Oak Ridge: Residual Plot vs. DW Dist - w/o ADJ_U* - LW2 Option - v15181
Pred (AERMOD Base 1-Layer, Vector WS, 10m-Zref, 0.6m-Zo) vs Obs
100.00
10.00
1.00
0.10
0.01
Predicted / Observed
100 - ns=11
200 - ns=11
400 - ns=10
Receptor Arcs

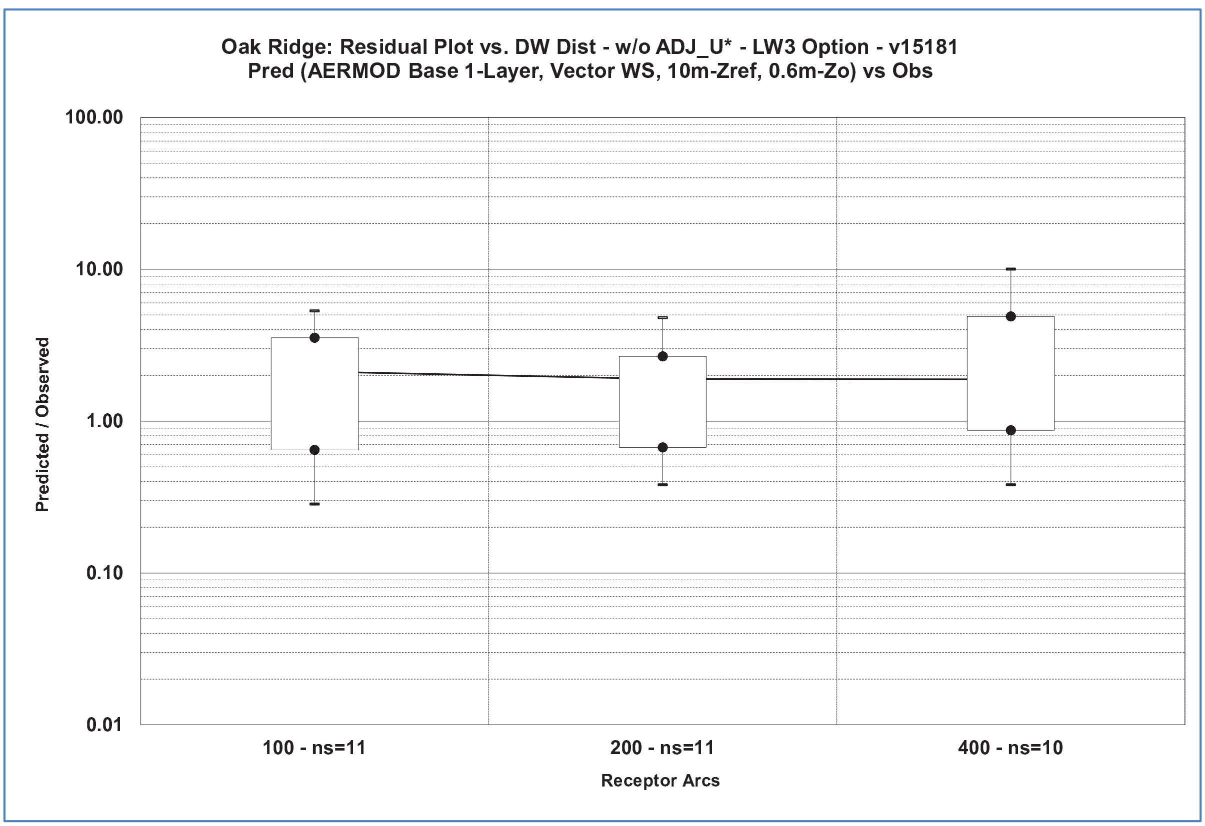
Oak Ridge: Residual Plot vs. DW Dist - w/o ADJ_U* - LW3 Option - v15181
Pred (AERMOD Base 1-Layer, Vector WS, 10m-Zref, 0.6m-Zo) vs Obs
100.00
10.00
1.00
0.10
0.01
Predicted / Observed
100 - ns=11
200 - ns=11
400 - ns=10
Receptor Arcs

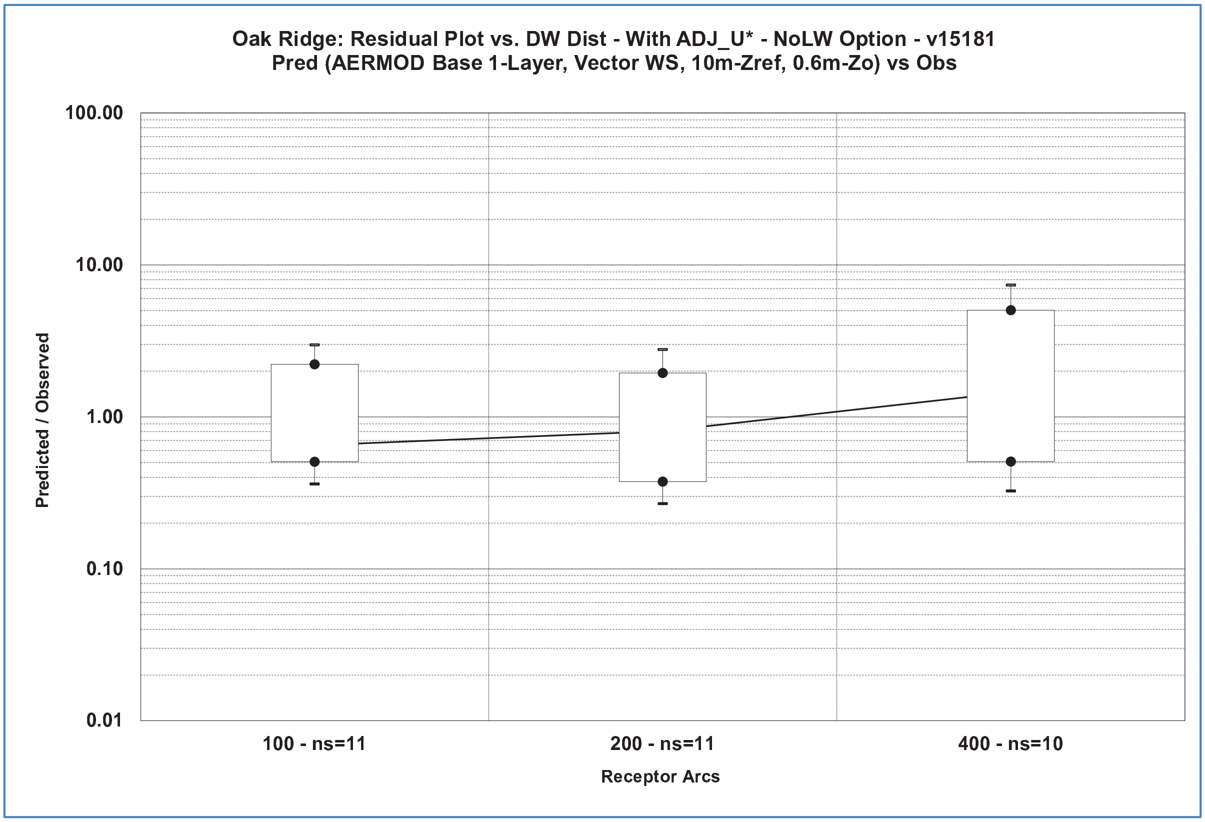

Oak Ridge: Residual Plot vs. DW Dist - With ADJ_U* - NoLW Option - v15181
Pred (AERMOD Base 1-Layer, Vector WS, 10m-Zref, 0.6m-Zo) vs Obs
100.00
10.00
1.00
0.10
0.01
Predicted / Observed
100 - ns=11
200 - ns=11
400 - ns=10
Receptor Arcs

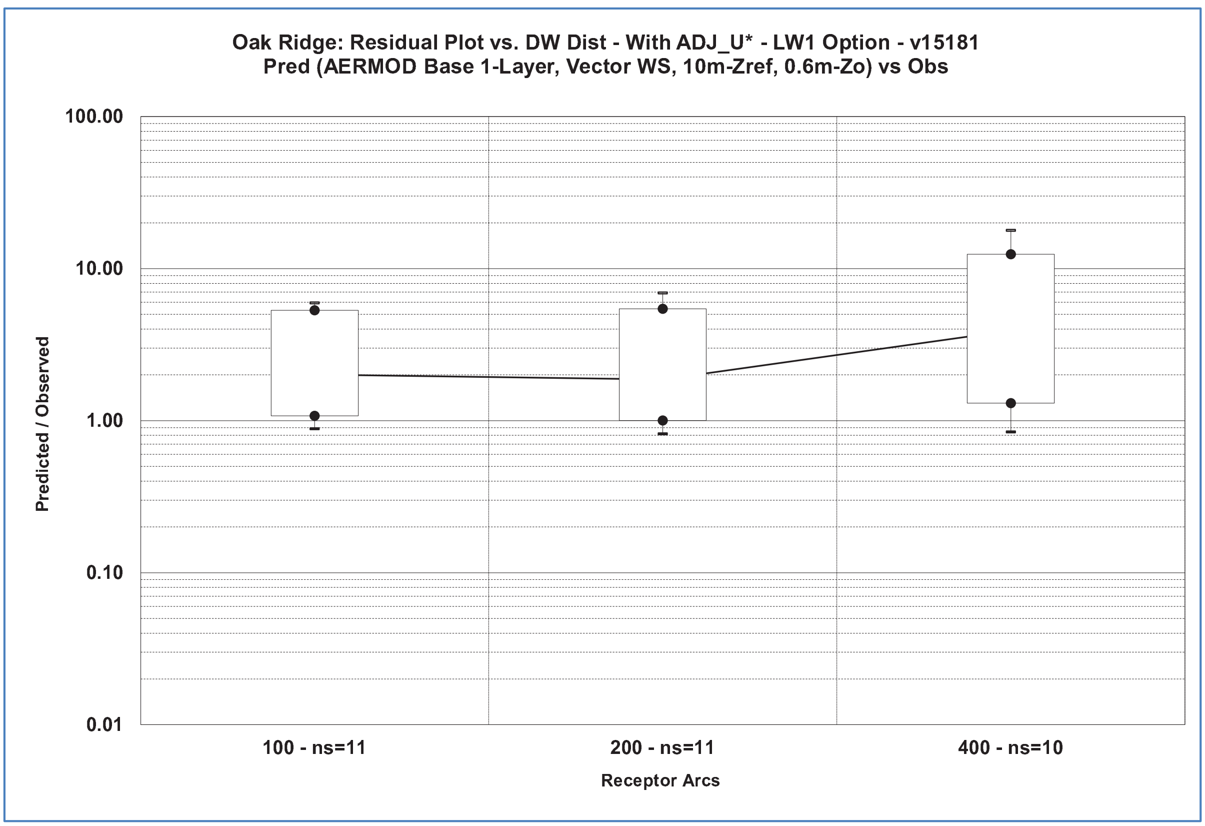

Oak Ridge: Residual Plot vs. DW Dist - With ADJ_U* - LW1 Option - v15181
Pred (AERMOD Base 1-Layer, Vector WS, 10m-Zref, 0.6m-Zo) vs Obs
100.00
10.00
1.00
0.10
0.01
Predicted / Observed
100 - ns=11
200 - ns=11
400 - ns=10
Receptor Arcs

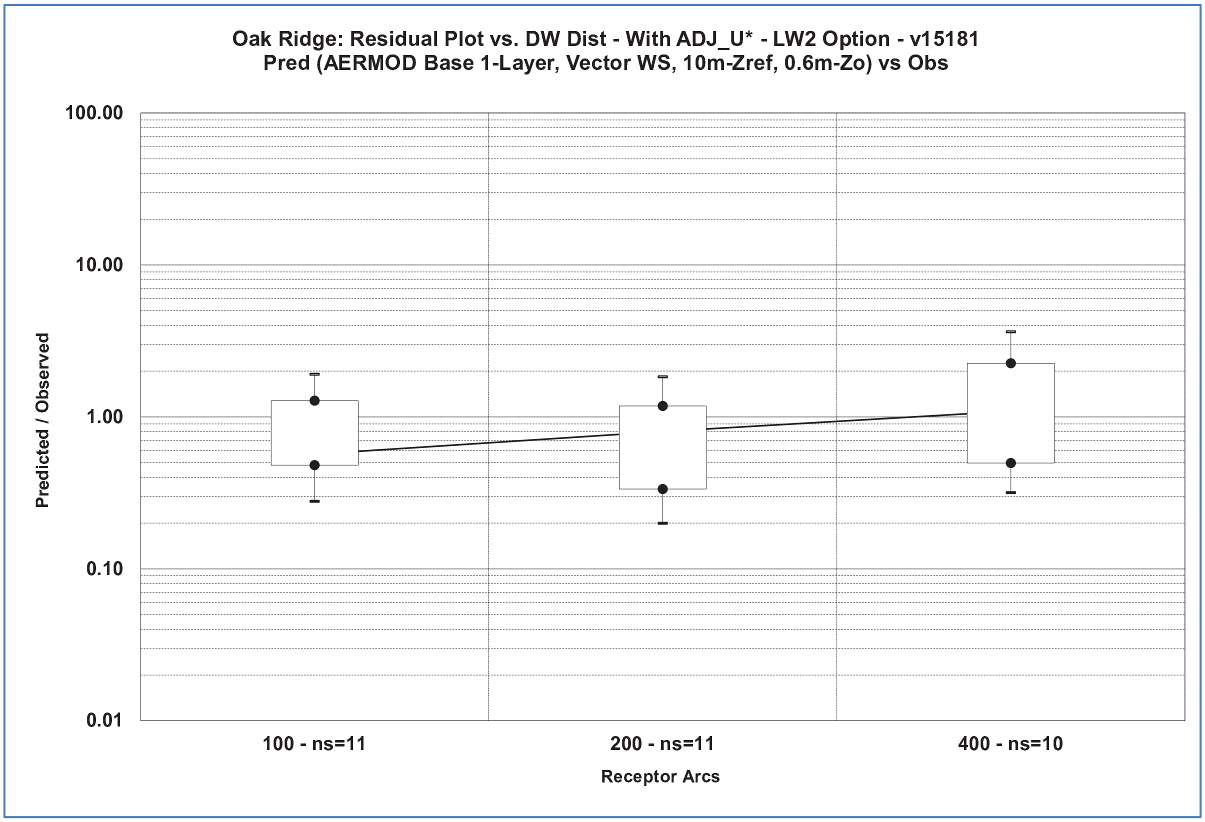
Oak Ridge: Residual Plot vs. DW Dist - With ADJ_U* - LW2 Option - v15181
Pred (AERMOD Base 1-Layer, Vector WS, 10m-Zref, 0.6m-Zo) vs Obs
100.00
10.00
1.00
0.10
0.01
Predicted / Observed
100 - ns=11
200 - ns=11
400 - ns=10
Receptor Arcs

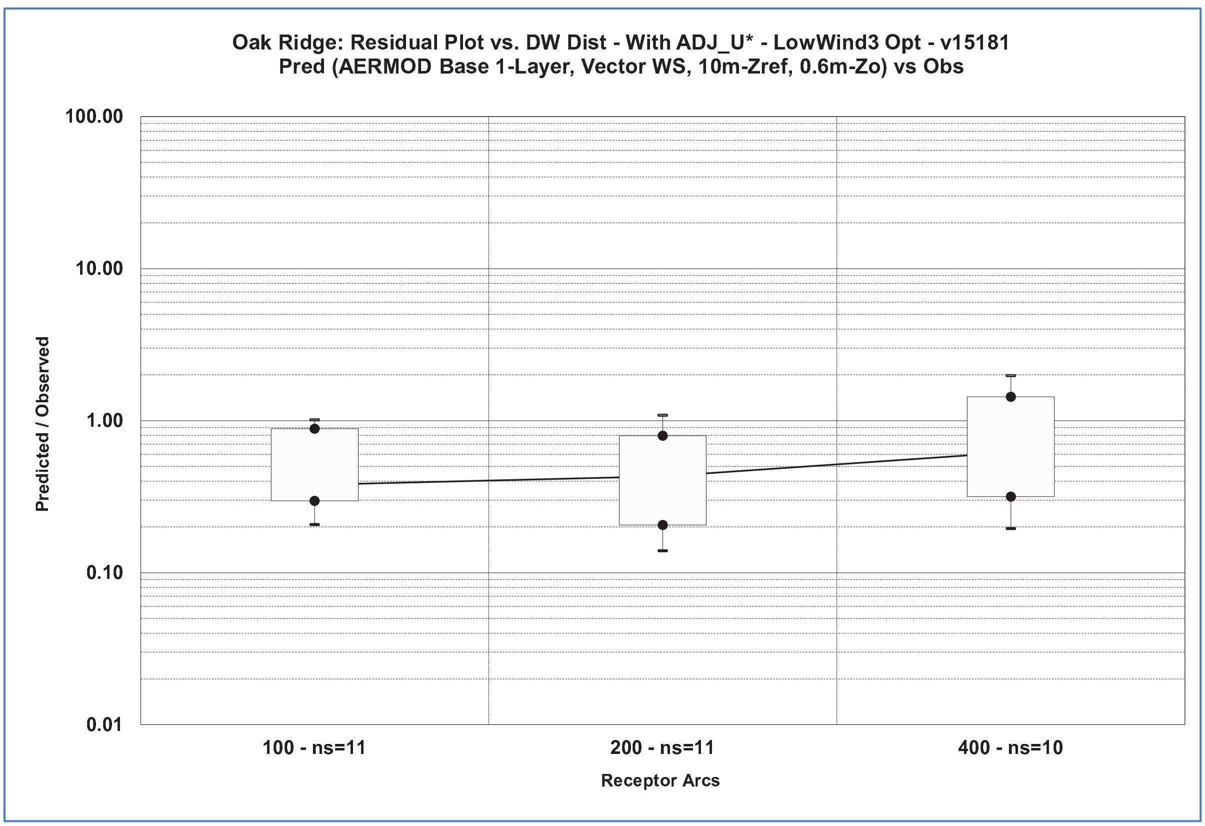
Oak Ridge: Residual Plot vs. DW Dist - With ADJ_U* - LowWind3 Opt - v15181
Pred (AERMOD Base 1-Layer, Vector WS, 10m-Zref, 0.6m-Zo) vs Obs
100.00
10.00
1.00
0.10
0.01
Predicted / Observed
100 - ns=11
200 - ns=11
400 - ns=10
Receptor Arcs

The figures shown above for the Oak Ridge field study show significant overprediction with the current default options in AERMET and AERMOD. The LowWind2 and LowWind3 options without the ADJ_U* option exhibit much better performance, with LowWind3 showing the best results, but both options still show significant overpredictions. The LowWind1 option actually degrades model performance relative to the default options. These figures also show significant improvement in model performance with the ADJ_U* option in AERMET with and without the LowWind options. The LowWind2 option with ADJ_U* appears to show the best overall performance, with the LownWind3/ADJ_U* option showing some bias toward underprediction. However, as noted above, the evaluation results presented here do not account for the potential influence of terrain on modeled concentrations. Given the potential for valley channeling and drainage flows one might expect modeling results based on an assumption of flat terrain to underestimate concentrations for this study. Figure 7 from the NOAA Technical Memorandum shows horizontal isopleths of concentrations for Test #6 which appears to be stretched along the axis of the valley where the tracer was released. A similar pattern shows up with other tests.

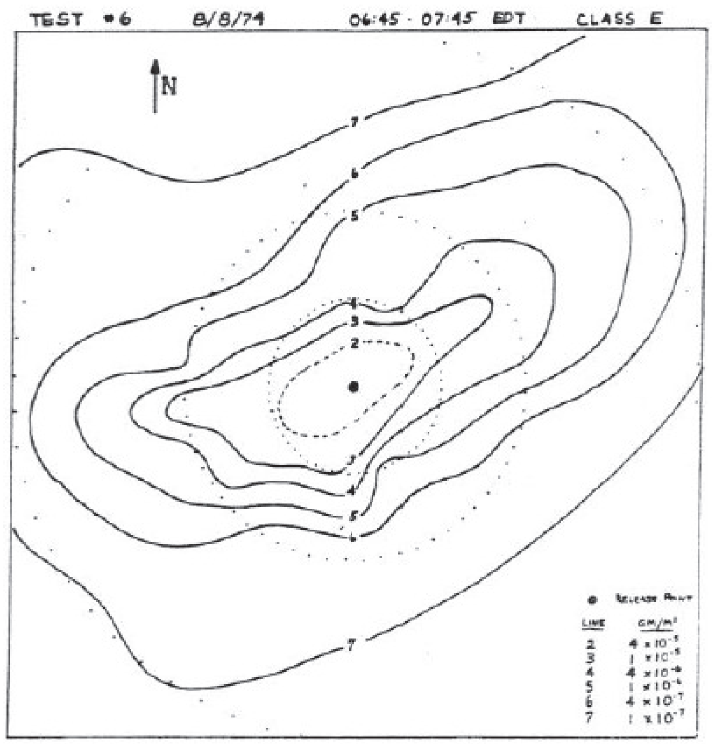

Figure 7. Horizontal isopleths of concentration for test 6 showing the typical 360° spread of gaseous tracer.

The next series of figures shows evaluation results for Idaho Falls based on the degraded 1-layer meteorological data (i.e., no delta-T data for the BULKRN option and no sigma-theta data, starting with the DFAULT option (without ADJ_U* and NoLW), followed by the LowWind1, LowWind2, and LowWind3 option, followed by the results with the ADJ_U* option.

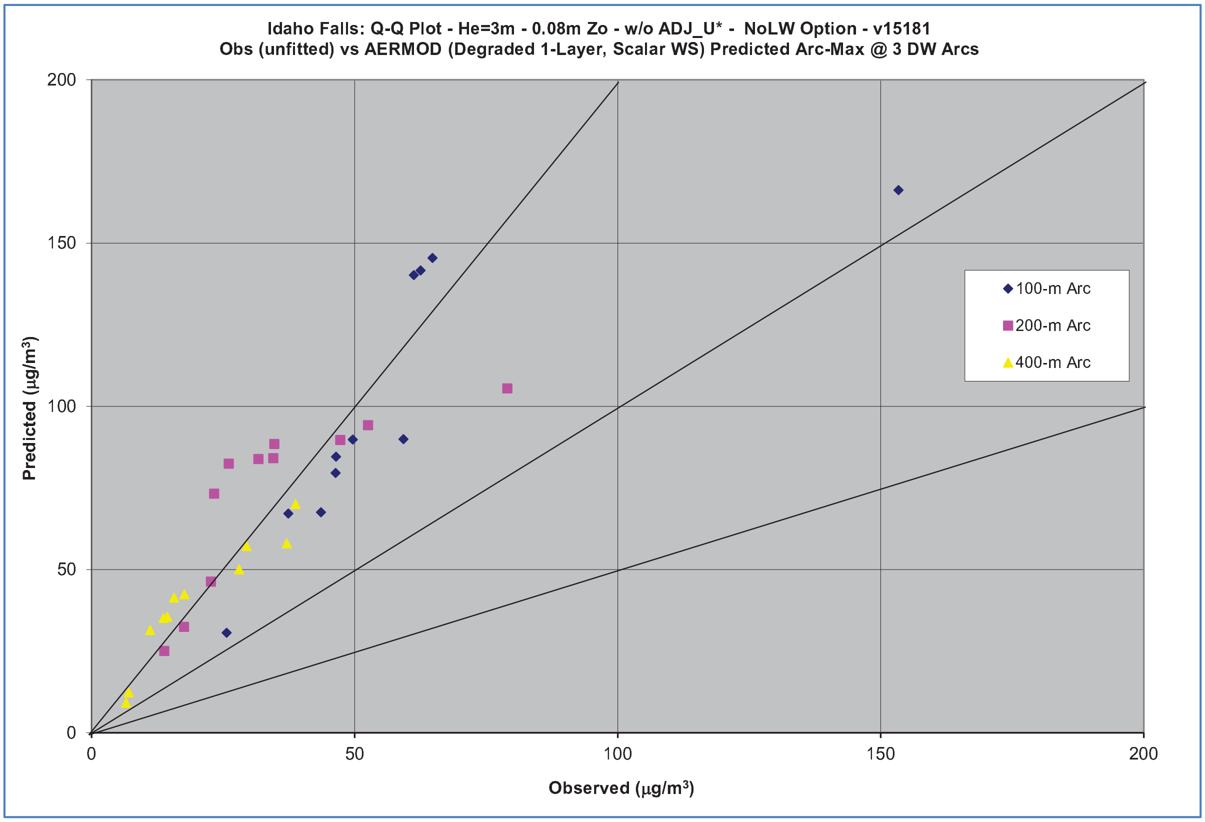
Idaho Falls: Q-Q Plot - He=3m - 0.08m Zo - w/o ADJ_U* - NoLW Option - v15181
Obs (unfitted) vs AERMOD (Degraded 1-Layer, Scalar WS) Predicted Arc-Max @ 3 DW Arcs
Predicted (µg/m³)
Observed (µg/m³)
0
50
100
150
200
100-m Arc
200-m Arc
400-m Arc

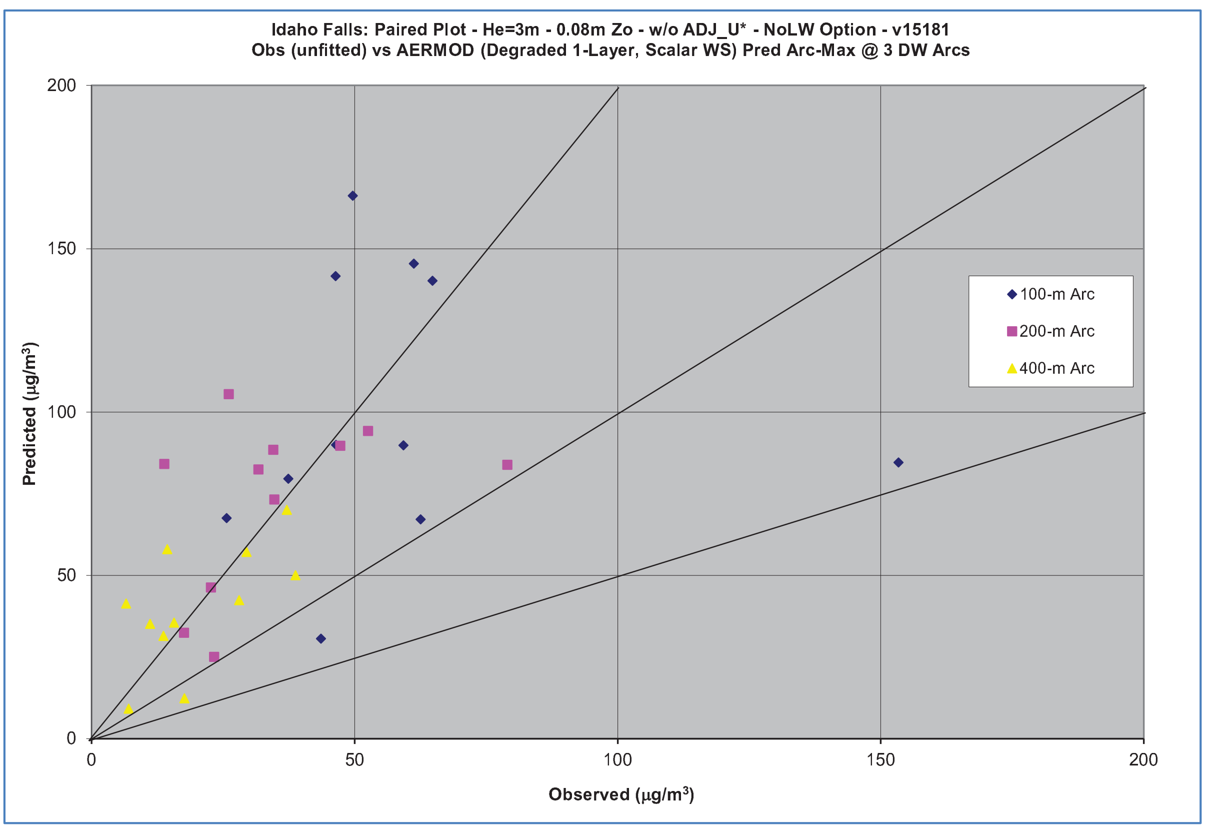
Idaho Falls: Paired Plot - He=3m - 0.08m Zo - w/o ADJ_U* - NoLW Option - v15181
Obs (unfitted) vs AERMOD (Degraded 1-Layer, Scalar WS) Pred Arc-Max @ 3 DW Arcs
Predicted (µg/m³)
Observed (µg/m³)
0
50
100
150
200
100-m Arc
200-m Arc
400-m Arc

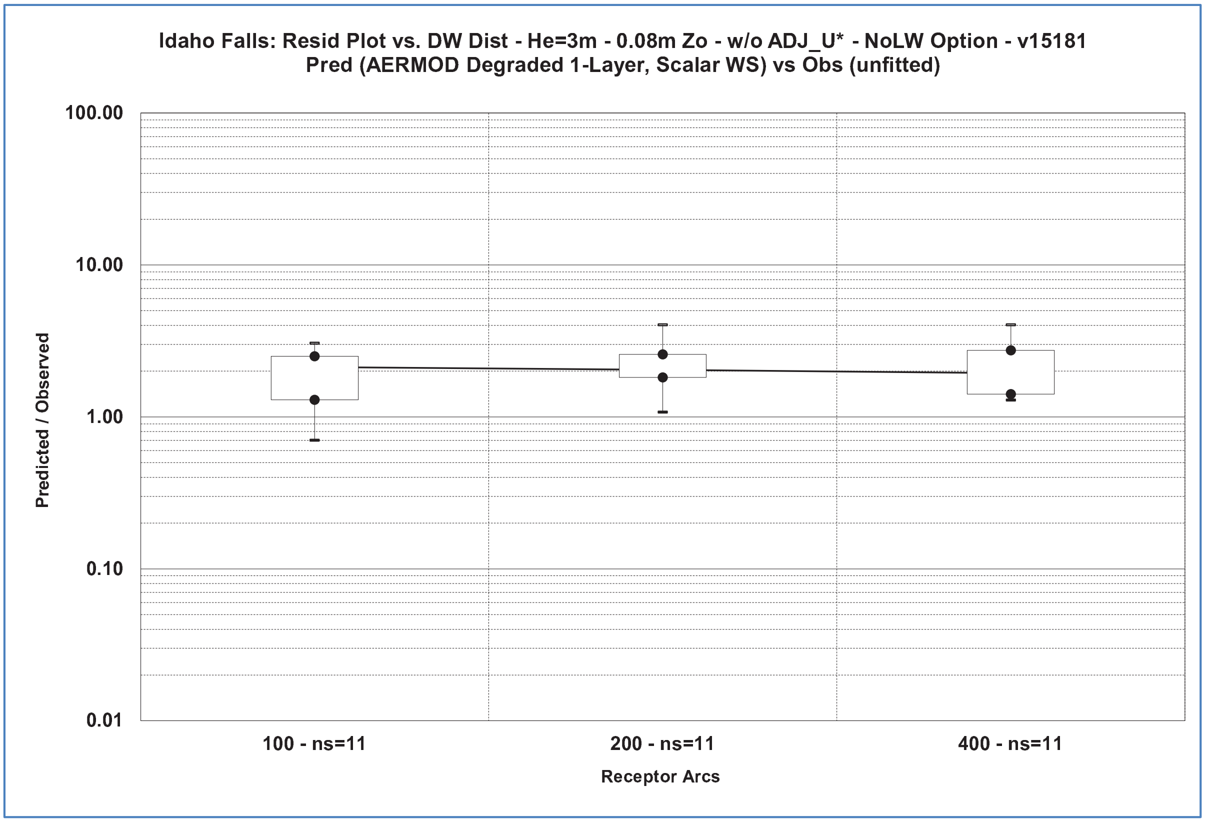

The results for Idaho Falls based on the default options in AERMET and AERMOD exhibit overprediction of the observed concentrations of approximately a factor of 2, with is a much smaller bias than for the Oak Ridge study. As shown below, the bias toward overprediction is largely eliminated with the LowWind options in AERMOD, without the ADJ_U* option in AERMET. The average Pred/Obs concentration ratios are also generally consistent with downwind distance.

The results for Idaho Falls with the ADJ_U* option in AERMET also show generally good performance at the first arc of receptors at 100m downwind, with some tendency toward underprediction further downwind, especially when the LowWind options are also used. For this type of source, i.e., a non-buoyant, ground-level or low-level source (e.g., fugitive emission), the maximum ambient impacts are likely to occur at the fenceline.

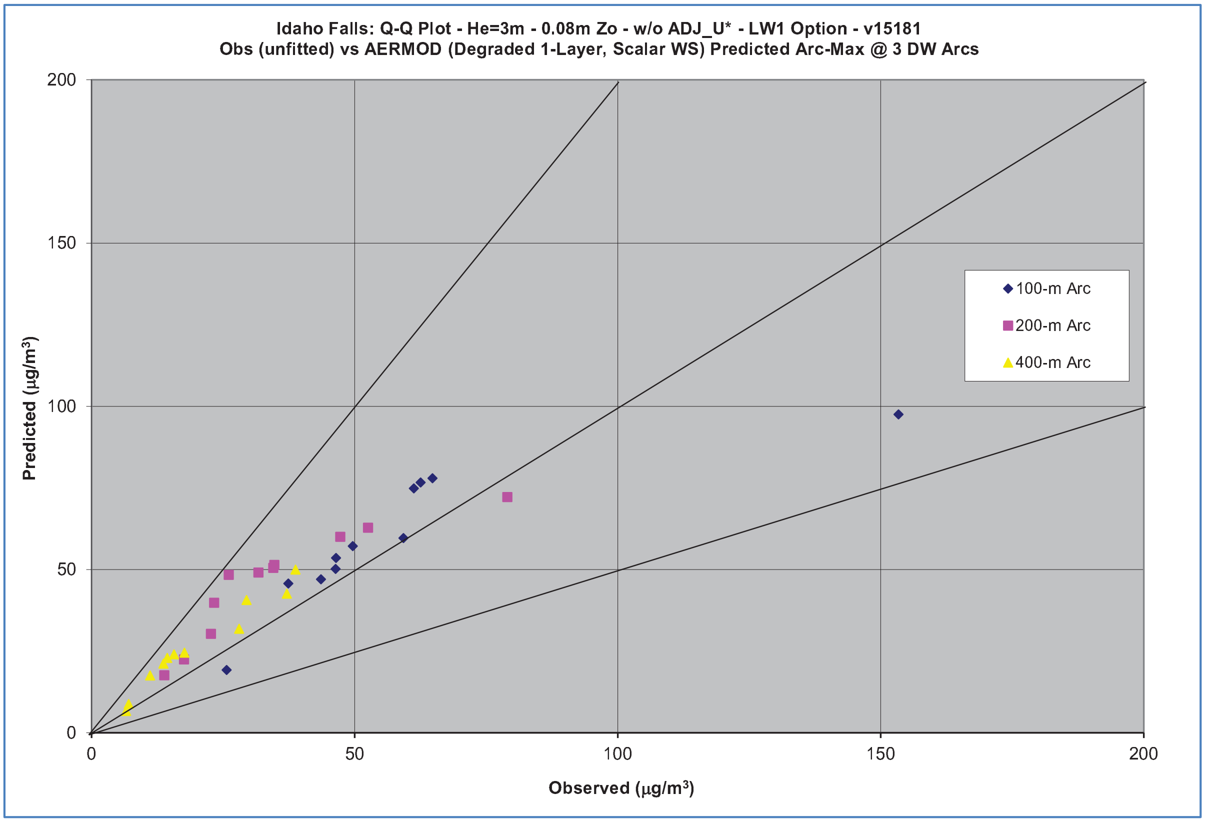
Idaho Falls: Q-Q Plot - He=3m - 0.08m Zo - w/o ADJ_U* - LW1 Option - v15181
Obs (unfitted) vs AERMOD (Degraded 1-Layer, Scalar WS) Predicted Arc-Max @ 3 DW Arcs
Predicted (µg/m³)
Observed (µg/m³)
100-m Arc
200-m Arc
400-m Arc
0
50
100
150
200

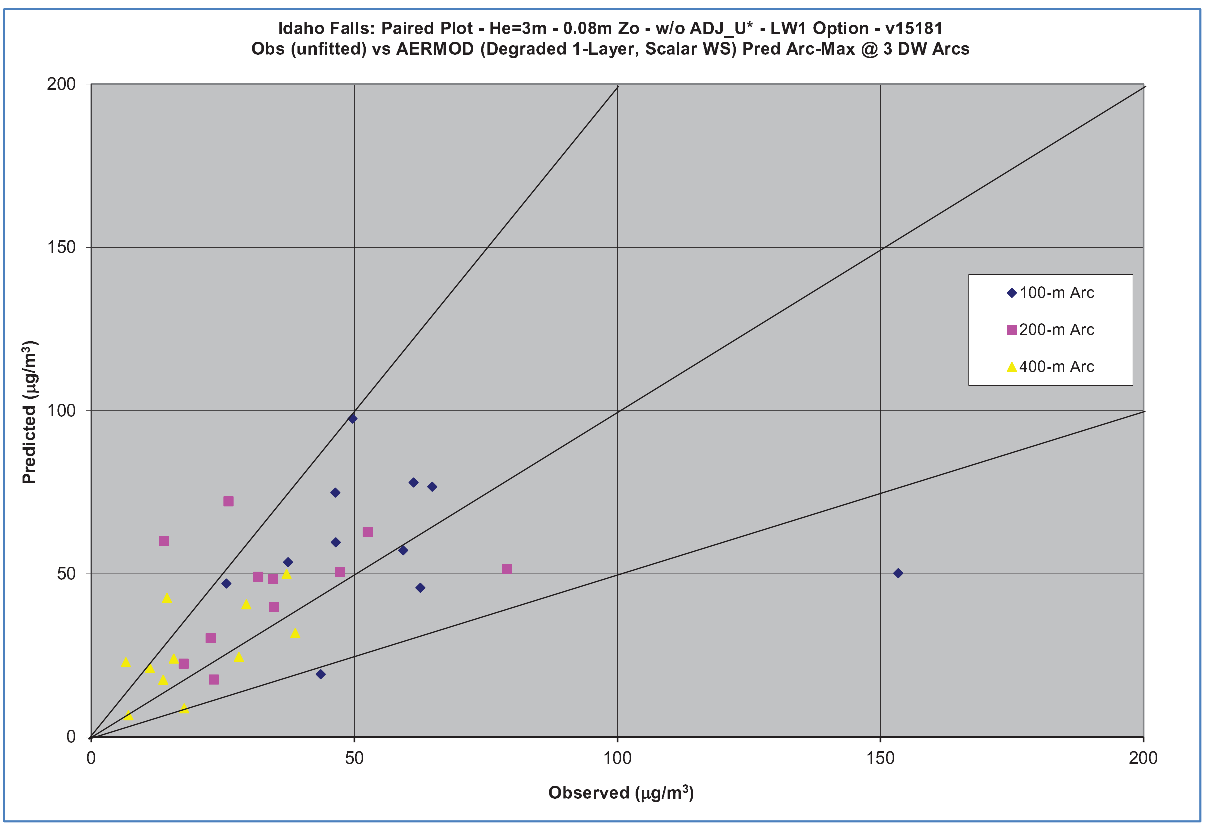
Idaho Falls: Paired Plot - He=3m - 0.08m Zo - w/o ADJ_U* - LW1 Option - v15181
Obs (unfitted) vs AERMOD (Degraded 1-Layer, Scalar WS) Pred Arc-Max @ 3 DW Arcs
Predicted (µg/m³)
Observed (µg/m³)
100-m Arc
200-m Arc
400-m Arc
0
50
100
150
200

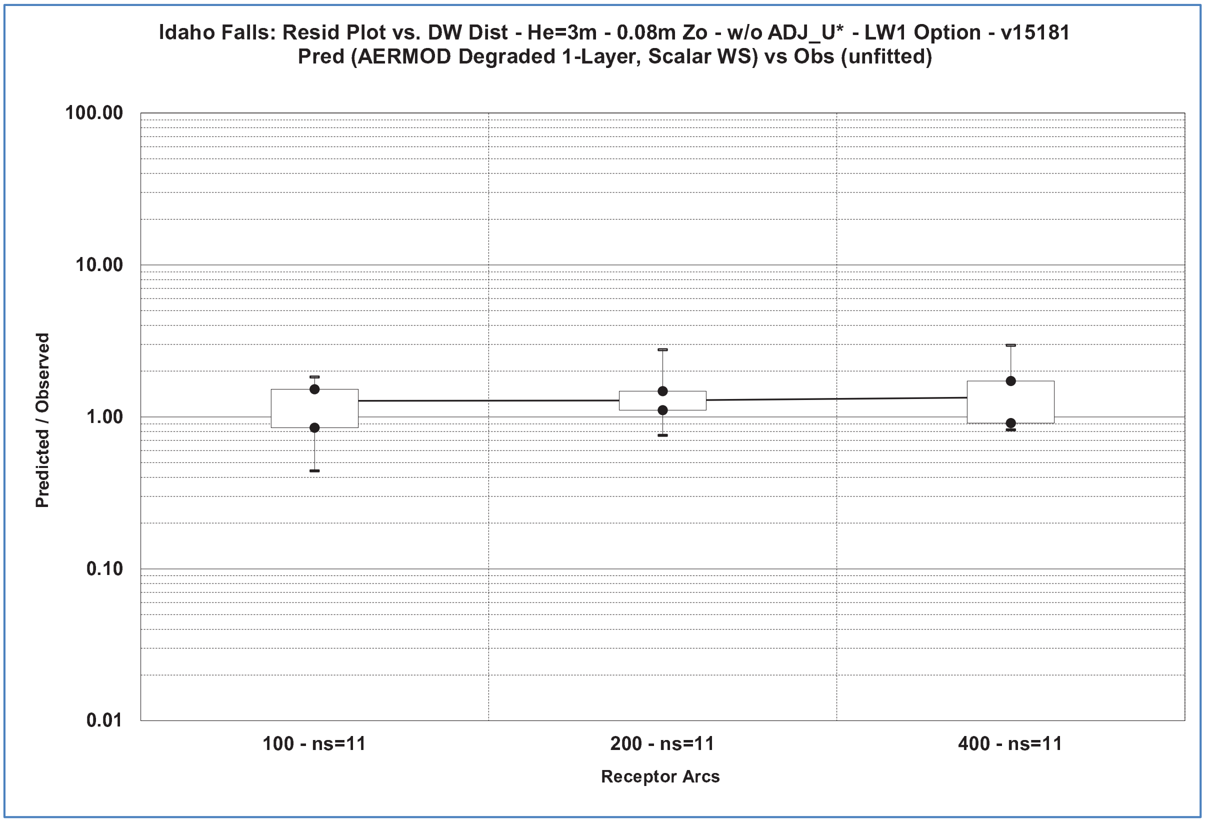
Idaho Falls: Resid Plot vs. DW Dist - He=3m - 0.08m Zo - w/o ADJ_U* - LW1 Option - v15181
Pred (AERMOD Degraded 1-Layer, Scalar WS) vs Obs (unfitted)
100.00
10.00
1.00
0.10
0.01
Predicted / Observed
100 - ns=11
200 - ns=11
400 - ns=11
Receptor Arcs

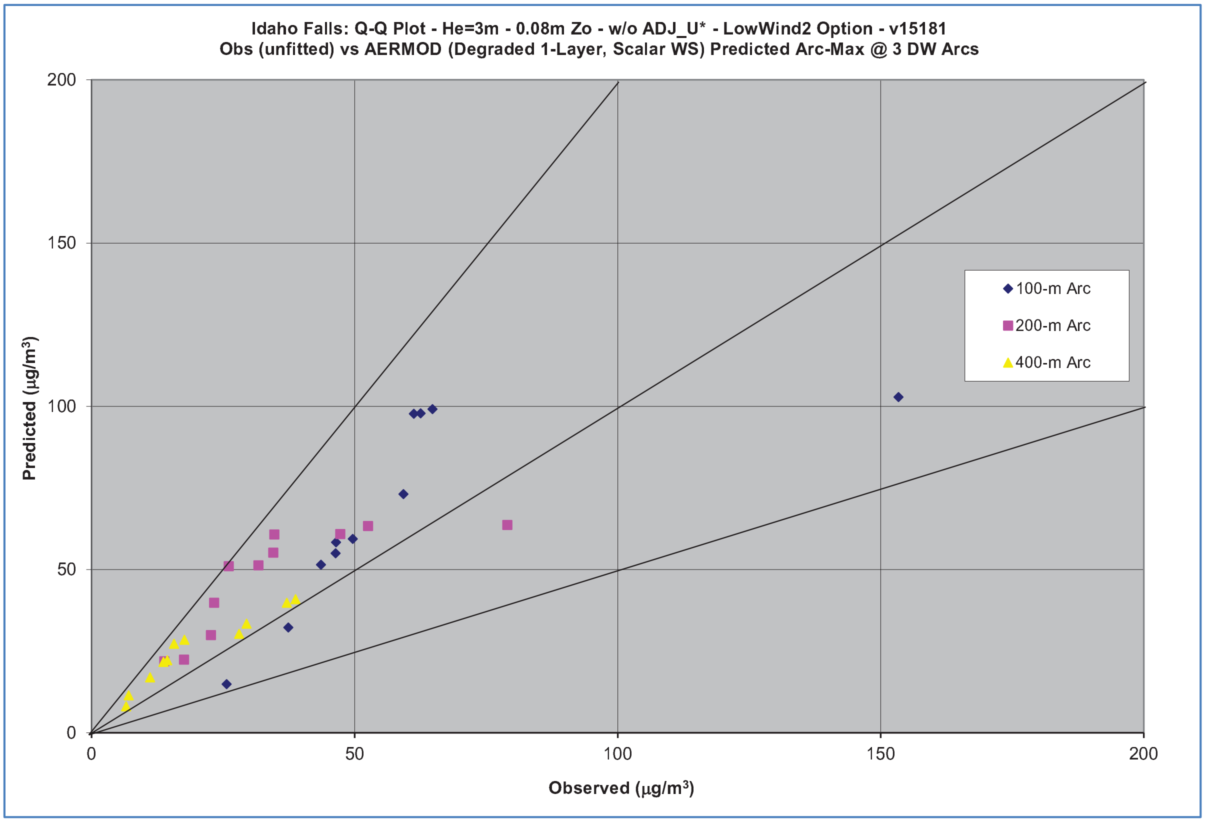
Idaho Falls: Q-Q Plot - He=3m - 0.08m Zo - w/o ADJ_U* - LowWind2 Option - v15181
Obs (unfitted) vs AERMOD (Degraded 1-Layer, Scalar WS) Predicted Arc-Max @ 3 DW Arcs
Predicted (µg/m³)
Observed (µg/m³)
100-m Arc
200-m Arc
400-m Arc
0
50
100
150
200

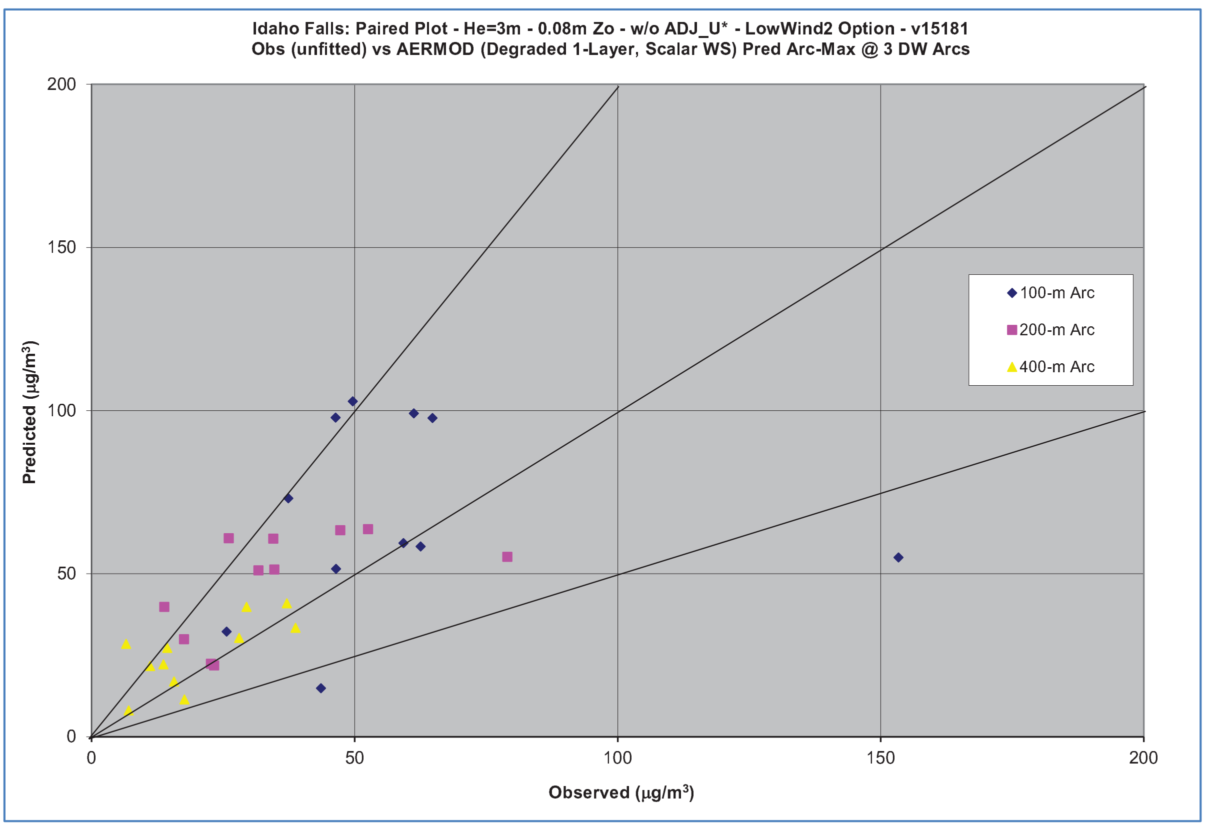
Idaho Falls: Paired Plot - He=3m - 0.08m Zo - w/o ADJ_U* - LowWind2 Option - v15181
Obs (unfitted) vs AERMOD (Degraded 1-Layer, Scalar WS) Pred Arc-Max @ 3 DW Arcs
Predicted (µg/m³)
Observed (µg/m³)
100-m Arc
200-m Arc
400-m Arc
0
50
100
150
200

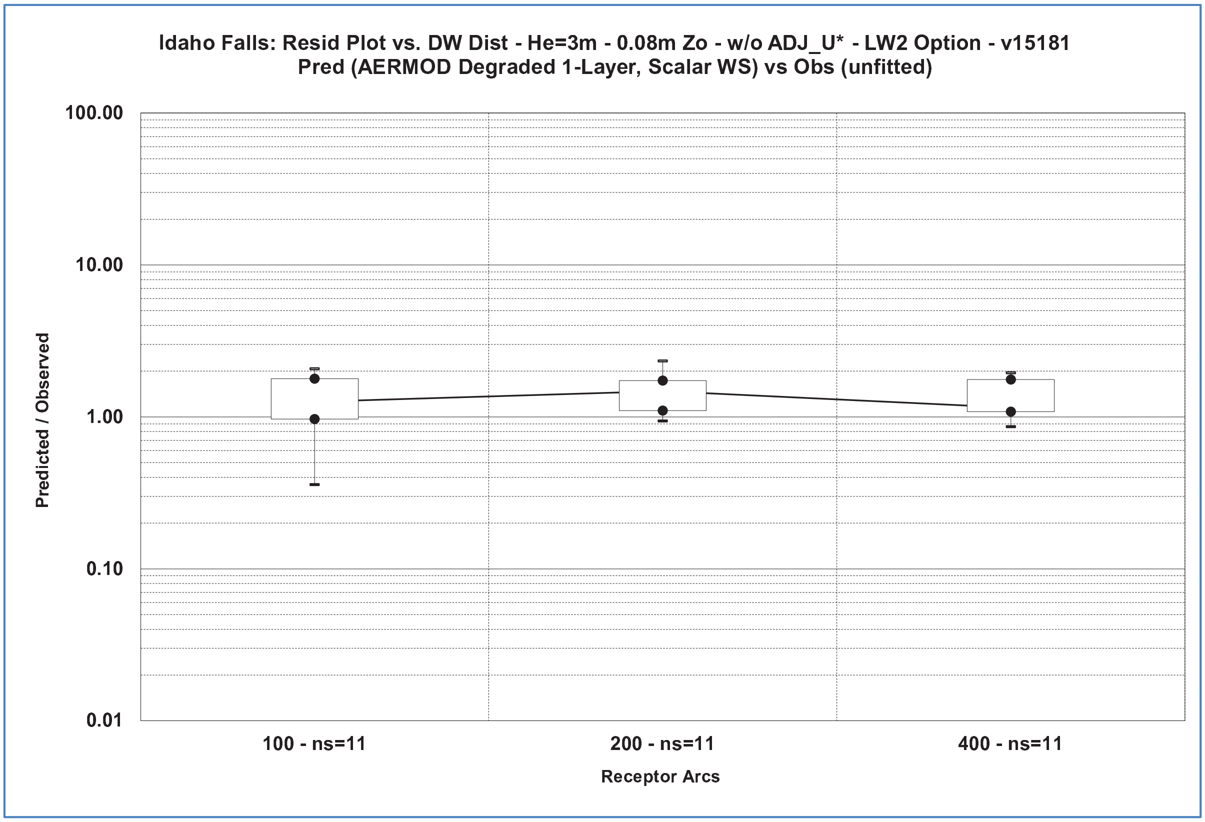
Idaho Falls: Resid Plot vs. DW Dist - He=3m - 0.08m Zo - w/o ADJ_U* - LW2 Option - v15181
Pred (AERMOD Degraded 1-Layer, Scalar WS) vs Obs (unfitted)
100.00
10.00
1.00
0.10
0.01
Predicted / Observed
100 - ns=11
200 - ns=11
400 - ns=11
Receptor Arcs

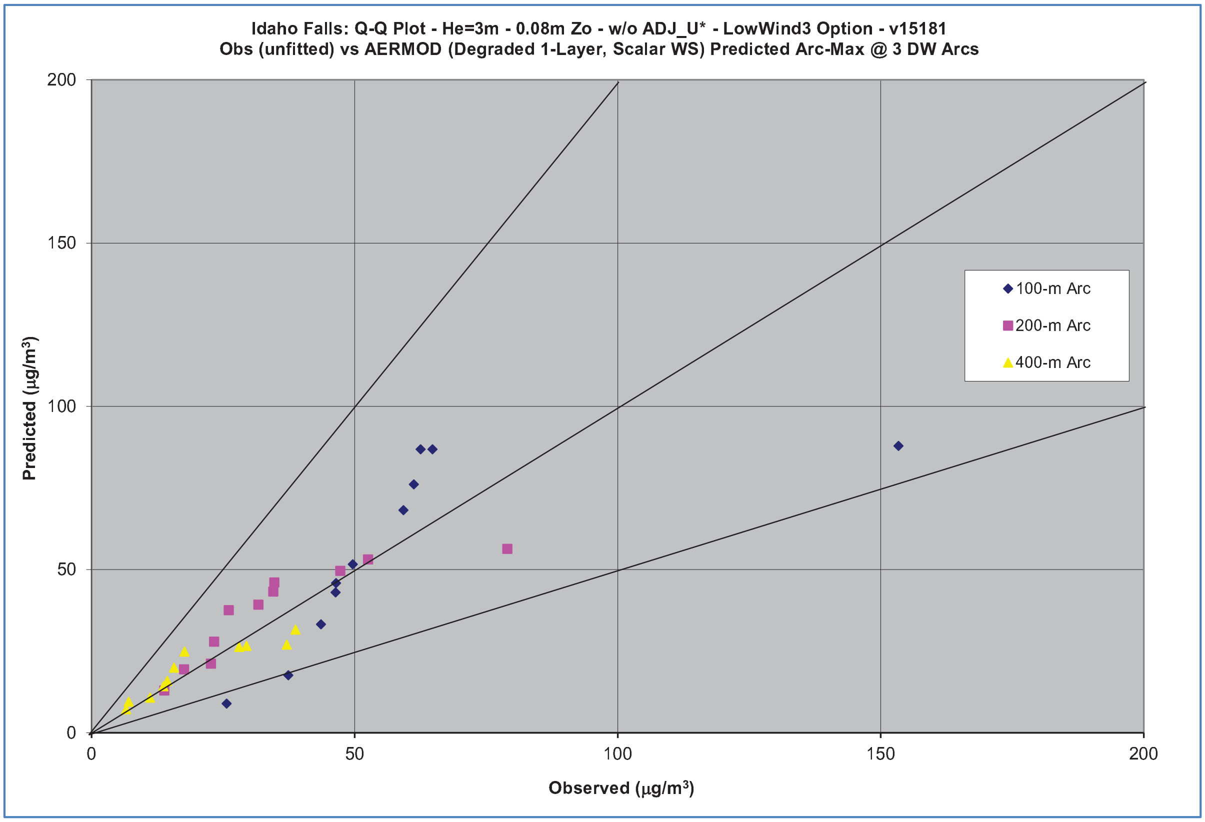
Idaho Falls: Q-Q Plot - He=3m - 0.08m Zo - w/o ADJ_U* - LowWind3 Option - v15181
Obs (unfitted) vs AERMOD (Degraded 1-Layer, Scalar WS) Predicted Arc-Max @ 3 DW Arcs
Predicted (µg/m3)
Observed (µg/m3)
0
50
100
150
200
100-m Arc
200-m Arc
400-m Arc

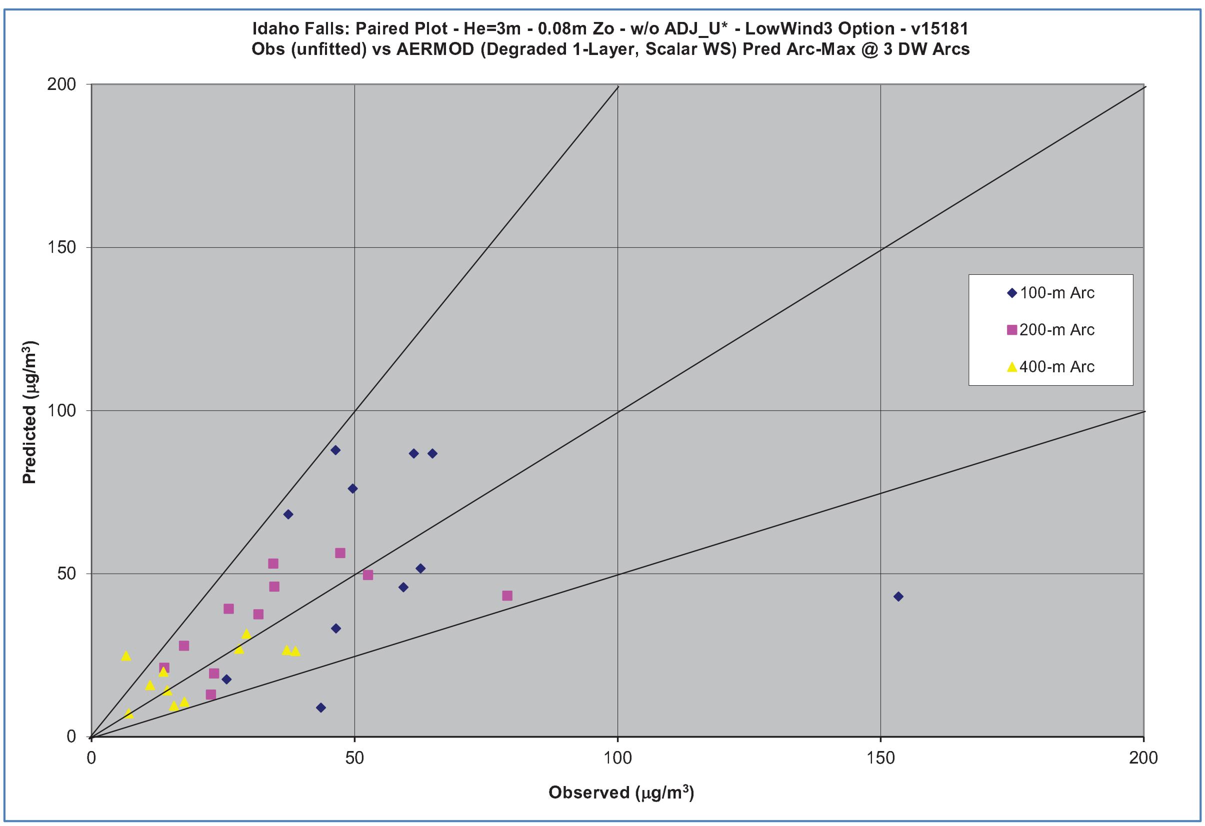
Idaho Falls: Paired Plot - He=3m - 0.08m Zo - w/o ADJ_U* - LowWind3 Option - v15181
Obs (unfitted) vs AERMOD (Degraded 1-Layer, Scalar WS) Pred Arc-Max @ 3 DW Arcs
Predicted (µg/m3)
Observed (µg/m3)
0
50
100
150
200
100-m Arc
200-m Arc
400-m Arc

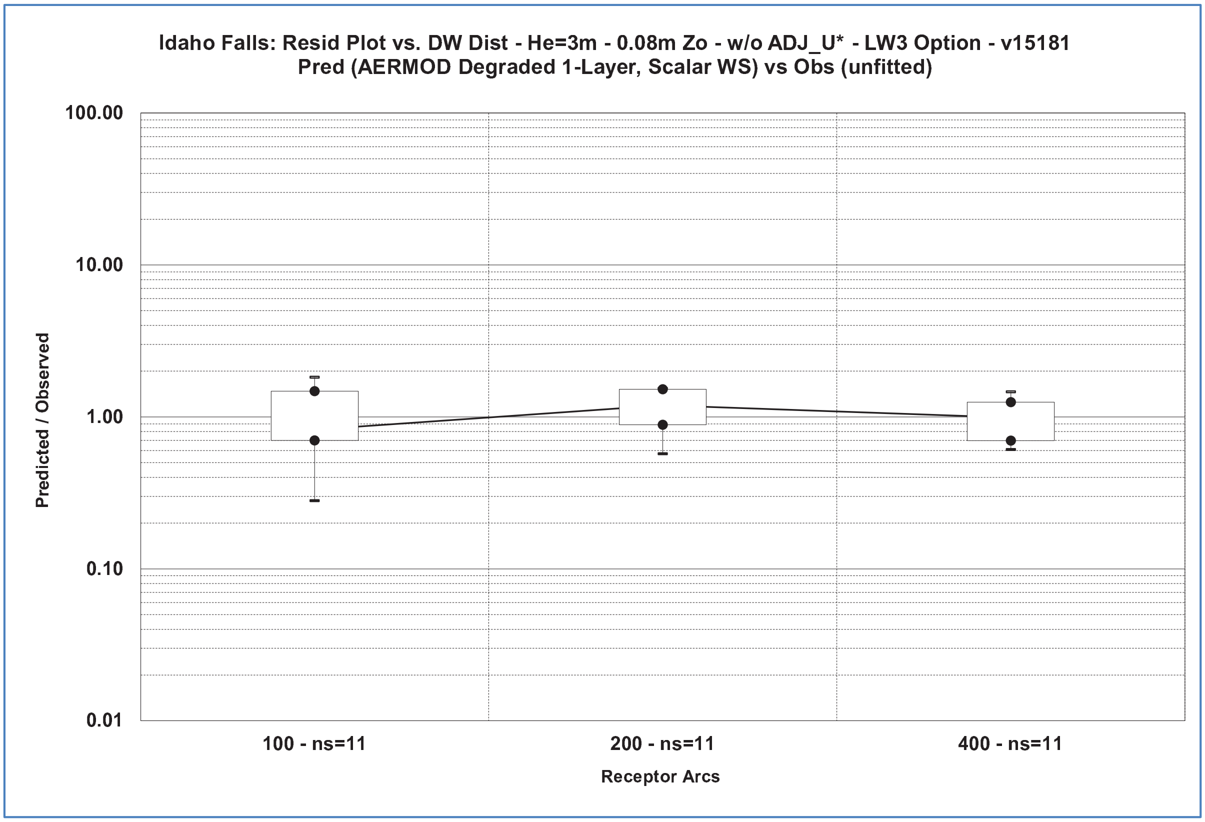
Idaho Falls: Resid Plot vs. DW Dist - He=3m - 0.08m Zo - w/o ADJ_U* - LW3 Option - v15181
Pred (AERMOD Degraded 1-Layer, Scalar WS) vs Obs (unfitted)
100.00
10.00
1.00
0.10
0.01
Predicted / Observed
100 - ns=11
200 - ns=11
400 - ns=11
Receptor Arcs

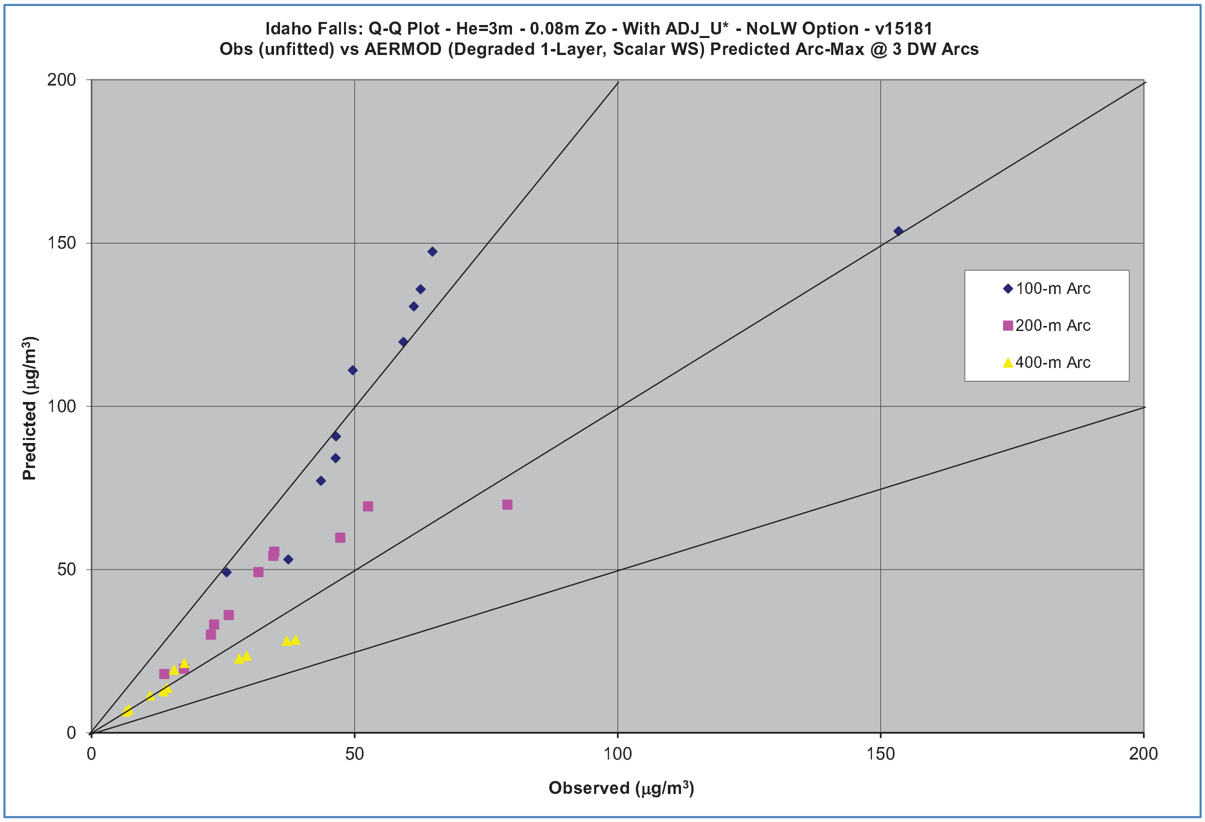
Idaho Falls: Q-Q Plot - He=3m - 0.08m Zo - With ADJ_U* - NoLW Option - v15181
Obs (unfitted) vs AERMOD (Degraded 1-Layer, Scalar WS) Predicted Arc-Max @ 3 DW Arcs
Predicted (µg/m³)
Observed (µg/m³)
0
50
100
150
200
100-m Arc
200-m Arc
400-m Arc

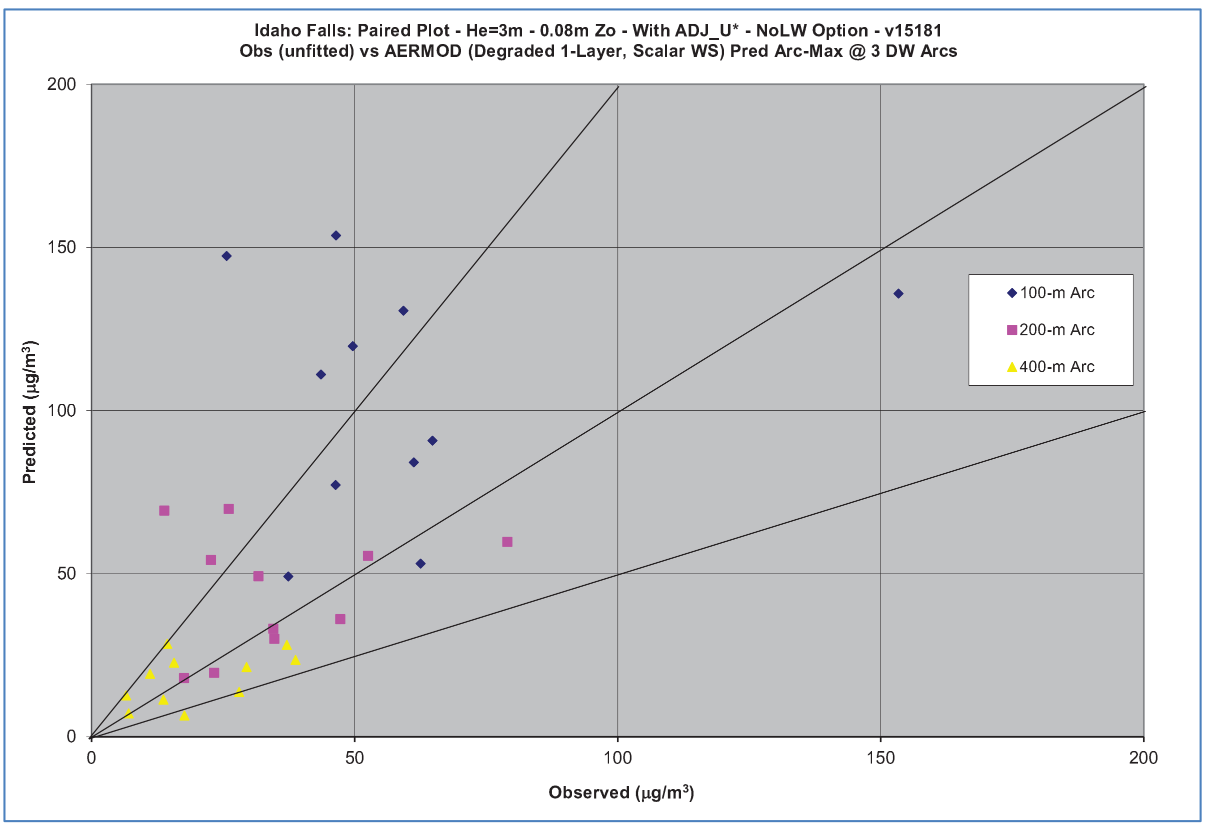
Idaho Falls: Paired Plot - He=3m - 0.08m Zo - With ADJ_U* - NoLW Option - v15181
Obs (unfitted) vs AERMOD (Degraded 1-Layer, Scalar WS) Pred Arc-Max @ 3 DW Arcs
Predicted (µg/m³)
Observed (µg/m³)
0
50
100
150
200
100-m Arc
200-m Arc
400-m Arc

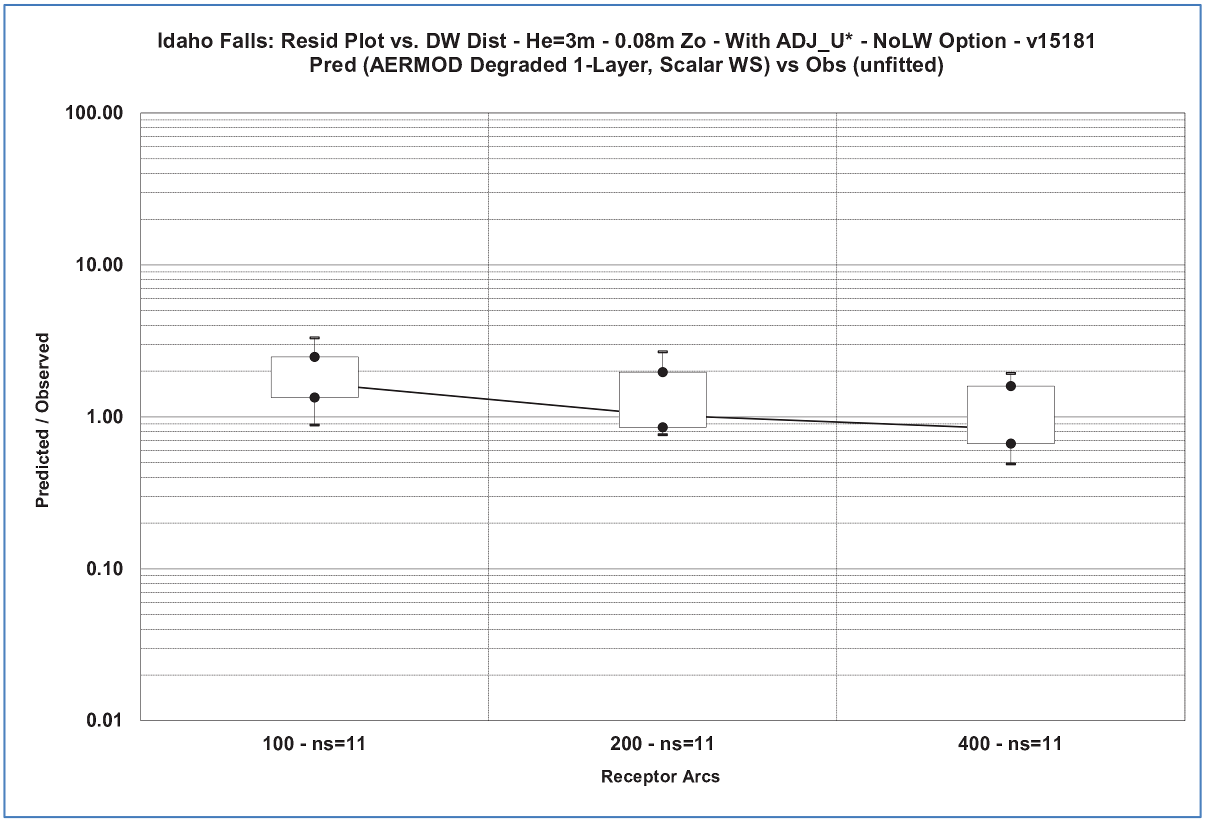
Idaho Falls: Resid Plot vs. DW Dist - He=3m - 0.08m Zo - With ADJ_U* - NoLW Option - v15181
Pred (AERMOD Degraded 1-Layer, Scalar WS) vs Obs (unfitted)
100.00
10.00
1.00
0.10
0.01
Predicted / Observed
100 - ns=11
200 - ns=11
400 - ns=11
Receptor Arcs

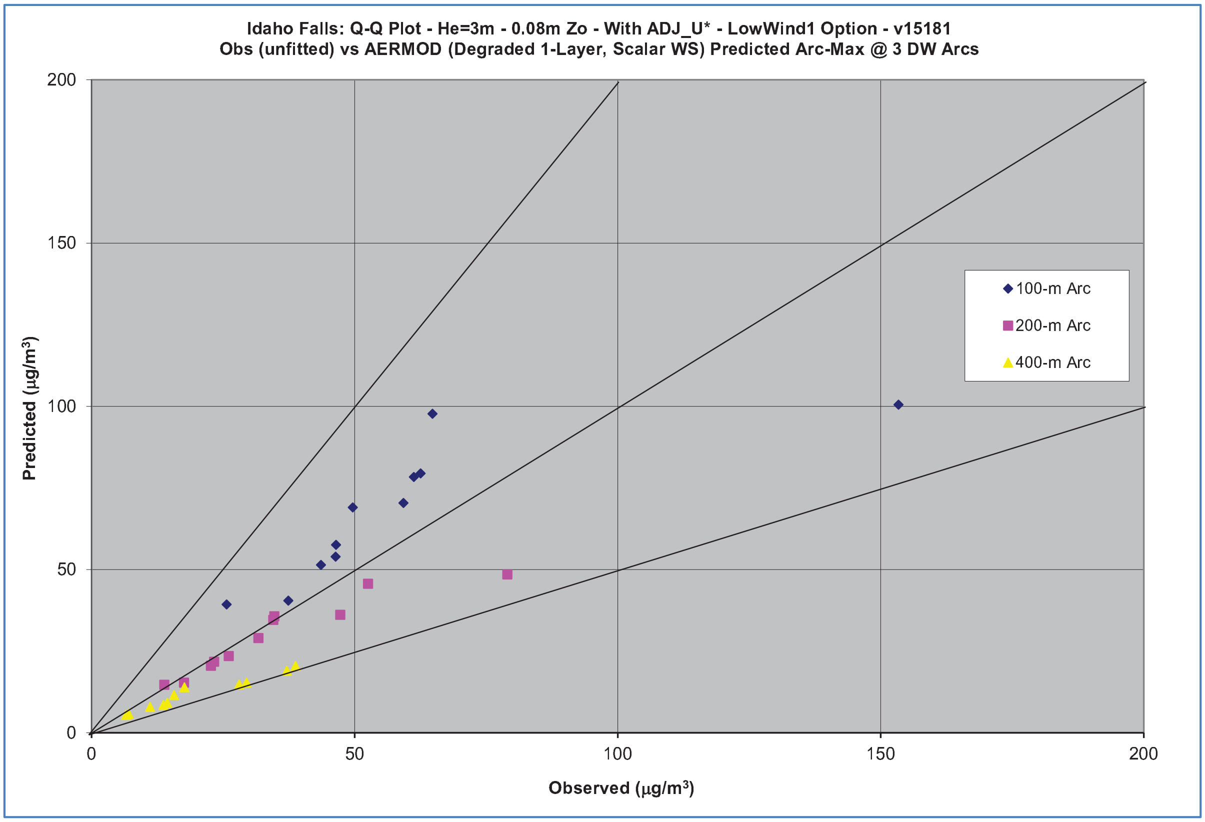
Idaho Falls: Q-Q Plot - He=3m - 0.08m Zo - With ADJ_U* - LowWind1 Option - v15181
Obs (unfitted) vs AERMOD (Degraded 1-Layer, Scalar WS) Predicted Arc-Max @ 3 DW Arcs
Predicted (µg/m³)
Observed (µg/m³)
0
50
100
150
200
100-m Arc
200-m Arc
400-m Arc

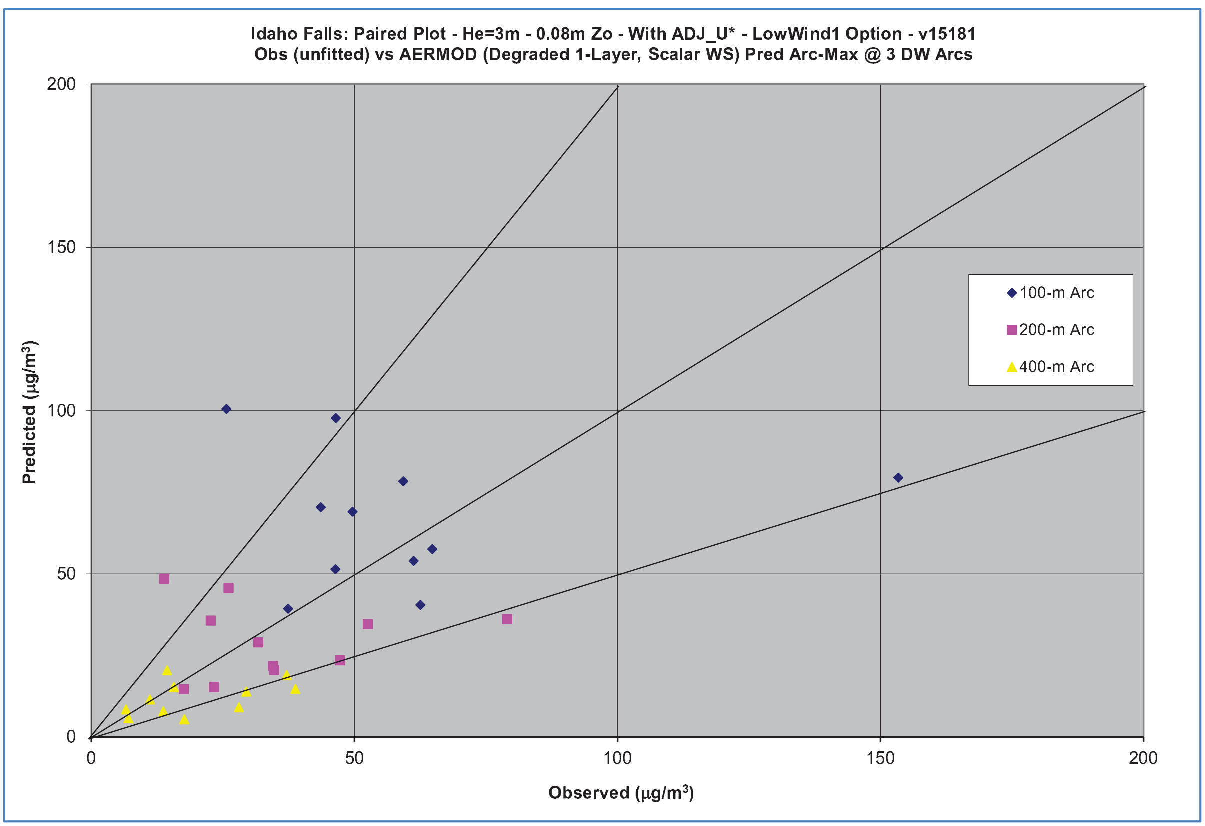
Idaho Falls: Paired Plot - He=3m - 0.08m Zo - With ADJ_U* - LowWind1 Option - v15181
Obs (unfitted) vs AERMOD (Degraded 1-Layer, Scalar WS) Pred Arc-Max @ 3 DW Arcs
Predicted (µg/m³)
Observed (µg/m³)
0
50
100
150
200
100-m Arc
200-m Arc
400-m Arc

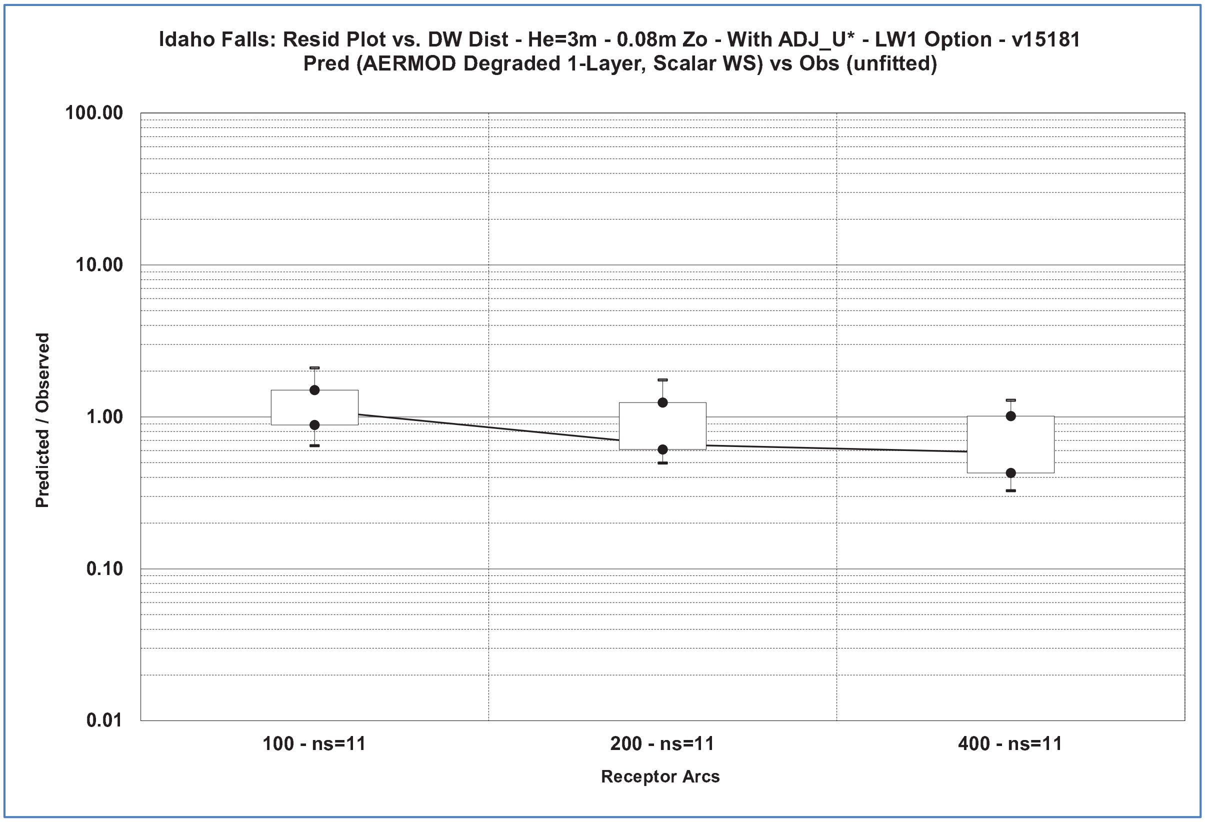
Idaho Falls: Resid Plot vs. DW Dist - He=3m - 0.08m Zo - With ADJ_U* - LW1 Option - v15181
Pred (AERMOD Degraded 1-Layer, Scalar WS) vs Obs (unfitted)
100.00
10.00
1.00
0.10
0.01
Predicted / Observed
100 - ns=11
200 - ns=11
400 - ns=11
Receptor Arcs

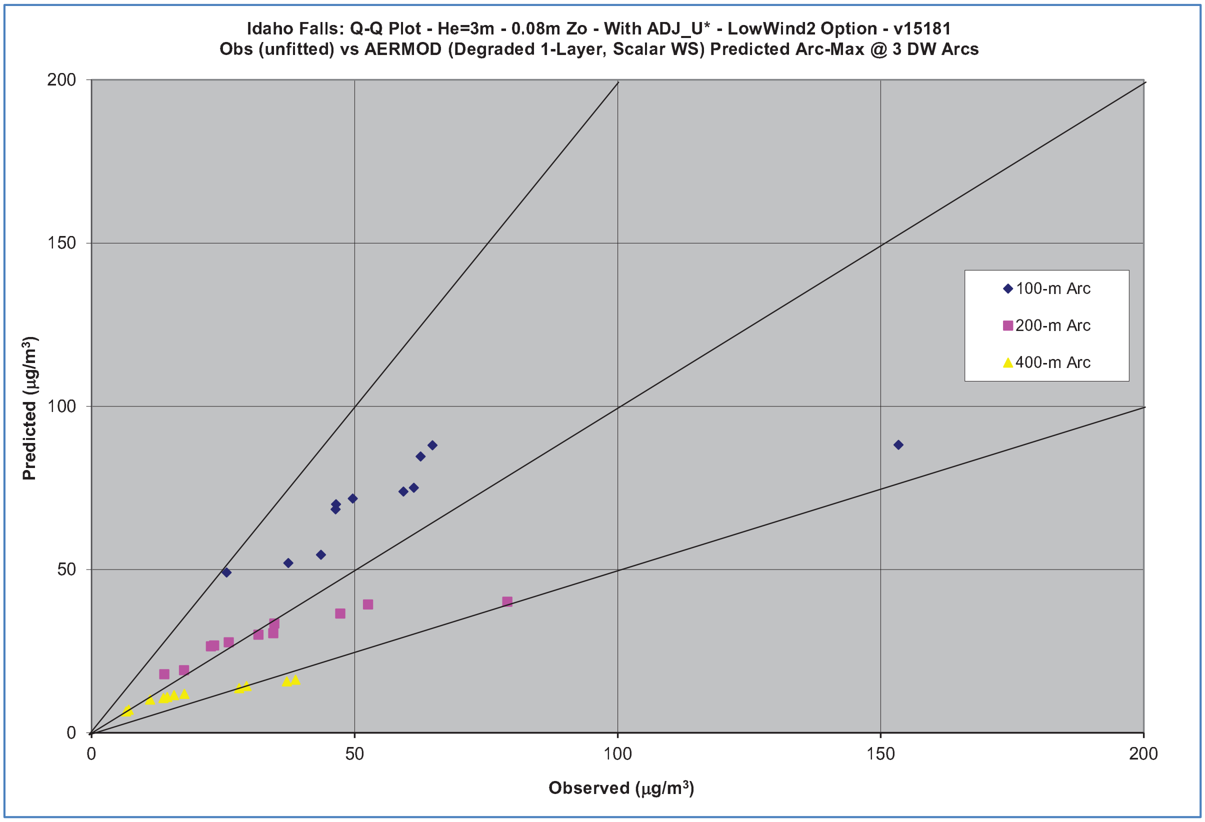
Idaho Falls: Q-Q Plot - He=3m - 0.08m Zo - With ADJ_U* - LowWind2 Option - v15181
Obs (unfitted) vs AERMOD (Degraded 1-Layer, Scalar WS) Predicted Arc-Max @ 3 DW Arcs
Predicted (µg/m3)
Observed (µg/m3)
100-m Arc
200-m Arc
400-m Arc
0
50
100
150
200

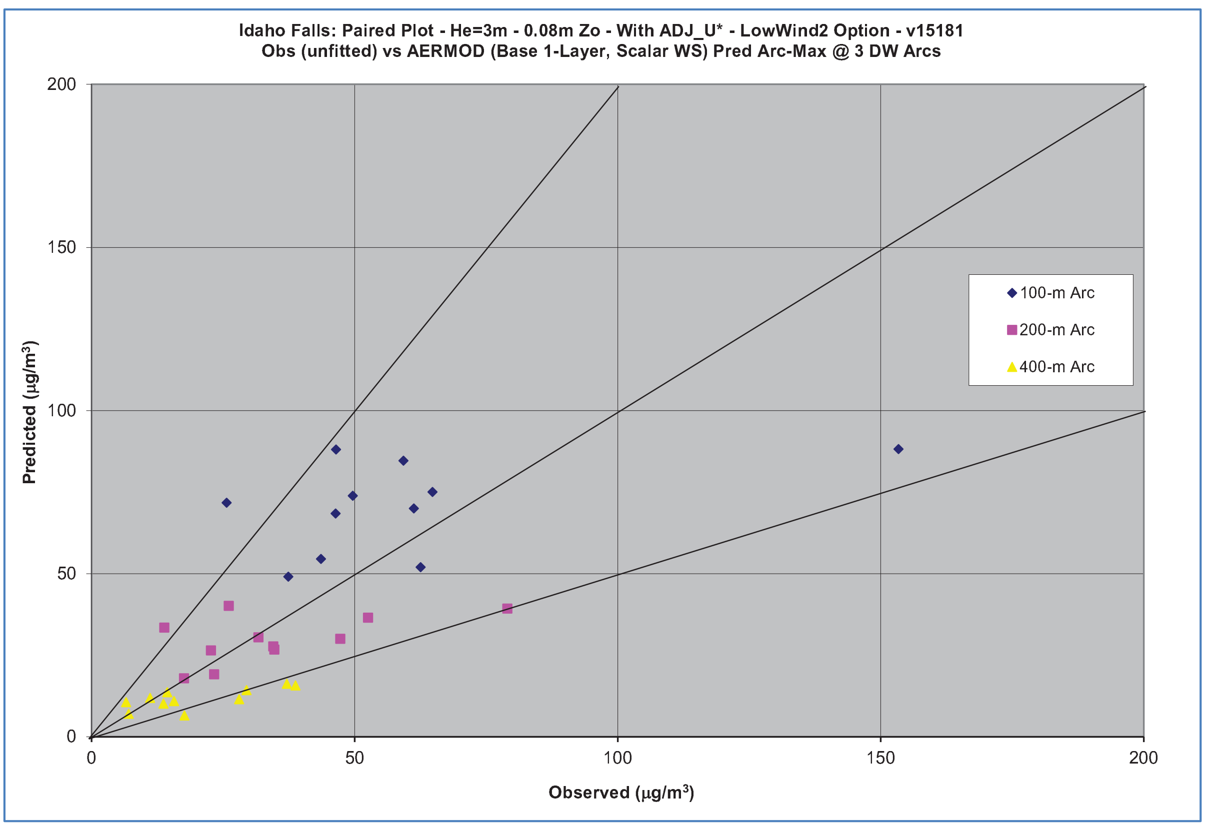
Idaho Falls: Paired Plot - He=3m - 0.08m Zo - With ADJ_U* - LowWind2 Option - v15181
Obs (unfitted) vs AERMOD (Base 1-Layer, Scalar WS) Pred Arc-Max @ 3 DW Arcs
Predicted (µg/m3)
Observed (µg/m3)
100-m Arc
200-m Arc
400-m Arc
0
50
100
150
200

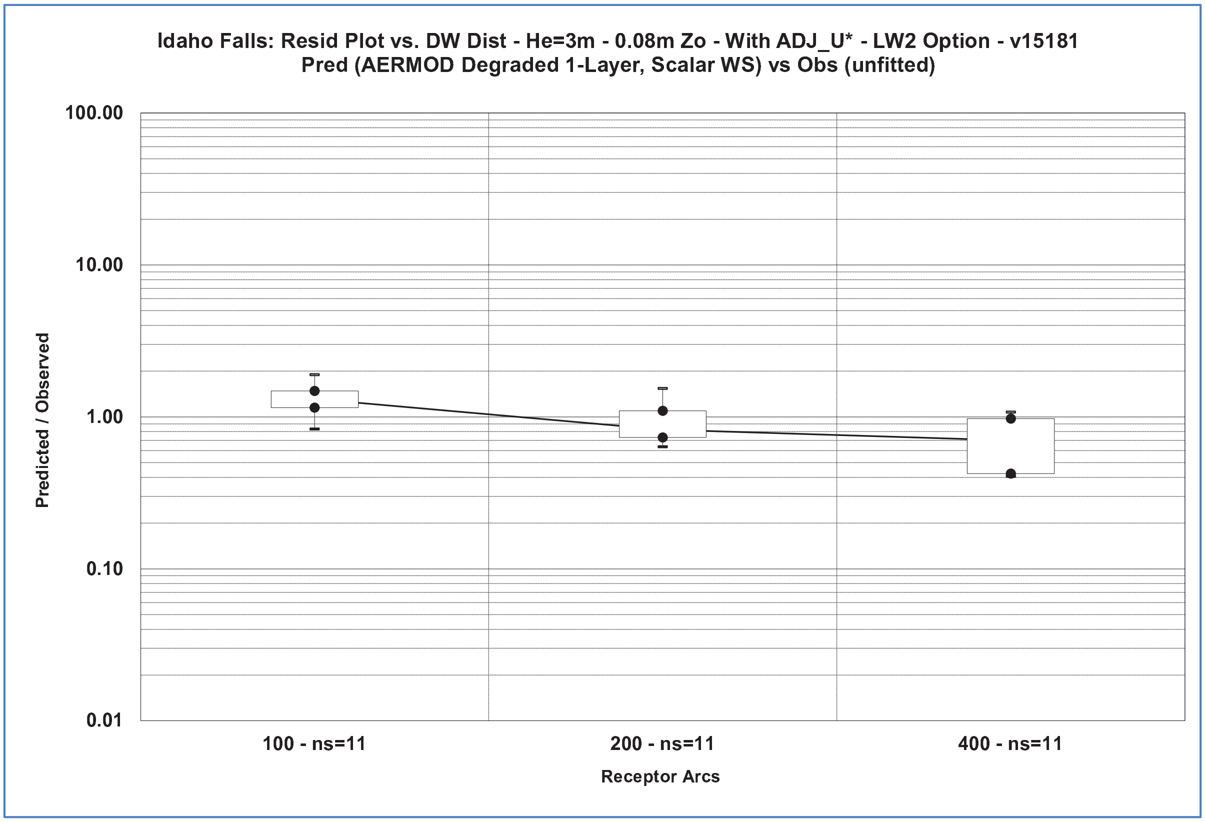
Idaho Falls: Resid Plot vs. DW Dist - He=3m - 0.08m Zo - With ADJ_U* - LW2 Option - v15181
Pred (AERMOD Degraded 1-Layer, Scalar WS) vs Obs (unfitted)
100.00
10.00
1.00
0.10
0.01
Predicted / Observed
100 - ns=11
200 - ns=11
400 - ns=11
Receptor Arcs

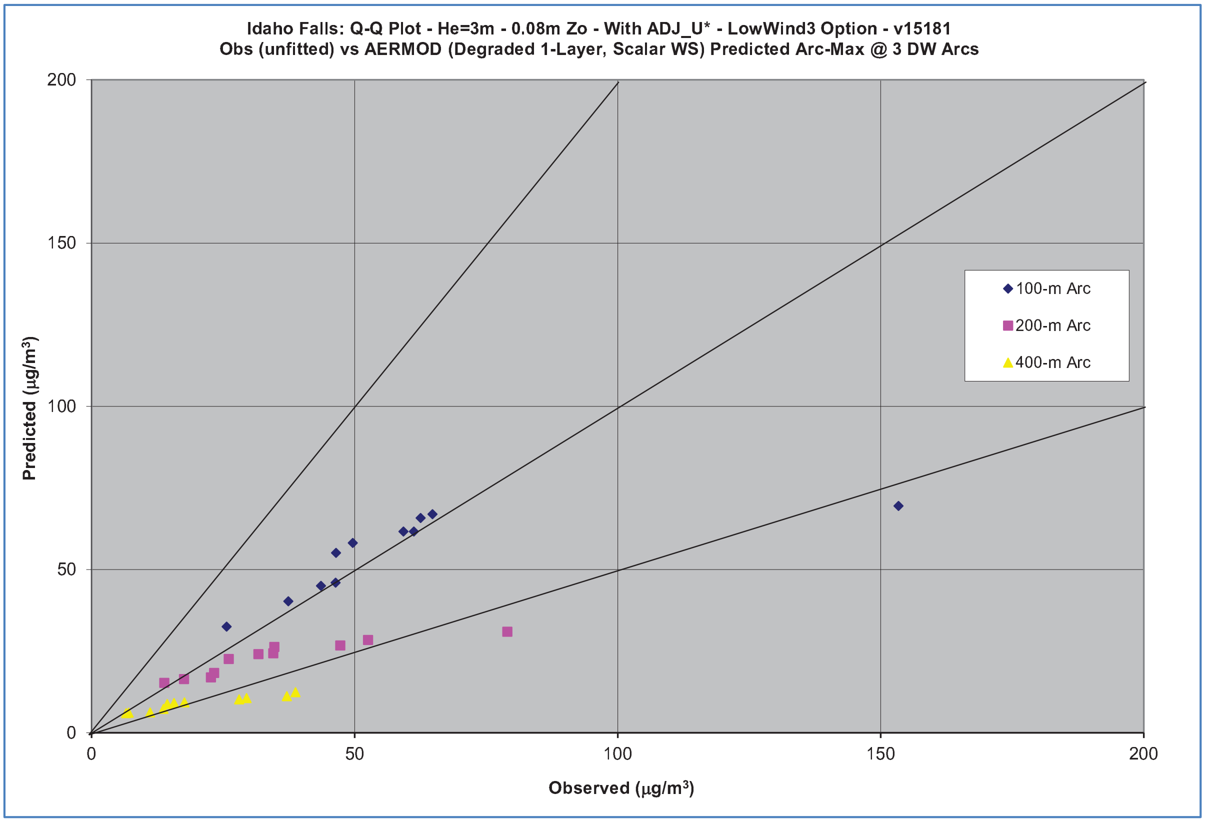
Idaho Falls: Q-Q Plot - He=3m - 0.08m Zo - With ADJ_U* - LowWind3 Option - v15181
Obs (unfitted) vs AERMOD (Degraded 1-Layer, Scalar WS) Predicted Arc-Max @ 3 DW Arcs
Predicted (µg/m³)
Observed (µg/m³)
100-m Arc
200-m Arc
400-m Arc
0
50
100
150
200

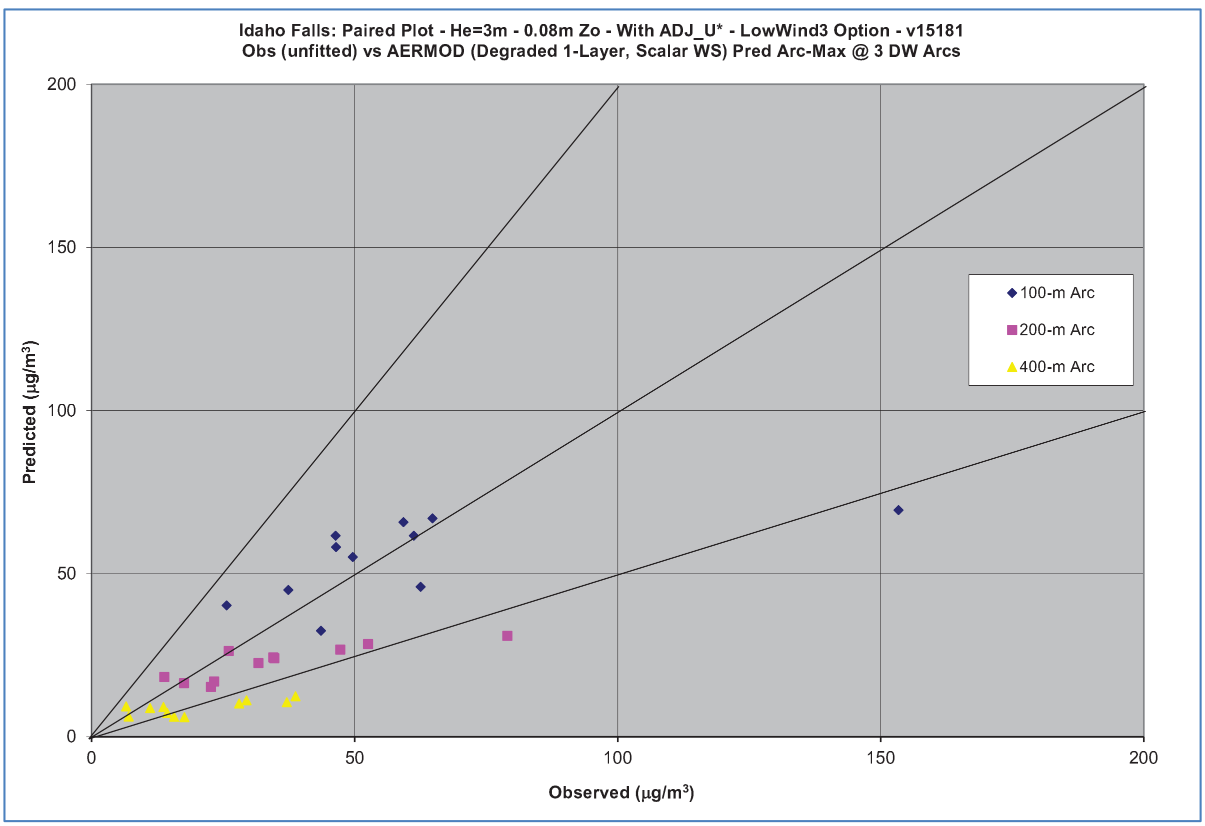
Idaho Falls: Paired Plot - He=3m - 0.08m Zo - With ADJ_U* - LowWind3 Option - v15181
Obs (unfitted) vs AERMOD (Degraded 1-Layer, Scalar WS) Pred Arc-Max @ 3 DW Arcs
Predicted (µg/m³)
Observed (µg/m³)
100-m Arc
200-m Arc
400-m Arc
0
50
100
150
200

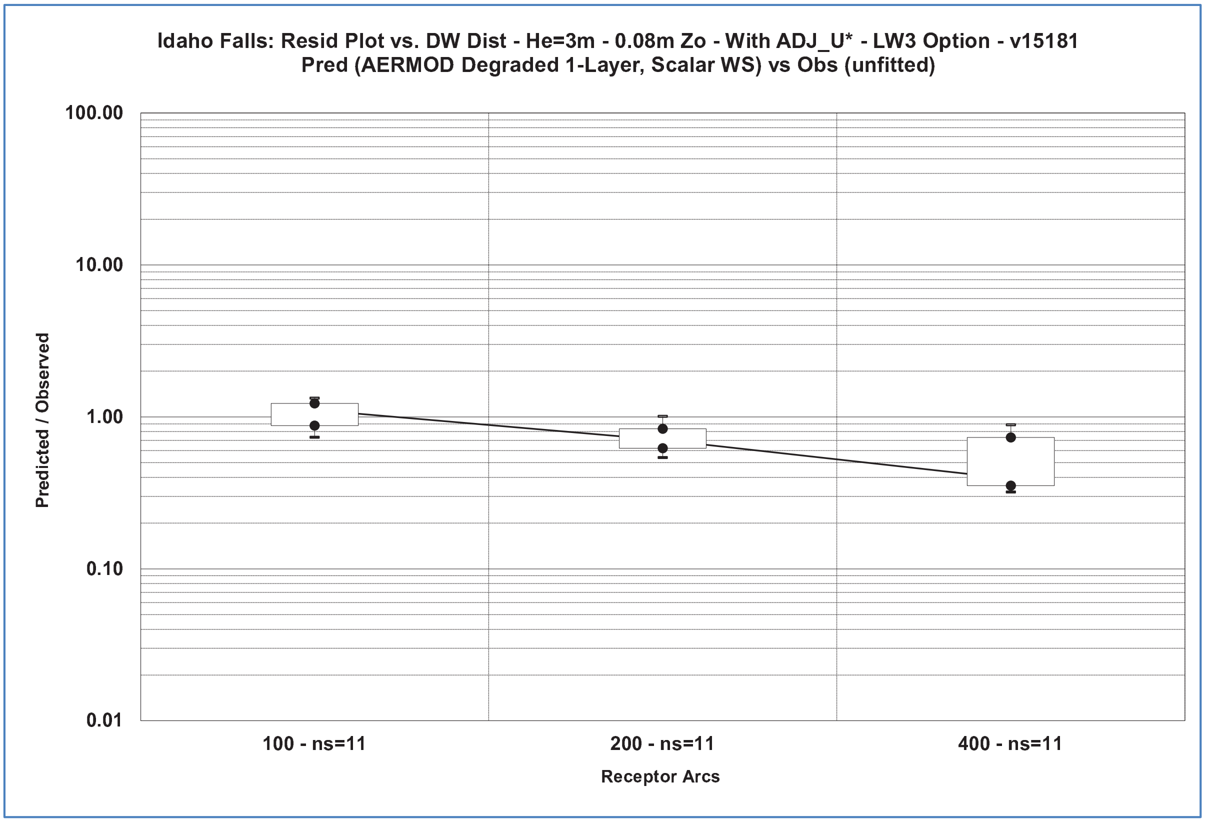

Idaho Falls: Resid Plot vs. DW Dist - He=3m - 0.08m Zo - With ADJ_U* - LW3 Option - v15181
Pred (AERMOD Degraded 1-Layer, Scalar WS) vs Obs (unfitted)
100.00
10.00
1.00
0.10
0.01
Predicted / Observed
100 - ns=11
200 - ns=11
400 - ns=11
Receptor Arcs

The Lovett data base includes a single 145m stack located within a few kilometers of complex terrain. The site area is shown below:

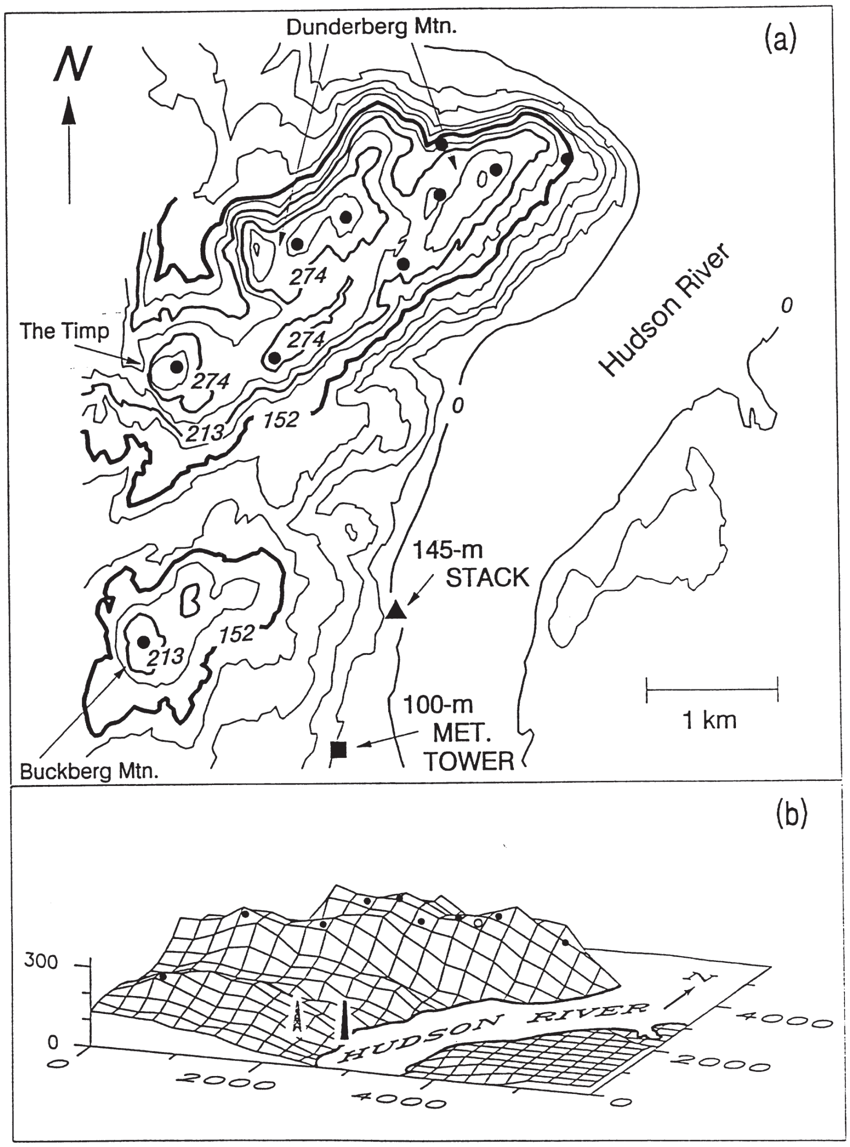

Figure 7 **Depiction of the Monitoring Network Used for the Lovett Complex Terrain Model Evaluation Study**

The Lovett data base includes a 100m meteorological tower with wind speed, wind direction, sigma-theta and temperature collected at the 10m, 50m, and 100m levels. In addition, sigma-w was also collected at the 10m and 100m levels. Past evaluations of AERMOD have shown good performance. Updated 1-hour results are presented below comparing model performance with full onsite meteorological data with and without the ADJ_U* and LowWind options, followed by comparisons with and without the ADJ_U* and LowWind options using degraded meteorological data inputs. Including the ADJ_U* option with full onsite meteorological data shows a slight improvement in model performance without the LowWind options, and little difference in performance for the LowWind2 compared to LowWind3 (the LowWind1 option was not included in this study.

The next set of comparisons are based on no temperature profile in the Lovett site-specific meteorological data. The model shows some overprediction without the temperature profile and without the ADJ_U* option, especially without the LowWind options. The model overprediction without the temperature profile is noticeably reduced when the ADJ_U* option is used. The modeled results shows more significant overprediction when the meteorological data is further degraded by eliminating the turbulence data (i.e., sigma-theta and sigma-w), with the overprediction bias exceeding a factor of 2. The overprediction without the temperature profile and turbulence data is significantly reduced when the ADJ_U* and LowWind options are used. It's also worth noting that results for the LowWind2 (LW2) and LowWind3 (LW3) options are nearly indistinguishable in this case.

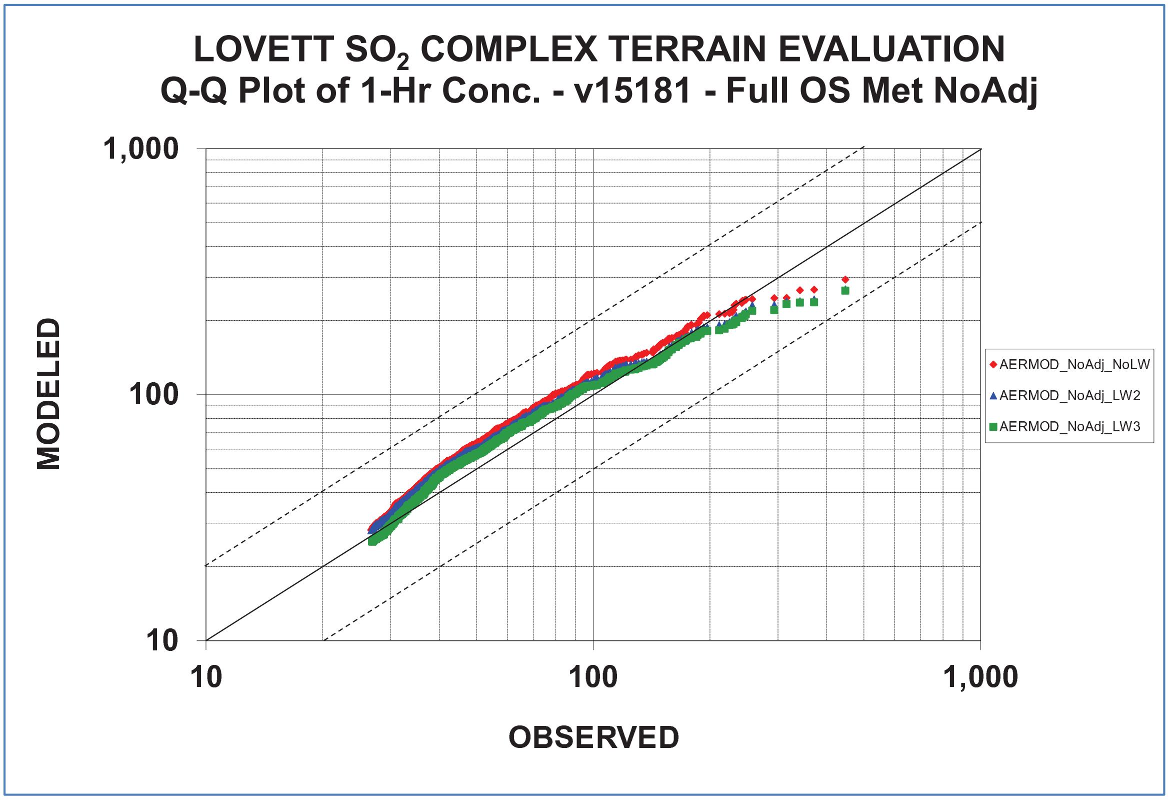
LOVETT SO_2 COMPLEX TERRAIN EVALUATION
Q-Q Plot of 1-Hr Conc. - v15181 - Full OS Met NoAdj
MODELED
OBSERVED
1,000
100
10
AERMOD_NoAdj_NoLW
AERMOD_NoAdj_LW2
AERMOD_NoAdj_LW3

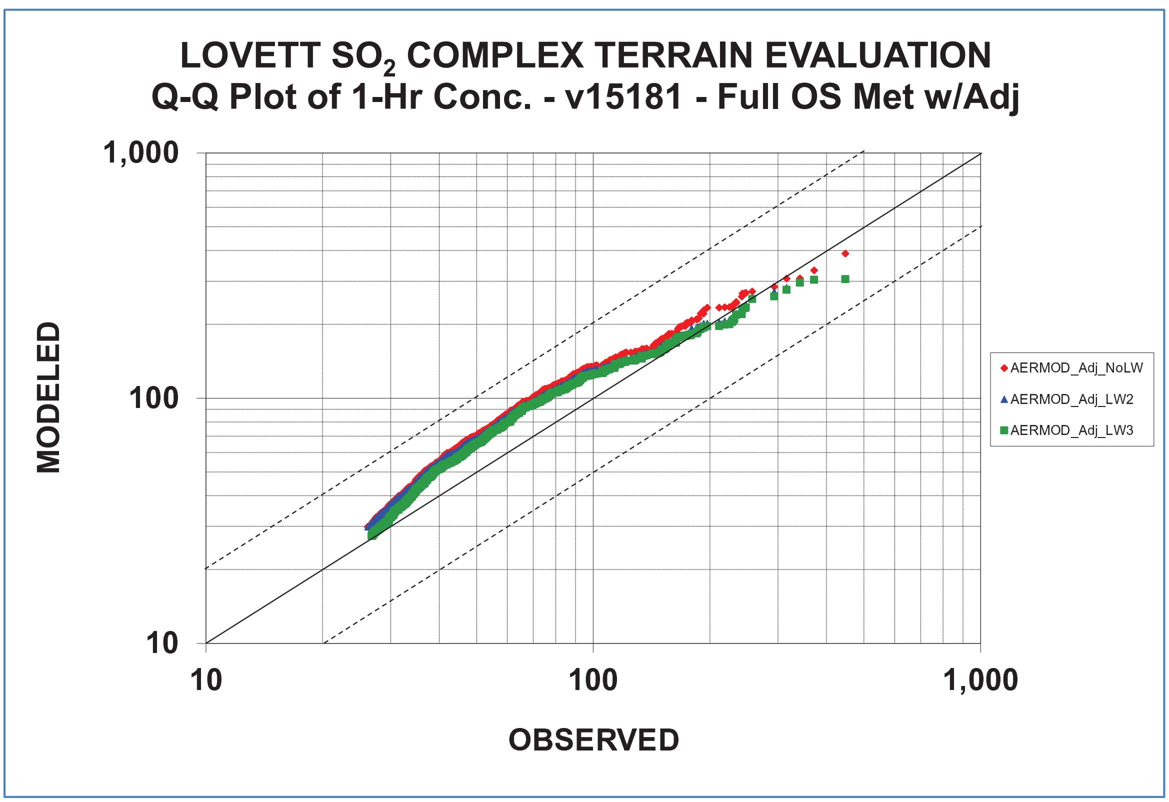
LOVETT SO_2 COMPLEX TERRAIN EVALUATION
Q-Q Plot of 1-Hr Conc. - v15181 - Full OS Met w/Adj
MODELED
OBSERVED
1,000
100
10
AERMOD_Adj_NoLW
AERMOD_Adj_LW2
AERMOD_Adj_LW3

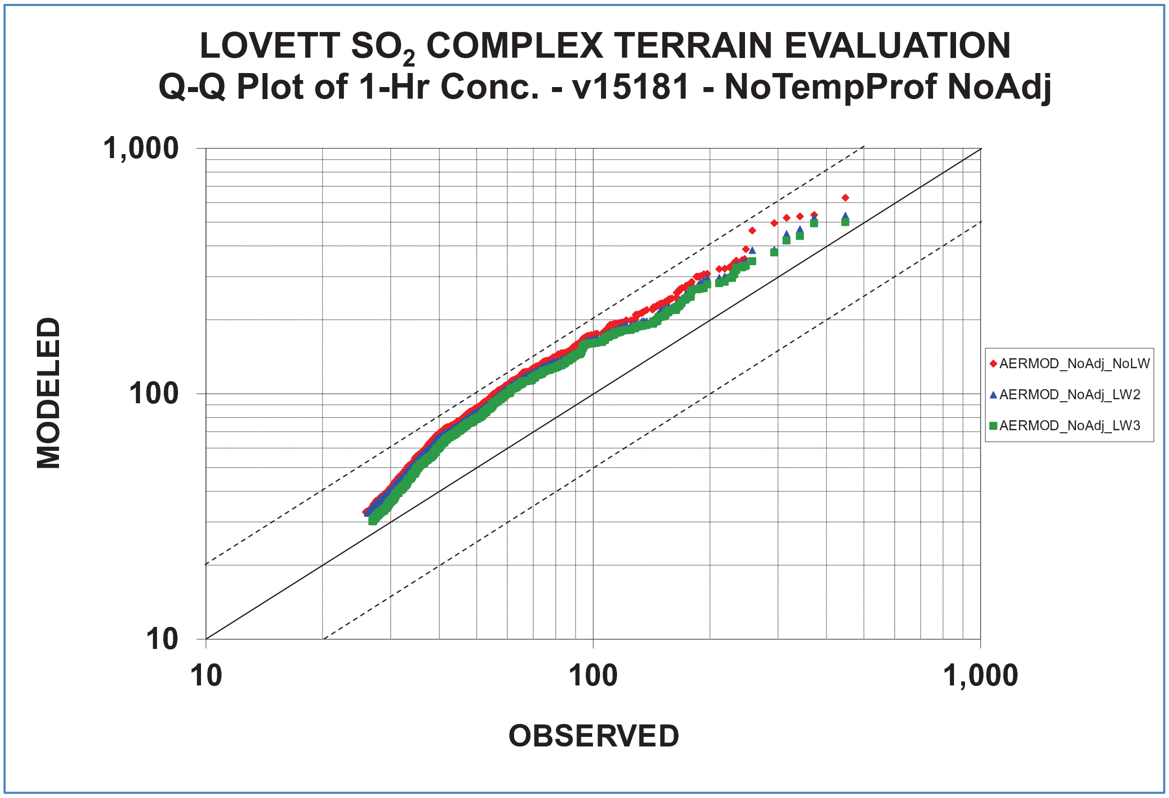

LOVETT SO2 COMPLEX TERRAIN EVALUATION
Q-Q Plot of 1-Hr Conc. - v15181 - NoTempProf NoAdj
1,000
100
10
MODELED
10
100
1,000
OBSERVED
AERMOD_NoAdj_NoLW
AERMOD_NoAdj_LW2
AERMOD_NoAdj_LW3

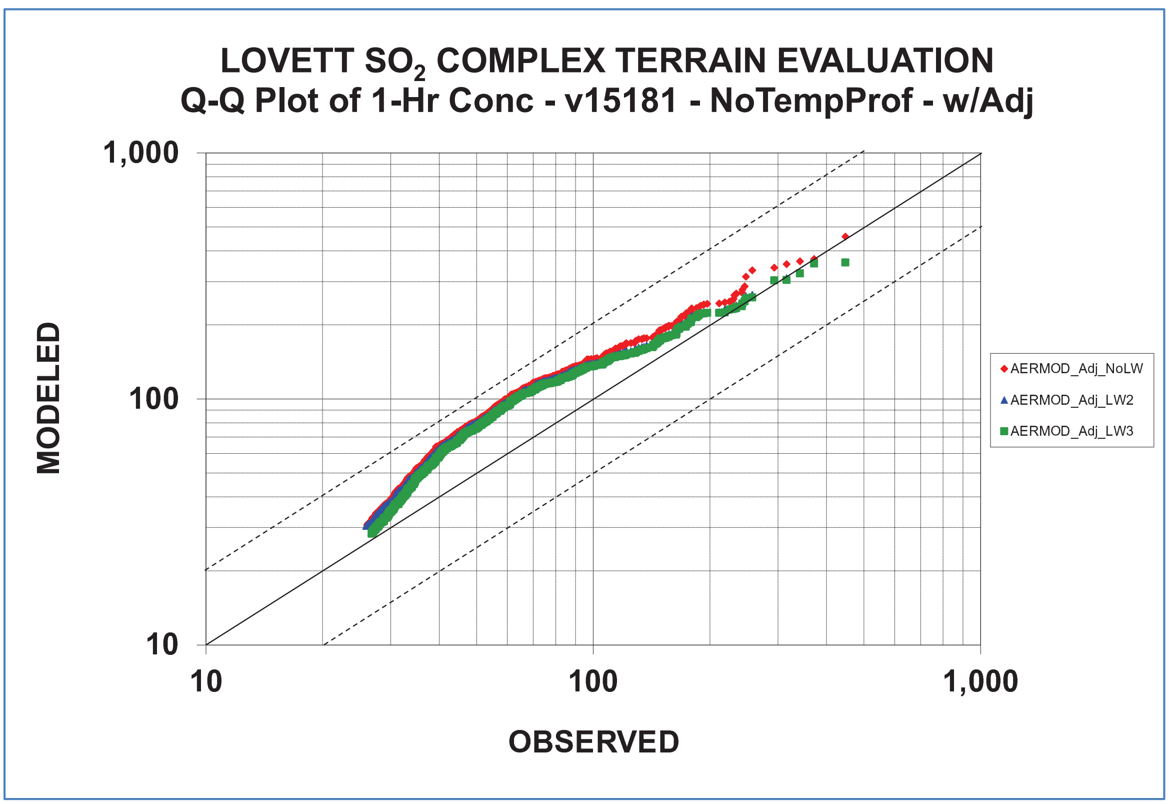

LOVETT SO2 COMPLEX TERRAIN EVALUATION
Q-Q Plot of 1-Hr Conc - v15181 - NoTempProf - w/Adj
1,000
100
10
MODELED
10
100
1,000
OBSERVED
AERMOD_Adj_NoLW
AERMOD_Adj_LW2
AERMOD_Adj_LW3

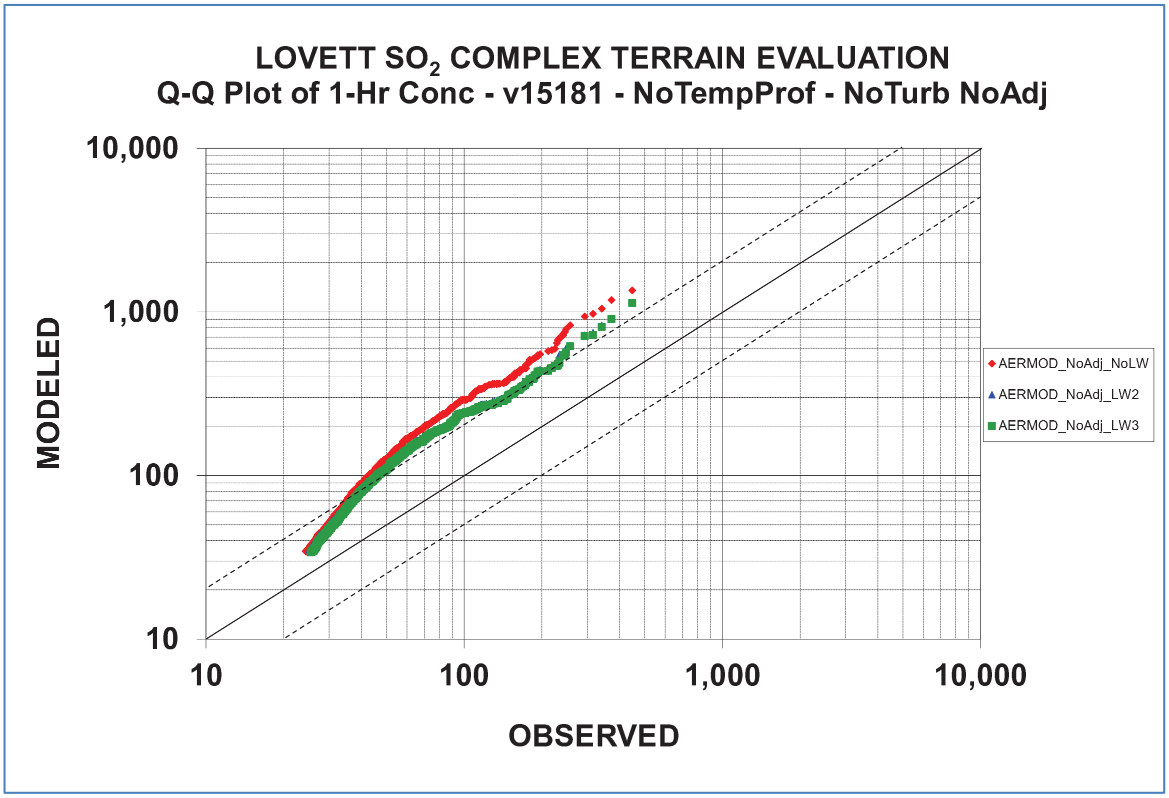
LOVETT SO2 COMPLEX TERRAIN EVALUATION
Q-Q Plot of 1-Hr Conc - v15181 - NoTempProf - NoTurb NoAdj
MODELED
10,000
1,000
100
10
10
100
1,000
10,000
OBSERVED
AERMOD_NoAdj_NoLW
AERMOD_NoAdj_LW2
AERMOD_NoAdj_LW3

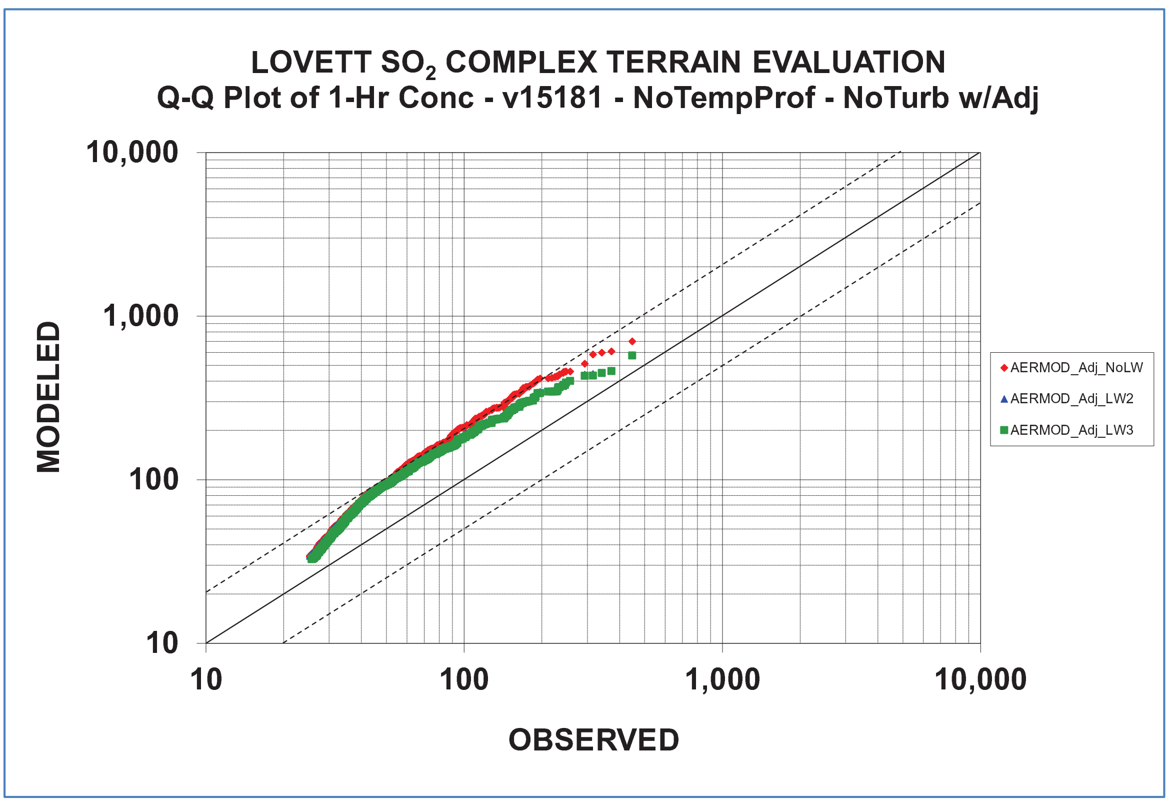
LOVETT SO2 COMPLEX TERRAIN EVALUATION
Q-Q Plot of 1-Hr Conc - v15181 - NoTempProf - NoTurb w/Adj
MODELED
10,000
1,000
100
10
10
100
1,000
10,000
OBSERVED
AERMOD_Adj_NoLW
AERMOD_Adj_LW2
AERMOD_Adj_LW3

Appendix D

Atmospheric Environment Paper on Source Characterization Refinements for Routine Modeling Applications

Atmospheric Environment 129 (2016) 55–67

Contents lists available at ScienceDirect

Atmospheric Environment

journal homepage: www.elsevier.com/locate/atmosenv

Source characterization refinements for routine modeling applications

Robert Paine, Laura L. Warren*, Gary E. Moore

AECOM, 250 Apollo Drive, Chelmsford, MA 01824, USA

HIGHLIGHTS

- Dispersion modeling source characterizations for unique facilities are described.
- Highly industrialized areas causing a heat island effect can be modeled as urban.
- Stacks with waste heat countering downwash can apply weighting to these effects.
- Extra rise for moist plumes is realistically estimated for use in "dry" models.
- Stacks in a row with merged plumes can be better represented to improve modeling.

ARTICLE INFO

Article history:
Received 24 September 2015
Received in revised form
18 December 2015
Accepted 4 January 2016
Available online 8 January 2016

Keywords:
Dispersion modeling
Model evaluation
Plume rise
Downwash
Source characterization

ABSTRACT

Steady-state dispersion models recommended by various environmental agencies worldwide have generally been evaluated with traditional stack release databases, including tracer studies. The sources associated with these field data are generally those with isolated stacks or release points under relatively ideal conditions. Many modeling applications, however, involve sources that act to modify the local dispersion environment as well as the conditions associated with plume buoyancy and final plume rise. The source characterizations affecting plume rise that are introduced and discussed in this paper include: 1) sources with large fugitive heat releases that result in a local urbanized effect, 2) stacks on or near individual buildings with large fugitive heat releases that tend to result in buoyant "liftoff" effects counteracting aerodynamic downwash effects, 3) stacks with considerable moisture content, which leads to additional heat of condensation during plume rise – an effect that is not considered by most dispersion models, and 4) stacks in a line that result in at least partial plume merging and buoyancy enhancement under certain conditions. One or more of these effects are appropriate for a given modeling application. We present examples of specific applications for one or more of these procedures in the paper.

This paper describes methods to introduce the four source characterization approaches to more accurately simulate plume rise to a variety of dispersion models. The authors have focused upon applying these methods to the AERMOD modeling system, which is the United States Environmental Protection Agency's preferred model in addition to being used internationally, but the techniques are applicable to dispersion models worldwide. While the methods could be installed directly into specific models such as AERMOD, the advantage of implementing them outside the model is to allow them to be applicable to numerous models immediately and also to allow them to remain applicable when the dispersion models themselves are updated. Available evaluation experiences with these techniques, which are discussed in the paper, indicate improved model performance in a variety of application settings.

1. Introduction

The AERMOD dispersion model (Cimorelli et al., 2005), recommended by United States Environmental Protection Agency (USEPA) for general short-range modeling applications out to a distance of 50 km, is widely used in air quality permit and compliance applications on an international scale (EPA Victoria, 2015). This model has been tested and evaluated against a number of traditional stack release databases (USEPA, 2003). However, aside from traditional building downwash situations, model evaluations for AERMOD and models used in other countries generally

* Corresponding author.
E-mail address: laura.warren2@aecom.com (L.L. Warren).

http://dx.doi.org/10.1016/j.atmosenv.2016.01.003

Abbreviations

ADMS	Atmospheric Dispersion Modelling System, an air quality dispersion model used for industrial emissions developed by Cambridge Environmental Research Consultants
AERMOD	A short range, steady-state air quality dispersion modeling system developed by the American Meteorological Society/U.S. Environmental Protection Agency Regulatory Model Improvement Committee (AERMIC)
ASTER	Advanced Spaceborne Thermal Emission and Reflection Radiometer, an instrument aboard the polar orbiting satellite called Terra
CALPUFF	A non-steady state air quality dispersion modeling system used for long range transport maintained and distributed by Exponent
HIA	Highly Industrialized Areas
OML	Short range air quality dispersion model that incorporates low wind effects related to aerodynamic downwash
PRIME	Plume Rise Model Enhancements, a building downwash algorithm used in the AERMOD model
SCICHEM	SCIPUFF air quality dispersion modeling system that includes chemistry
SCIPUFF	Second-order Closure Integrated Puff, an air quality dispersion modeling system maintained and distributed by Sage Management
SO_2	Sulfur Dioxide
TAPM	The Air Pollution Model, a photochemical grid modeling system
USEPA	U.S. Environmental Protection Agency

do not include scenarios in which the emission source itself substantially alters the dispersion environment. Because model performance can be an even greater challenge for some nontraditional emission sources, accurate representation of the source and its surrounding environment that influence plume rise is important.

To address this general issue, we have implemented and tested four different source characterization procedures with AERMOD, which could also be implemented in other models. All of these approaches affect buoyant plume rise, and in the case of the urban approach for highly industrialized areas, also affects plume dispersion. These approaches are different than other dispersion modeling refinements that might affect chemical transformation of released pollutants (such as NOx) because they generally do not change meteorological processing or dispersion (except for the urban approach). These effects are also independent of (and do not duplicate or replace) the low wind AERMOD enhancements described by USEPA (2012). While AERMOD itself could be modified to incorporate these changes, applying the source characterizations outside the model is beneficial because the procedures can be applicable to other dispersion models and would be more readily available for implementation. Any model changes to AERMOD would likely take several years for formal incorporation into the USEPA regulatory version. Therefore, as designed, each of the advanced plume rise techniques can be performed now using processors outside of AERMOD. In countries where other models are recommended, the methods described in this paper can be considered for those models as well. Other models for which these approaches could be used include, among others, CALPUFF (Scire et al., 2000), The Air Pollution Model (TAPM) (Hurley, 2008), Atmospheric Dispersion Modelling System (ADMS) (CERC, 2015), SCIPUFF (Sykes et al., 1999), and OML (Olesen et al., 2007).

The first source characterization method addresses sources with large "fugitive" heat releases that result in a local urban-like dispersion environment. As used in this paper, "fugitive" refers to sources of heat that are not specifically considered as input to the dispersion model. While the stack exhaust temperature and velocity are considered for plume rise calculations, the heat releases of unrelated processes in large industrial complexes are generally ignored, although they affect the dispersion environment, as noted below. AERMOD estimates urban heat island effects using an urban/rural classification based on population or land use (USEPA, 2004a), but it does not consider the effects created by large industrial complexes located in remote, rural areas. The "highly industrialized area" (HIA) effect can be addressed by a technique that accounts for the heat from an industrial complex and derives an effective urban population equivalent to the scale of the HIA as input to AERMOD, which would model the source as urban.

A second source characterization issue unaccounted for within AERMOD is similarly related to fugitive heat releases on or near individual buildings that affect plume rise from nearby stacks. These unaccounted-for heat releases generally occur on a horizontal scale well below a kilometer and affect stack plume rise in the vicinity of individual buildings. While the areal extent of the fugitive heat releases may be too small to qualify as an urban-like HIA, they can exhibit a tendency to cause buoyant effects that counteract localized aerodynamic downwash effects that would otherwise result in plumes being caught in downdrafts behind buildings. Building aerodynamic effects are handled within AERMOD by the Plume Rise Model Enhancements (PRIME) (Schulman et al., 2000) model, which was developed with limited evaluation in low winds or with buildings associated with fugitive heat releases. To account for downwash effects for cases with fugitive heat releases from buildings, a procedure called "LIFTOFF" is described, along with a model-to-monitor field study evaluation demonstrating improved prediction of receptor impacts.

Thirdly, stacks with substantially moist plumes can lead to latent heat release of condensation after the plume exits the stack, providing additional plume rise relative to a "dry" plume scenario. Although some of the initial added buoyancy is later lost due to partial evaporation, a net gain in plume rise occurs. AERMOD (and many other steady-state plume models) have plume rise formulations that are based on the assumption of a dry plume, in that the chimney plume is considered to be far from being saturated and carries essentially no moisture. A procedure to incorporate the moist plume effect by adjusting the input exit temperature data can be performed prior to an AERMOD model analysis using a pre-processor called "AERMOIST." This pre-processor makes use of a European validated plume rise model called "IBJpluris" that already incorporates moist plume effects and has been found to accurately predict the final rise of a moist plume (Janicke and Janicke, 2001; Janicke Consulting, 2015). The adjustments to plume rise using IBJpluris with and without moist plume effects can be transferred to AERMOD (or other models, as appropriate) by adjusting the input stack temperature of each affected source on an hourly basis, as a function of ambient temperature and relative humidity.

Finally, multiple stacks in a line can result in plume merging and buoyancy enhancement under certain conditions. The tendency of adjacent stack plumes to at least partially merge is a function of several factors which include the separation between the stacks, the angle of the wind relative to the stack alignment, and the plume rise for individual stack plumes (associated with individual stack buoyancy flux and meteorological variables such as stack-top wind speed). A procedure called "AERLIFT" has been created as a processor that works in conjunction with AERMOD for assessing and incorporating plume merging from aligned emission sources. It uses an hourly emissions file from an initial AERMOD run to refine the exhaust characteristics of the merging plumes on an hourly basis, and then AERMOD is run a second time with this new input of effective hourly exhaust parameters for each affected source.

In the sections below, we discuss the formulation and implementation of each of these source characterization effects. Note that these effects are generally independent from each other and can be run in combination, if appropriate. For example, in the case of a large industrial facility such as a steel mill, the characterization for a modeling application could include the urban characterization, liftoff effects of the plumes near buildings, moist plume effects (e.g., quench towers), and partial merging of plumes from stacks in a line.

2. Highly industrialized area heat islands

The urban heat island effect is a well-known phenomenon as it relates to urban and suburban areas that experience higher temperatures when compared to their rural surroundings. The key issue for plume dispersion in an urban area is that the urban heat island prevents the boundary layer from becoming stable at night, and results in weakly convective mixing at night within a deeper layer than that which exists in rural areas.

Urban surface characteristics such as albedo and surface roughness continuously affect boundary layer parameters (USEPA, 2004a). However, the boundary layer structure is most influenced by these urban surface characteristics at night (Oke, 1998). At night, an urban boundary layer is created when stable rural air reaches a warmer urban surface. Because buildings and urban surfaces trap heat more efficiently than rural areas, urban areas are slower to cool at night than the rural environments.

AERMOD currently accounts for urban environments by adjusting the urban area's surface heat flux and boundary layer height based on the urban-rural temperature difference of the urban core's temperature to the neighboring rural area's temperature (USEPA, 2004a). To calculate the urban-rural temperature difference, $\Delta T_{u\text{-}r}$, population information is used in the following equation:

$$\Delta T_{u-r} = \Delta T_{max}[0.1 \ln (P/P_o) + 1.0] \quad (1)$$

where $\Delta T_{max} = 12$ K, $P_o = 2{,}000{,}000$, the population related to the maximum temperature difference in Oke (1973, 1978, 1982), and P is the population of the urban area being modeled (USEPA, 2004a). AERMOD uses the population input value to simulate the height of the urban boundary layer.

The area of population considered for input into this AERMOD model formulation is defined using methods described in USEPA model guidance (USEPA, 2005). For locations considered to be isolated urban areas, published census data are used. Guidance further states that, "[f]or urban areas adjacent to or near other urban areas, or part of urban corridors, the user should attempt to identify that part of the urban area that will contribute to the urban heat island plume affecting the source(s)." (USEPA, 2015) For other situations, the user may determine the population within the area where the population density exceeds 750 people per square kilometer as described in the AERMOD Implementation Guide (USEPA, 2015).

To determine upward surface heat flux, H_u, resulting from the urban-rural temperature difference at night, the following relationship can be derived:

$$H_u = \alpha\, \rho\, c_p\, \Delta T_{u-r} u_* \quad (2)$$

where α is an empirical constant (0.03) described in the AERMOD model formulation document, ρ is the density of air (about 1.2 kg/m^3), c_p is the specific heat at constant pressure (1 W-s/g-K), and u_* is on the order of 0.1 m/s (USEPA, 2004a). This equation can be solved for $\Delta T_{u\text{-}r}$ (in units of K):

$$\Delta T_{u-r} \approx H_u/4 \quad (3)$$

where H_u is the anthropogenic heat release in units of watts per square meter in the "urban core."

A lesser known cause of urban heat island effects, and unaccounted for in AERMOD, but described by Hanna and Britter (2002) is an industrial complex that mimics a heat signature similar to cities. Fugitive heat releases at industrial facilities can be equivalent to the level of heat trapped by urban surfaces and buildings, and contribute to the effects seen in highly industrialized areas on a more compact scale, but more centered at the location of the emissions. These HIAs are not considered in the traditional urban classification approaches used for AERMOD, even though Irwin (1978) suggested this approach in an internal USEPA memo. The population near such areas is often much reduced because of zoning issues, and the area beyond the immediate industrial park may be rural in nature, resulting in a misleading characterization for this type of source. This mischaracterization was recognized in an independent study by Schewe and Colebrook (2013), who recognized the appropriateness of the urban approach for a large industrialized area.

2.1. Surrogate population for highly industrialized area characterization

Based upon Irwin's suggestions and with some adaptations to the AERMOD formulation, we are providing an approach here to specify a nontraditional type of urban source that is subject to urban dispersion due to industrial anthropogenic heat release rather than due to the presence of a traditional city. The user would specify the anthropogenic heat flux resulting from the source, or an urban-rural temperature difference, if available. This would be used to determine a surrogate "effective" population value for input to AERMOD. The effective population could be calculated through the use of eq (1) if $\Delta T_{u\text{-}r}$ is specified or eqs (1)–(3) if the anthropogenic heat flux is specified. A value of $\Delta T_{u\text{-}r}$ less than 3–4 K is likely insufficient to support an urban designation with a large effective population because, according to eqs (1)–(3), the resulting effective population would be too small (e.g., only 2,500 for a 4 K temperature difference). A more practical temperature difference threshold is about 8 K, which corresponds to an effective population of 70,000.

In eqs (2) and (3), it is important to note that the "urban core" of a HIA heat release (H_u) depicts an area with a horizontal extent of at least a few hundred meters on a side. In a follow-up to Hanna and Britter (2002), Dr. Hanna indicated that the minimum size of an industrial area needed to take on urban characteristics has been the subject of much discussion (Hanna et al., 2011; Hanna, 2014 – personal communication to authors). In his personal communication, Hanna referred to his 2011 reference (noted below) and indicated that an "expert elicitation" would likely result in a minimum size estimate of a few hundred meters. The anthropogenic heat release per unit area of major cities such as Indianapolis (extensively studied by the Electric Power Research Institute (EPRI) in the 1980s) would be on the order of 50 W/m^2. This value lies within the 10–100 W/m^2 range stated by Hanna et al. (2011) for urban areas.

2.2. Satellite analysis and model evaluation

A modeling study was undertaken using an evaluation database in Lake County in northwestern Indiana USA to test the performance of the AERMOD model for a HIA. Several AERMOD options were tested to determine the most representative scenario of 1-h average ground-level SO_2 modeled concentrations due to emissions from industrial complexes such as steel mills with respect to ambient monitoring stations in Gary and Hammond, Indiana (Fig. 1). The Gary monitor was located about 300 m from the nearest source, and generally within 2 km of the cluster of sources in close proximity to the monitor. The Hammond monitor was generally between 1 and 4 km away from nearby sources. Downwash effects, if present, would have affected the Gary monitor more than the Hammond monitor.

USEPA guidance for land use characterization indicated that this area should be modeled as rural, but the heat releases from the numerous iron and steel industry sources in this area create a dispersion environment that is effectively representative of an urban area with a large population.

For this model evaluation, the thermal imagery method was selected to determine the temperature difference between the populated areas and the industrial facilities. The procedures for conducting this estimate, discussed in more detail in open literature (e.g., Fung et al., 2009; Nichol, 2005; Voogt and Oke, 2003), are to obtain thermal infrared radiation (TIR) data for multiple time periods from polar-orbiting satellite instruments such as Advanced Spaceborne Thermal Emission and Reflection Radiometer (ASTER) and Landsat 8 (NASA, 2004; USGS, 2015). These data are then processed to account for surface emissivity, based on additional land use-related satellite data coinciding with the same time periods of interest, to derive a form of land surface temperature called brightness temperature. The satellite data used in these analyses must have relatively cloud-free skies so that the resulting temperature is representative of the ground rather than a cloud layer. The ASTER and Landsat 8 instruments have the ability to reliably detect land surface temperature perturbations as small as 1–2 K (Fung et al., 2009).

Whenever possible, multiple satellite images should be selected representing $\Delta T_{u\text{-}r}$ to examine diurnal trends as well as seasonal temperature variations of the HIA's surroundings. Ultimately, satellite data availability and the need for a nearly cloud-free image often limit a comparison of this nature. The $\Delta T_{u\text{-}r}$ uncertainty is reduced when the HIA emits heat at a constant rate such as steel, iron, or aluminum processing plants which generally operate 24 h per day, 7 days per week.

Brightness temperature in northwest Indiana was reviewed to estimate the temperature difference for the area of interest, derived from measurements by the ASTER instrument. On a summer day, maximum temperatures associated with industrial facilities were approximately 310–315 K which led to a temperature difference of about 11–12 K (Fig. 2). Although the satellite-measured temperature difference between the HIAs and the populated areas would often be greater at night, the temperature difference in this case was based upon a summer day due to satellite data availability. Note that this temperature difference measured by the satellite automatically accounts for the “urbanized” temperature excess of the HIA caused by the overall industrial heat releases not otherwise accounted for in the model. Using eq (1), this temperature difference was consistent with heavily populated areas with typical populations on the order of 1,000,000 instead of the region's U.S. Census Bureau population data of 10,000.

Three scenarios for the northwest Indiana application were run with building downwash and actual emissions for the year 2008 using AERMOD with default options: 1) rural land use, 2) urban land use with a small (actual) population of 10,000, and 3) urban land use with a large population of 1,000,000. Two model receptors were used to coincide with the SO_2 monitoring locations nearest to the facilities. In all three scenarios, the highest concentrations most frequently occurred during the night or early morning hours. The rural and small urban population modeling approaches led to AERMOD overpredictions of 1-h SO_2 as high as a factor of 10 at two monitors ranging from 1 to 10 km from the sources being modeled. The urban, large population scenario resulted in improved model performance by reducing the atmospheric stability at night, leading to higher plume rise and a deeper mixing layer for plume dispersion. The results still indicate that AERMOD overpredicted the 99th percentile daily maximum 1-h SO_2 ground-level concentration

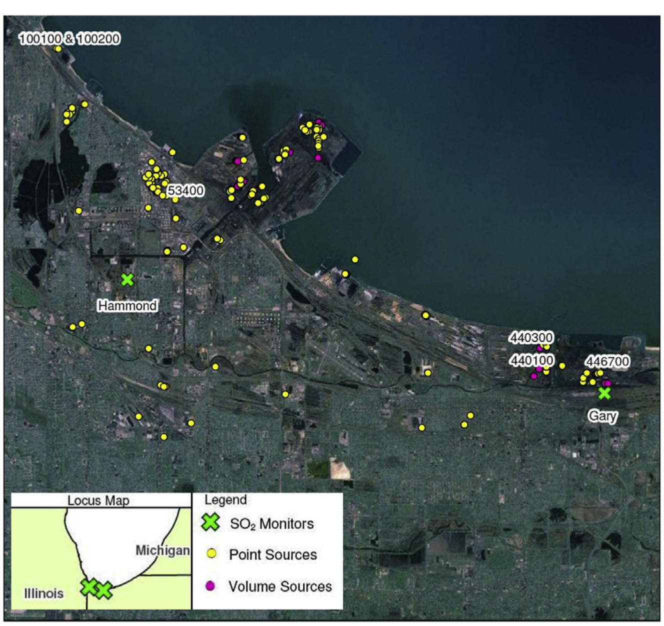

Fig. 1. Location of various emission sources in the Gary and Hammond, IN area in relation to the SO_2 ambient air monitors.

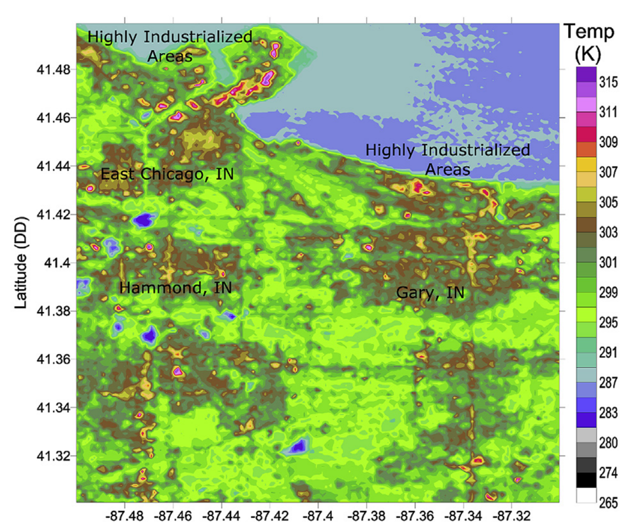

Fig. 2. Brightness temperature from ASTER band 14 on June 10, 2008 at 11 a.m. local time.

Table 1
AERMOD modeling results for rural and urban land use scenarios.

Monitor	Land use	Population	99th percentile of the daily maximum 1-h SO_2 ($\mu g/m^3$)
Hammond (96 $\mu g/m^3$)	Rural	NA	290.4
	Urban	10,000	935.5
	Urban	1,000,000	179.0
Gary (175 $\mu g/m^3$)	Rural	NA	1298.2
	Urban	10,000	1855.9
	Urban	1,000,000	392.2

Note: 1-h SO_2 99th percentile (4th highest) monitored values are listed in by monitor in parenthesis.

(which is the basis for the ambient standard in the United States) by a factor of about 2 at the Hammond and Gary monitors (Table 1). Additional refinements such as the use of liftoff effects as noted below might have further reduced this overprediction, but that analysis was not performed in this evaluation. In general, these results in comparison to the other scenarios indicate that improved model performance could be obtained by using an urban dispersion approach with an effective large population (e.g., on the order of 1,000,000).

Since actual rather than potential emissions were used in this evaluation, it is not likely that emission input uncertainty would cause the large overpredictions noted. It is possible that downwash effects are part of the overprediction problem, but such predictions are a function of the nocturnal temperature lapse rate, which is significantly different in urban vs. rural dispersion conditions in AERMOD. We strongly believe that the use of the urban characterization, as well as implementation of low wind speed improvements, are the enhancements leading to improved model performance. This northwest Indiana study involved the two monitors for which results have been reported. Additional case studies are needed to further verify these findings and approaches of which we present to encourage independent researchers to conduct such studies.

3. Plume liftoff in industrial complex environments with fugitive heat and low wind conditions

AERMOD estimates building downwash effects by applying its downwash model, PRIME, concentration estimates in the near-field where building wakes are predicted, while transitioning to the AERMOD estimates without building wake considerations in the far field (USEPA, 2004a). This transition is performed without consideration of low wind speed conditions, which can lead to poor model performance, particularly when building aerodynamic effects are estimated by the model under nearly calm conditions. Downwash conditions in near calm winds are likely to be subject to the effects of wind meander, leading to an intermittent downwash effect in any given direction. Such low wind effects have not been adequately evaluated.

In the current AERMOD implementation using default model options on a facility with short stacks close to the heights of nearby buildings, very high 1-h ground-level concentrations due to building downwash have been found by the authors to be predicted even with nearly calm winds in stable conditions. The top three predicted concentrations occurred with wind speeds less than 1.5 m/s. This is a condition for which persistent downwash effects might not be expected due to strongly buoyant plumes and weak building aerodynamic effects. For example, the CALPUFF model (Scire et al., 2000) does not consider building downwash to occur for wind speeds less than 0.5 m/s. In discussions among co-designers of the PRIME downwash algorithm in AERMOD, Dr. Lloyd Schulman and Mr. Robert Paine, Dr. Schulman confirmed that the PRIME downwash algorithm was never tested for such light wind, stable conditions, and there is no mechanism in the model for addressing the lack of or intermittent nature of the wake behind a building in very light wind conditions (Schulman, personal communication to the author, November 4, 2011). The model is assuming a plume is caught in a building wake, even in such light wind conditions, and then impacting ground-level receptors at the fenceline under very low dilution conditions. Note that when the PRIME algorithm was developed, modeling and evaluating downwash under very light winds was not a major concern when airport wind speeds in the United States were not reported below 3 knots (about 1.5 m/s). In recent years, the further use of sonic anemometers at airports and the processing of 1-min data have made the need to accommodate very low wind speeds a significant challenge. It is also noteworthy that for airport databases (including that for the northwest Indiana study), there are no turbulence measurements, and so the simulation of turbulence is affected by the boundary layer parameterization. This is one reason why the use of urban dispersion and possibly the low wind improvements to AERMOD will lead to better performance for the plume liftoff field study and its associate model evaluation presented in more detail in a subsequent section. To the extent that building downwash may be a factor, it should be noted that the depth of the enhanced turbulence region in PRIME may be overstated, as indicated by Petersen (2015).

In light winds with significant wind meander, building wake effects are unsteady, as noted by Robins (1994). However, AERMOD's basic meander treatment for low winds only applies to non-downwash dispersion, and was never implemented in the PRIME model within AERMOD. Therefore, the building downwash impacts due to PRIME predictions do not account for the intermittency of downwash effects that would tend to reduce hourly-averaged ground-level concentrations in one location. A downwash approach that accounts for low wind speeds and the inherent intermittency of steady wake effects under such conditions is already incorporated into regulatory models similar to AERMOD such as the Danish OML model (Olesen and Genikhovich, 2000) and the United Kingdom ADMS model (Robins et al., 2013).

In addition to the mistreatment of low wind conditions, a plume is able to gain buoyancy within an environment where the source's buildings provide fugitive heat on a smaller scale in comparison to a highly industrialized area. AERMOD and other steady-state plume models do not consider the additional buoyancy plume uplift due to these waste heat releases (in addition to stack releases of the pollutants of interest) in the area of an emission source, especially on or around the controlling building. An example of this is a cooler vent from taconite production furnaces; the vents do not release pollutants, but they duct very hot air to the building roof environment that will affect the aerodynamics around the building. For these cases with significant additional heat releases in the same vicinity, but not related to the pollutant stacks, plumes will resist downwash effects, especially in light wind cases. This resistance allows the plume to avoid downdrafts behind the building, which are nullified by "liftoff" conditions due to the excess heating (Hanna et al., 1998).

3.1. The LIFTOFF approach

The heat flux associated with thermal releases triggering plume liftoff can be estimated and used in an alternative approach with the use of a buoyancy flux term, F_b. Hanna et al. (1998) suggest a combined dimensionless buoyancy flux:

$$F^{**} = F_b/\left(W\,U^3\right) \quad (4)$$

where F_b is the buoyancy flux, U is a reference wind speed, and W is the initial plume width. An approach that can be used as a post-processor to any dispersion model such as AERMOD, called "LIFTOFF", accounts for conditions with no downdraft effects using a weighting factor between one extreme (liftoff conditions, no downwash) and non-liftoff conditions (normal downwash) modeled in separate AERMOD runs. This weighting factor, γ, ranges from 0 to 1 on an hourly basis (Hanna et al., 1998):

$$\gamma = \exp\left(-6F^{**0.4}\right) \quad (5)$$

where with large buoyancy, the downwash weight approaches 0 and with minimal buoyancy, it approaches 1. To perform these calculations, an estimate of the heating is needed for the buoyancy flux term, F_b. To quantify the combined effects of the heat release, wind, and plume width, it is necessary to estimate these values. Once these values are obtained, the final calculation can be performed using the hourly weighting factor between modeled concentrations with and without downwash ($C_{Downwash}$ and $C_{No\ Downwash}$, respectively) to determine the final LIFTOFF concentrations, $C_{LIFTOFF}$:

$$C_{LIFTOFF} = \gamma\, C_{Downwash} + (1-\gamma)\, C_{No\ Downwash} \quad (6)$$

To account for low wind effects, LIFTOFF reads the 10-m reference wind speed information from the AERMET SURFACE file for each hour. In combination with the heat release and plume width information, LIFTOFF applies a weighting scheme as shown in eq (6), which is similar to the dependence on the wind intermittency for the approach used in the OML model (Olesen and Genikhovich, 2000). In general, during low wind events, it is expected that the no-downwash solution will be weighted more heavily than the downwash solution. The degree of weighting is also dependent upon the magnitude of the heat release and the initial plume width which is conservatively taken to be as large as the building width. Although the USEPA's Building Profile Input Program (USEPA, 2004b) is generally used to determine the building width, these input values can be manually edited in the event that this pre-processor overestimates the effective building width which can occur when the wind direction coincides with a long and narrow building.

For modeling applications without source-related fugitive heat releases, LIFTOFF should not be used because the calculated effect will be zero with no heat release rate. It is likely that the current PRIME model overpredicts in low winds due to its lack of considering wind meander and the related intermittent wake effects. However, with fugitive heat releases, there is a dependency of the liftoff potential on wind speed because a high wind speed would tend to dilute the effects of the heating. Therefore, the dependence of the LIFTOFF approach on all three components: heat release rate, wind speed, and initial source width is warranted. It is important, however, that any current evaluations of LIFTOFF with a substantially modified PRIME model would be useful to determine whether the weighting factor between the downwash and no downwash solutions should be adjusted.

For buoyancy effects due to source-related heat release scenarios, LIFTOFF calculates F^{**} and applies the resulting weighting factor between the downwash and no downwash model runs. These calculations are performed for each hour using the wind direction and require building width information which serves as a conservatively large estimate of the initial plume width. Additionally, an estimation of the heating is needed for the buoyancy flux term. External heating measurements can be obtained from an engineering evaluation or by estimating the temperature excess in satellite thermal imagery data using the same procedure described to estimate $\Delta T_{u\text{-}r}$ for a highly industrialized area. The temperature difference is used to solve for H_u in eq (3), where the buoyancy flux, F_b, is proportional to the heat release rate, H_u (USEPA, 1995; Briggs, 1969).

3.2. Model evaluation case study of the LIFTOFF approach

Model performance of the LIFTOFF procedure at an industrial facility featuring process areas with considerable fugitive heat releases was assessed using data from a three-month field study with four SO_2 monitors located on-site. These SO_2 monitors were oriented around the facility's three point sources in areas where the highest modeled impacts occurred based on AERMOD using default options and downwash without consideration of liftoff conditions. Monitors were approximately 400–1200 m away from the point sources (Fig. 3). The buildings affecting the point sources are shown in Fig. 4. The aspect ratio of the horizontal to vertical building dimensions was approximately 2.5:1.

Using the facility's continuous emission monitor data, several model scenarios were tested including AERMOD with default options and building downwash, AERMOD with default options and no building downwash, and the LIFTOFF technique. Although the facility was located in an isolated, rural area, it had a significant source-to-ambient temperature difference of approximately 8 K as measured by satellite imagery (Fig. 5). The area of fugitive heat was approximately 300 × 600 m, leading to a heat release of approximately 6 MW.

Modeled and monitored 1-h ground-level concentrations were

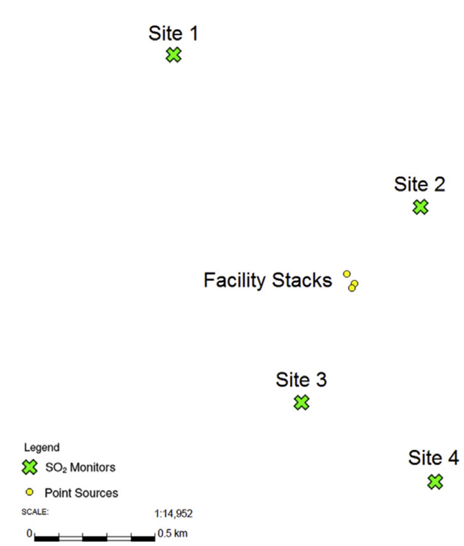

Fig. 3. At left, the industrial facility point source emissions in relation to SO_2 ambient air monitor locations.

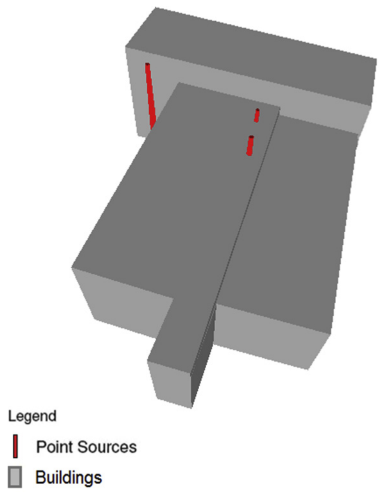

Fig. 4. At right, a 3D view, looking toward the northeast, of the industrial facility's building dimensions and point source locations.

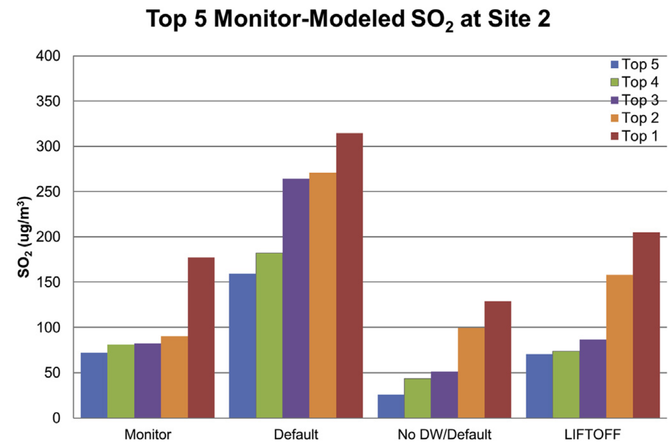

Fig. 6. Top 5 ranked daily maximum 1-h SO_2 at site 2. "Default" uses default options and downwash. "No DW" uses default options without downwash effects. "LIFTOFF" refers to the approach weighs the downwash and no downwash effects on an hourly basis.

ranked from highest to lowest and compared. In general, for the top five ranked concentrations, AERMOD with downwash indicated large overpredictions, while AERMOD without downwash exhibited a modest underprediction tendency. However, the LIFTOFF scenario (which is a weighted average of the downwash and no downwash cases computed from hourly wind and building dimension data) was relatively unbiased, and generally exhibited a modest overprediction tendency as shown by Fig. 6 for Site 2. Site 2 is the location that measured the highest SO_2 concentration during the field study. At all monitors, the top five ranked LIFTOFF concentrations were generally higher than the top five ranked observations, which is most evident in quantile-quantile comparisons of monitored to modeled concentrations as shown in Fig. 7 for each site. The LIFTOFF results have a modest overprediction and avoid the large overpredictions that are evident if no consideration is made for the fugitive heat release. More information on this model evaluation is provided in the corresponding supplemental material.

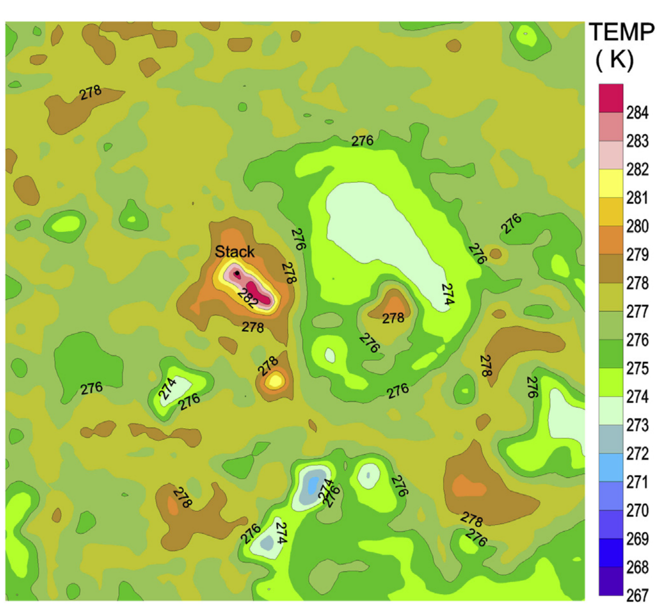

Fig. 5. Brightness temperature from Landsat 8 TIR band 11 April 21, 2013 10 p.m. local time.

4. Effects of a moist plume on plume rise calculations

The final plume rise formula in AERMOD and most other dispersion models is based on the assumption of a dry plume, where the stack plume is far from being saturated and carries essentially no liquid water load. However, in many cases for moist plumes, the effect on plume rise can be significant due to heat of condensation and should be accounted for, particularly for emission sources that operate flue gas desulphurization equipment, or scrubbers, designed to remove several pollutants from combustion plumes. The scrubbing process acts to partially or fully saturate exhaust gases while minimizing any liquid "drift" emerging from the scrubber to minimize chemically erosive processes. This process acts to cool the plume relative to the unscrubbed exhaust, resulting in a reduction of plume rise. However, the moist plume exits the stack and the heat of condensation released by the liquid water particles acts to make the plume gases warmer, giving the plume additional buoyancy. Some of this buoyancy is lost as the droplets evaporate on mixing, but a net gain in plume rise is realized from the heating/cooling process. The largest net rise is realized for the situation where the ambient air itself is near saturation.

A validated, moist plume rise model called "IBJpluris" has been found to accurately predict the final rise of a moist plume (Janicke and Janicke, 2001) and can be used to complement the dispersion modeling process when moisture content can be a significant factor. The IBJpluris model formulation includes a general solution for bent-over moist (initially saturated) chimney plumes (Janicke and Janicke, 2001). The model was reviewed by Presotto et al. (2005), which indicated that despite a number of entrainment formulas available, IBJpluris possessed the physical capability of representing the impacts of heat of condensation on symmetric chimney plume rise. The Presotto et al. (2005) paper also reported field evaluation results for the IBJpluris model involving aircraft measurements through moist plumes emitted by stacks and cooling towers. Therefore, IBJpluris was selected as the core model for developing and applying a simple adjustment method to the standard Briggs (1975) plume rise formula used by AERMOD to account for thermodynamic modification of plume rise.

4.1. The moist plume pre-processor

A method has been developed and incorporated into a pre-processor called "AERMOIST", whereby adjustments can be made

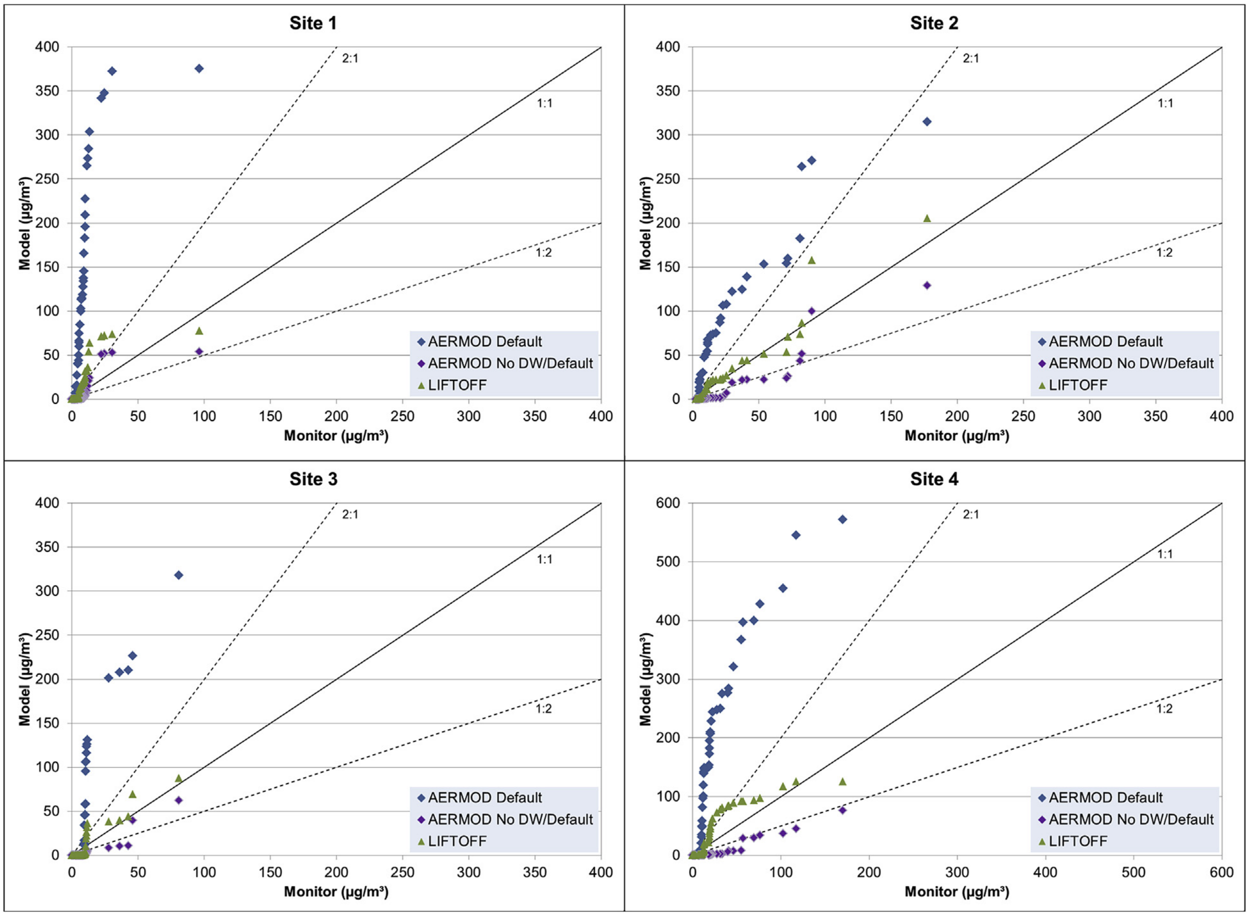

Fig. 7. Quantile-quantile comparisons between monitored and modeled daily maximum 1-h SO_2 concentrations at sites 1–4. "AERMOD Default" uses default options and downwash while "AERMOD No DW/Default" uses default options without downwash. "LIFTOFF" refers to the approach that weighs the downwash and no downwash effects on an hourly basis.

to better simulate the rise of a moist plume using a dry plume model like AERMOD. This is done by performing IBJpluris model runs for both the actual moist plume and a dry plume so that the adjustments for the difference can be made and transferred to hourly plume input data for models such as AERMOD. By assuming the ambient environment that the plume rises through is identical for both a dry and wet plume, a reasonable assumption is that the ratio of the wet to dry plume rise for IBJpluris can be used to adjust the dry dispersion model plume rise to a moist plume rise prediction:

$$[\Delta h_w(\text{model})]/[\Delta h_d(\text{model})] = [\Delta h_w(\text{IBJpluris})]/[\Delta h_d(\text{IBJpluris})] \quad (7)$$

where Δh is the change in final plume rise, and subscripts "w" and "d" correspond to moist and dry plumes, respectively. The approach assumes that this scaling ratio is independent from changes in wind speed and stability, although the variations in rise may be rather large. This assumption is reasonable since the rise is functionally related to the sum of exiting buoyancy and vertical momentum fluxes and the difference between dry and moist rise depends mainly on buoyancy, which is primarily temperature- and relative humidity-dependent.

The rising plume, by analogy, can be treated as if it were a rising moist thermal and cloud dynamic process. Concepts such as the buoyancy factor (Jacobson, 2005) can be applied since this same buoyancy factor appears in the Briggs (1975) dry plume rise. The major difference is that the cloud buoyancy depends on the virtual temperature, which depends on temperature, pressure, and relative humidity of both the plume and the environment. The buoyancy factor, F_b, for both plume and cloud water as normalized density can be expressed by the difference between plume temperature and ambient temperature, divided by the plume temperature, when virtual temperature is equal to dry bulb temperature. The approximate term appears in Briggs (1975) final plume rise formula for the dry buoyancy flux term. The final rise Δh_f is a power law function of F_b, where the power is '1/3' as derived by Briggs (1975). Following Jacobson (2005), the moist buoyancy can be expressed in terms of the virtual temperatures and water vapor partial pressures of the plume and the ambient environment as T_{va}, T_{vp}, and P_a, P_{wa}, P_{wp}, where P_{wp} is assumed to be saturated, P_s. The virtual temperature, T_v, can be expressed in terms of dry bulb temperature, T (Arya, 2001):

$$\begin{aligned} T_v &= T(1 + 0.608\, q_v) \\ &= T\{1 + 0.608[0.622\,(RH)\,P_s/(P_{da} + 0.622\,(RH)\,P_s)]\} \end{aligned} \quad (8)$$

where q_v is the mixing ratio in kg of moisture per kg of dry air, P_{da} is the dry atmosphere pressure, and RH is relative humidity as a fraction. For a plume exit temperature of 325 K, the virtual temperature of a saturated plume is 390 K. As the saturated plume temperature increases, so do the effects of virtual temperature, especially for higher stack temperature and relative humidity.

Using a relationship for estimating the saturation vapor pressure of water derived from the Clausius-Clapeyron equation (Arya, 2001), the relative humidity of a plume can be estimated from the moisture content (%) at the plume exit temperature:

$$P_s = 6.112 \exp\{6816[(1/273.15) - (1/T)] + 5.1309 \ln(273.15/T)\} \quad (9)$$

where all pressures are in hectopascals (millibars). The IBJpluris model has the ability to treat sub-saturated plumes as long as the plume emission temperature is held constant. Using eq (9) and the moisture content of the exiting plume, the relative humidity of the plume can be estimated. As the ambient air retains more moisture, the plume travels higher before reaching equilibrium with the ambient air.

4.1.1. Equivalent dry plume temperature approach

An effective approach for representing moisture in plumes is to adjust only the plume temperature rather than changing both plume and ambient temperatures, which would be required if virtual temperature were to be used directly. This revised plume temperature is generated by AERMOIST and can be referred to as an "equivalent dry plume temperature", and it is always greater than the original plume temperature and does not equal the virtual temperature. This hourly equivalent plume temperature is input to a dispersion model such as AERMOD in an hourly emissions input file so that the moist plume rise is more accurately modeled. The scaling relationship based on the right hand side of eq (7) forms the first part of the adjustment model. The plume height scaling parameter is given by the moist over the dry buoyancy flux:

$$\beta = \left(\Delta h_w^3 \middle/ \Delta h_d^3\right) \quad (10)$$

where subscripts w and d refer to moist and dry buoyancy fluxes, respectively.

Two equations relating final rise to equivalent plume and ambient temperature are:

$$\Delta h_d^3 = \lambda F_{bdry} = \lambda\left[(T_p - T_a)/T_p\right] \quad (11)$$

$$\Delta h_w^3 = \lambda F_{bwet} = \lambda\left[(T_p^{eq} - T_a)/T_p^{eq}\right] \quad (12)$$

The exponent of 3 in eq (10) is due to the Briggs (1975) plume rise dependence on the buoyant flux, F_b, to the '1/3' power. As the vertical momentum flux becomes a larger fraction of the total flux, the effective exponent for the buoyant rise becomes smaller because the momentum plume rise is proportional to the momentum flux, F_m, to the 1.5 power. In AERMOIST, the exponent is treated as a user input to be conservative (<3) when the total plume rise may have appreciable momentum at release. A smaller buoyant rise exponent, such as 2.5, helps to insure that the model is conservative and the plume rise is not overstated.

From the equations stated above, the equivalent plume temperature, T_p^{eq}, can be solved for directly as:

Table 2
Moist plume characteristics used in the test case.

Stack height (m)	Exit diameter (m)	Exit temperature (K)	Exit velocity (m/s)
171.45	14.23	325.37	15.16

$$T_p^{eq} = T_p\, T_a/\left[(1-\beta)T_p + \beta T_a\right] \quad (13)$$

The ratio, β, is a function of both humidity and temperature and is found by the dry and moist IBJpluris simulations. As β goes to 1, the equivalent plume temperature approaches the dry plume temperature, T_p.

To provide the hourly equivalent plume temperature to AERMOD, a simple interpolation bilinear model is constructed using a series of βs across a range of temperature and relative humidity. At the end points of each range, β is calculated using IBJpluris and applied in a Taylor first-order expansion to create a bilinear model for the wet to dry ratio of plume rise within each range, $\beta(T_a,RH_a)$. The model assumes that ambient air at stack exit will be in the range from 253 to 313 K. Ambient temperatures outside of this range are clipped. The ambient relative humidity is assumed to lie between 0% and 95%. Values above 95% are clipped because these lie in a range of extreme sensitivity to conditional instability.

In AERMOIST, the IBJpluris model is exercised in both dry and wet mode for each range and an array of temperatures and humidity over the range of possible values, $\beta(T_i,RH_j)$ ratios, is saved for each stack that is modeled and are used to estimate the model adjustment coefficients, $C_{i,j}$ and $D_{i,j}$. The continuous model for the moist to dry plume rise ratio becomes:

$$\beta(T_a, RH_a) = \beta(T_i, RH_j) + (T_a - T_i)\, C_{i,j} + (RH_a - RH_j)\, D_{i,j} \quad (14)$$

The $\beta(T_a,RH_a)$ are used to estimate the equivalent hourly plume temperatures for input to the dispersion model for each hour of emissions. By modifying only the plume temperature, multiple sources can be included in the model run, each with their own series of equivalent hourly plume temperatures. Dry plumes can also be modeled with standard, constant input data.

4.1.2. Moist plume rise testing

The IBJpluris model was exercised for a typical saturated, scrubbed power plant, with characteristics as listed in Table 2. The exiting plume moisture content for this test stack is 13.4%, and for a surface pressure of 1000 hPa, $P_s = 134$ hPa which, according to eq (8), translates into a saturated plume ($RH_p = 100\%$) for an observed stack temperature of 325 K. The source's plume characteristics suggest that such an observed temperature (dry bulb) is actually near 340 K in terms of the virtual temperature for the saturated plume.

The profile used by AERMOIST assumes neutral conditions with a height constant humidity and turbulence profile. For a given environmental humidity value, the plume was modeled with dry humidity (0%) and a moist humidity based on the actual moisture content of the plume. The resulting plume rises as a function of downwind distance are illustrated for the dry (0% RH_p) and the moist (100% RH_p) plume cases with a dry ambient humidity (0% RH_a), and for a saturated plume emitted into a nearly saturated environment in Fig. 8. The rise at 2000 m downwind is 189.8 m for the dry plume and dry environment, 209.3 m for a saturated plume in a dry ambient environment, and 219 m for the saturated plume rise in a 90% constant RH environment. At an ambient temperature of 293 K, the percent increase over the dry case is 10.3% and when a moist environment is considered, it is 15.4%.

AERMOIST systematically exercises IBJpluris for each of the temperatures and relative humidity ranges (bins). Assuming final rise estimates at 2000 m downwind for a select set of temperature and relative humidity ranges, it is apparent that the largest rise of the saturated plume occurs at 90% humidity environmental conditions for the cooler ambient temperatures. The dependency on ambient humidity of final rise at any ambient temperature is rather

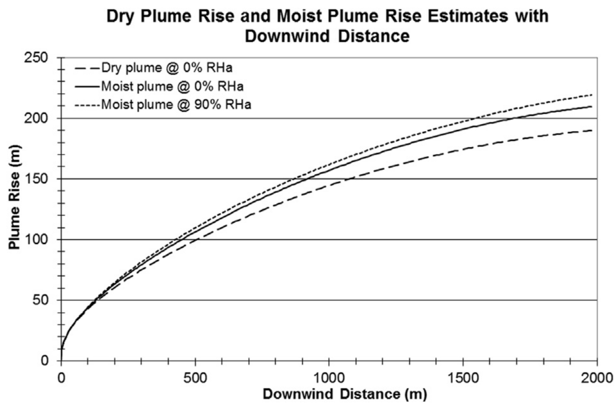

Fig. 8. Plume rise as a function of downwind distance for dry rise and an initially saturated plume by the test source for two constant relative humidity environmental conditions.

small for a dry plume, allowing for ambient RH to be ignored for dry plumes. However, moist plume rise will increase substantially as the ambient humidity approaches saturation with an increase of over 10% from dry, cool air to moist cool air. Using virtual temperature by itself does not explain this effect. As the ambient temperature increases and the buoyancy factor decreases, the change in plume rise with humidity is reduced. The resulting equivalent plume temperatures for use in dispersion modeling generated by AERMOIST, which actually runs the validated IBJpluris plume rise model, produce improved plume rise estimates for moist plumes. As evaluated by Presotto et al. (2005), the IBJpluris model predicts a more realistic plume rise for moist plumes than a model that represents a moist plume as a dry plume. Therefore, using the AERMOIST technique in conjunction with a dry plume model such as AERMOD will result in improved model performance by reduction its inherent model overprediction.

5. Plume merging of stacks in a line

When adjacent stacks are positioned in a line, the individual plumes have shown to have a tendency to merge causing a buoyancy enhancement under certain conditions. This plume merging tendency is influenced by the stacks' proximity, the wind direction relative to the stack configuration, and individual stack plume rises. Briggs (1984), refers to the results of wind tunnel studies for a row of identical stacks that indicate the usefulness of a merger parameter, S′, to determine the effect of the angle of the wind relative to the stack alignment:

$$S' = (\Delta s \sin\theta) \Big/ \left[L_b^{1/3} (\Delta s \cos\theta)^{2/3}\right] \quad (15)$$

where Δs is the average spacing between the aligned stacks, θ is the wind angle relative to the alignment angle of the adjacent, inline stacks, L_b is the buoyancy length scale where:

- $L_b = F_b/U^3$,
- F_b is the buoyancy flux where $F_b = g\, V_s^2 D_s^2/4\, [(T_p - T_a)/T_p]$,
- U is the wind speed at plume height,
- V_s is the stack gas exit velocity,
- T_p is the stack gas temperature,
- T_a is the ambient temperature, and
- D_s is the stack diameter.

By definition, S′ is undefined when the wind is exactly normal to the alignment angle, so in practice for that case, an angle not exceeding 89.99° is used in the approach described in the next section.

Wind tunnel studies using neutral conditions showed that S′ less than 2.3 results in buoyancy enhancement while values above 3.3 indicate no enhancement (Briggs, 1984). Intermediate values would indicate partial enhancement. For those wind angles that allow plume merging, a formulation for the buoyancy enhancement accounting for other factors noted above due to the merging of adjacent plumes can be taken from the Manins implementation (Manins et al., 1992) of the Briggs formulation:

$$E = (N + S)/(1 + S) \quad (16)$$

$$S = 6\left\{[(N-1)\,\Delta s]/\left(N^{1/3}\,\Delta h\right)\right\}^{3/2} \quad (17)$$

where E is the buoyancy enhancement factor, N is the number of stack in the row, S is a separation factor, and Δh is the plume rise for one stack. While the buoyancy flux would be enhanced, the momentum flux should be unchanged. The formula for the momentum flux in AERMOD and many other dispersion models is:

$$F_m = (T_a/T_p)\, V_s^2\, D_s^2/4 \quad (18)$$

Therefore, the buoyancy enhancement would increase T_p and V_s in a manner to provide the appropriate multiplier to F_b while retaining F_m by retaining the ratio of V_s^2/T_p.

Several investigators noted in Briggs (1984) have studied and reported buoyancy enhancement for only two stacks. Briggs noted that "all of the authors referenced in this section compared the predictions of their models, at least for N = 2, with the semi-empirical results of Briggs (1974) and concluded that, as different as these approaches seem, their predictions were very similar." Additionally, the plume rise enhancements plotted in neutral conditions by Anfossi (1985) indicated that even for stacks separated by 77 m, some enhancement was observed in conditions of substantial buoyancy.

Additional supporting evidence for plume merging from two stacks is available from more recent journal articles. These articles are consistent in reporting an angular dependence on the extent of the merging. Macdonald et al. (2002) indicated that there is a definite enhancement for flow parallel to the line of stacks. For larger angles, due to dual rotors from plumes (clockwise looking downwind on the right side and counterclockwise on the left side), there can sometimes be some plume rise suppression between two closely spaced stacks for wind angles approaching a perpendicular to the line of stacks. These authors also noted plume rise enhancement for power plant stacks separated by a distance of more than 1 km, providing support for no arbitrary distance cutoff for this algorithm. The Briggs algorithm will automatically reduce the plume rise enhancement as the distance between the stacks increases.

Furthermore, Overcamp and Ku (1988) conclude that "tests with azimuthal angles of 0° and 30° showed enhanced rise". Tests with azimuthal angles of 60° and 90° did not appear to exhibit enhanced rise (Overcamp and Ku, 1988), information that was incorporated into the Briggs formulation. Similar confirmation of plume merging effects from two identical, separated stacks is documented by Contini et al. (2006). The dependence of the enhanced buoyancy on the approach angle to the stacks is similar to findings by the other investigators.

5.1. The AERLIFT technique

The AERLIFT technique has been developed to account for potential merging of plumes from aligned emission sources and the resulting partial to full enhanced plume buoyancy. This intermediate processor, run outside of the AERMOD modeling system for this implementation, creates an enhanced hourly emissions file using information from an initial model run with information for effective stack exhaust characteristics of the partially merged plumes. The model is then run a second time using the adjusted source parameters.

To define the parameters necessary for calculating the buoyancy enhancement on an hourly basis, the initial dispersion model run for the stacks involved is set up to run with a 10-km ring of 360 receptors set 1° apart in flat terrain. Next, the AERLIFT processor takes the meteorology and the model output data (i.e., the hourly and source specific final plume rise and effective wind speed) to determine first whether plume merging occurs, and if so, by how much.

The maximum enhancement factor applied to the buoyancy flux is the number of stacks in the line. The AERLIFT processor applies the enhancement factor to the original stack velocity and temperature, and derives an altered set of parameters that increases the buoyancy flux by the appropriate factor while preserving the momentum flux. This is done to conservatively apply the enhancement to only the buoyancy component. During stable hours, AERLIFT uses the plume rise directly in eq (17). For added degree of conservativeness, during unstable hours for when the stack top is less than the mixing height, AERLIFT selects the minimum between the final plume rise and the mixing height, which is defined as the maximum of the mechanical and convective mixing heights, for use in eq (17).

Finally, a second dispersion model run is performed using the appropriate terrain options and modeling receptors for the emission source as well as the enhanced hourly emission file from AERLIFT.

5.2. Evaluation of AERLIFT

AERMOD has been tested with the AERLIFT approach with a model evaluation field study conducted by Eastman Chemical Company in Kingsport, Tennessee, USA (described by Paine et al., 2013; Szembek et al., 2013). This study featured a 1-year monitoring period with 4 monitors featuring a line of 5 coal-fired boiler stacks. The inclusion of the AERLIFT approach significantly reduced AERMOD overpredictions, as noted by Szembek et al. (2013). The need for this feature was particularly evident when plumes from a row of 5 stacks indicated overprediction for impacts at a monitor located in elevated terrain, in spite of other model improvements from the low wind options (adjusted u* and LOWWIND options in AERMOD). When this single feature was tested in isolation, it resulted in a higher plume rise and a better model evaluation result in both flat and elevated terrain. This improvement was due to the effect of AERLIFT on plume rise and the attendant effect on predicted concentrations.

6. Examples of source characterization applications

Examples of the use of both the highly industrialized area (urban) application and the LIFTOFF approach would be a large aluminum smelter or large steel mill. These sources typically feature extensive areas of excess heat releases and stacks in the midst of the heated building areas. The heat release can be quantified with either a satellite thermal imagery analysis or through engineering estimates of the heat loss.

An example of a facility with only the LIFTOFF effect would be a smaller heated industrial area such as a taconite ore processing facility. This type of facility might typically have the heat release area encompassing only a few hundred meters. If the facility's point sources have considerable plume moisture, then the AERMOIST approach may also be used.

Stack releases from processes involving flue gas desulfurization controls would be good candidates for the AERMOIST approach. Flue gas desulfurization controls treat the plume by injecting an alkaline reagent into the flue gas to remove SO_2 from the gas. This treatment results in higher plume moisture content than those without the treatment, thus making it viable for the AERMOIST approach.

For any of these applications, a situation with a row of stacks (even if only 2) would qualify for the AERLIFT approach, especially if they are within a few stack diameters of each other. As noted above, the stack separation distance affects the plume rise change due to stack merging.

At the time this paper was submitted in revised form, there were a few modeling applications in the United States for which these methods have been proposed and are either being applied based upon the past evaluations reported in this paper, or are going to be evaluated in the near future based upon new field data. In the case of the Eastman Chemical evaluation study (Paine et al., 2013; Szembek et al., 2013), the urban characterization as well as LIFTOFF have been used in the same application as approved USEPA techniques.

7. Summary

Steady-state plume models such as AERMOD have not been extensively tested or designed for scenarios where an emission source modifies the dispersion environment. Model performance for these conditions has become increasingly important in light of short-term pollutant standards, e.g., for 1-h SO_2 and 1-h NO_2 United States ambient standards. Four independent source characterization techniques described in this paper have been adapted and evaluated to better represent plume rise effects for nontraditional sources and their surrounding environment. These techniques are implemented as universally applicable to many dispersion models and are thus designed to be used as external processors that interact with the main dispersion model.

Two of these source characterization methods address fugitive heat releases at industrial complexes. The first occurs on a large scale resulting in a local urban-like dispersion environment called a “highly industrialized area”. To account for this excess heat, an effective population equivalent to the scale of the HIA can be calculated using an already existing relationship between population to urban-rural temperature difference and used as input to the dispersion model. We recommend that this approach is applied to areas with a scale of at least several hundred meters and an excess temperature between the HIA and the surrounding area of at least 8 K. The second, smaller scale excess heat release issue relates to building downwash effects, and can be addressed by using the LIFTOFF procedure and a weighting relationship using procedures developed by Hanna et al. (1998). Both the HIA's effective population and LIFTOFF technique can be applied in the same modeling application. Both have been evaluated and shown to provide modest overpredictions.

Stacks with moist plumes can lead to latent heat release of condensation after the plume exits the stack, providing additional plume rise relative to a dry plume case. This effect has been neglected in many dispersion models, but with the increasing use of flue gas desulfurization controls that inject considerable water vapor into the plume exhaust, accommodating this effect is very important. The AERMOIST procedure incorporates this moist plume effect by refining the hourly input exit temperature data based on a scaling ratio developed using a previously validated European model (the IBJpluris model) which incorporates moist plume effects. Stack sources for which this approach is particularly relevant is for processes involving wet and dry flue gas desulfurization controls.

Lastly, multiple stacks in a line can result in plume merging and buoyancy enhancement under certain conditions. The AERLIFT processor assesses and incorporates plume merging from aligned emission sources using an hourly emissions file from an initial model run. The exhaust characteristics of the merging plumes are refined by AERLIFT on an hourly basis, and then the dispersion model is run a second time with a new input of effective hourly exhaust parameters for each affected source.

These advanced plume rise procedures have been designed for use with dispersion models without the need to change the modeling system code, and are shown to improve model performance. They can be used individually, or in combination. By including these procedures outside of the modeling code as source characterization techniques, these procedures are available to a large suite of modeling approaches. In addition, their use as more accurately portraying the source plume behavior is inherently a refinement outside the model's treatment of plume transport and dispersion. Although we have provided available model performance results, we encourage much wider testing and evaluation of these approaches in a variety of settings.

Acknowledgements

The authors would like to gratefully acknowledge the American Iron and Steel Institute for providing funding for this research.

Appendix A. Supplementary data

Supplementary data related to this article can be found at http://dx.doi.org/10.1016/j.atmosenv.2016.01.003.

References

Anfossi, D., 1985. Analysis of plume rise data from five TVA steam plants. J. Appl. Meteorol. Clim. 24, 1225–1236. http://dx.doi.org/10.1175/1520-0450(1985)024<1225:AOPRDF>2.0.CO;2.

Arya, S., 2001. Chapter 5: air temperature and humidity in the PBL. In: Introduction to Micrometeorology. Academic Press, Oxford, UK.

Briggs, G.A., 1969. Plume Rise. USAEC Critical Review Series, National Technical Information Service, Springfield, VA.

Briggs, G.A., 1974. Cooling Tower Environment – 1974: Plume Rise from Multiple Sources (CONF-740302). ERDA Symposium Series, National Technical Information Services, U.S. Dept. of Commerce, Springhill, VA.

Briggs, G.A., 1975. Plume rise predictions. In: Lectures on Air Pollution and Environmental Impact Analyses. American Meteorological Society, Boston, MA.

Briggs, G.A., 1984. Chapter 8: plume rise and buoyancy effects. In: Atmospheric Science and Power Production. Technical Information Center, Office of Scientific and Technical Information, U.S. Dept. of Energy, Oak Ridge, TN; Springfield, VA.

Cambridge Environmental Research Consultants Ltd, 2015. ADMS 5 Atmospheric Dispersion Modelling System User Guide. http://www.cerc.co.uk/environmental-software/assets/data/doc_userguides/CERC_ADMS_5_1_User_Guide.pdf (accessed 30.11.15).

Cimorelli, A.J., Perry, S.G., Venkatram, A., Weil, J.C., Paine, R.J., Wilson, R.B., Lee, R.F., Peters, W.D., Brode, R.W., 2005. AERMOD: a dispersion model for industrial source applications. Part I: general model formulation and boundary layer characterization. J. Appl. Meteorol. 44, 682–693. http://dx.doi.org/10.1175/JAM2227.1.

Contini, D., Hayden, P., Robins, A., 2006. Concentration field and turbulent fluxes during the mixing of two buoyant plumes. Atmos. Environ. 40 (40), 7842–7857. http://dx.doi.org/10.1016/j.atmosenv.2006.07.024.

Environmental Protection Authority Victoria, Australia. Monitoring the Environment: AERMOD Air Pollution Modelling. http://www.epa.vic.gov.au/our-work/monitoring-the-environment/monitoring-victorias-air/aermod-air-pollution-modelling (accessed 22.09.15).

Fung, W.Y., Lam, K.S., Nichol, J., Wong, M.S., 2009. Derivation of nighttime urban air temperatures using a satellite thermal image. J. Appl. Meteorol. Clim. 48, 863–872. http://dx.doi.org/10.1175/2008JAMC2001.1.

Hanna, S.R., Briggs, G.A., Chang, J.C., 1998. Lift-off of ground-based buoyant plumes. J. Hazard. Mater. 59, 123–130.

Hanna, S.R., Britter, R.E., 2002. Chapter 2: overview of meteorology and atmospheric dispersion. In: Wind Flow and Vapor Cloud Dispersion at Industrial and Urban Sites. John Wiley & Sons, Inc., Hoboken, NJ http://dx.doi.org/10.1002/9780470935613.refs.

Hanna, S., Marciotto, E., Britter, R., 2011. Urban energy fluxes in built-up downtown areas and variations across the urban area, for use in dispersion models. J. Appl. Meteorol. Clim. 50, 1341–1353.

Hurley, P., 2008. TAPM V4. Part 1: Technical Description. In: https://publications.csiro.au/rpr/download?pid=procite:0cff4149-4feb-4b86-abcb-c707168ecb0b&dsid=DS1 (accessed 30.11.15).

Irwin, J.S., 1978. Proposed Criteria for Selection of Urban versus Rural Dispersion Coefficients. Draft Staff Report (Docket No. A-80–46, II-B-8). Meteorology and Assessment Division, U.S. Environmental Protection Agency.

Jacobson, M.Z., 2005. Fundamentals of Atmospheric Modeling. Cambridge University Press, New York, NY.

Janicke, U., Janicke, L., 2001. A three-dimensional plume rise model for dry and wet plumes. Atmos. Environ. 35, 877–890.

Janicke Consulting, Environmental Physics, 2015. Plume Rise Model IBJpluris. http://www.janicke.de/en/download-programs.html (accessed 11.03.15).

Macdonald, R.W., Strom, R.K., Slawson, P.R., 2002. Water flume study of the enhancement of buoyant rise in pairs of merging plumes. Atmos. Environ. 36 (29), 4603–4615. http://dx.doi.org/10.1016/S1352-2310(02)00464-8.

Manins, P., Carras, J., Williams, D., 1992. Plume rise from multiple stacks. Clean. Air – Aust. 26 (2), 65–68.

National Aeronautics and Space Administration Jet Propulsion Laboratory, 2004. Advanced Spaceborne Thermal Emission and Reflection Radiometer. http://asterweb.jpl.nasa.gov (accessed 14.12.15).

Nichol, J., 2005. Remote sensing of urban heat islands by day and night. Photogramm. Eng. Remote Sens. 71, 613–621.

Olesen, H.R., Genikhovich, E., Ministry of Environment and Energy, 2000. Building Downwash Algorithm for OML Atmospheric Dispersion Model. http://www2.dmu.dk/1_viden/2_Publikationer/3_arbrapporter/rapporter/AR123.pdf (accessed 09.03.15).

Olesen, H.R., Berkowicz, R.B., Lofstrom, P., 2007. OML: Review of Model Formulation. National Environmental Research Institute, Denmark, p. 130. NERI Technical Report No. 609. www.dmu.dk/Pub/FR609.pdf (accessed 30.11.15).

Oke, T.R., 1973. City size and the urban heat island. Atmos. Environ. 7 (8), 769–779.

Oke, T.R., 1978. Boundary Layer Climates. John Wiley and Sons, New York, NY, p. 372.

Oke, T.R., 1982. The energetic basis of the urban heat island. Quart. J. Roy. Meteor. Soc. 108, 1–24.

Oke, T.R., November 2–4, 1998. An algorithmic scheme to estimate hourly heat island magnitude. In: Paper presented at the Second Symposium on Urban Environment. Am. Meteorol. Soc., Boston, MA.

Overcamp, T.J., Ku, T., 1988. Plume rise from two or more adjacent stacks. Atmos. Environ. 22 (4), 625–637.

Paine, R., Tringale, F., Gossett, S., 2013. Resolution of 1-hour SO_2 non-attainment area in Kingsport, TN: advanced meteorological and monitoring study. In: Control #7, Air & Waste Management Association Specialty Conference, Guideline on Air Quality Models: the Path Forward, Raleigh, NC. March.

Petersen, R., 2015. Building downwash – problems, solutions and next generation. In: 11th USEPA Modeling Conference, August 13. http://www3.epa.gov/ttn/scram/11thmodconf/presentations/3-6_Building_Downwash-CPP-11thMC.pdf (accessed 30.11.15).

Presotto, L., Bellasia, R., Bianconi, R., 2005. Assessment of the visibility impact of a plume emitted by a desulphuration plant. Atmos. Environ. 39 (4), 719–737.

Robins, A., 1994. Flow and dispersion around buildings in light wind conditions. In: Castro, Rockliff (Eds.), Stably Stratified Flows. Clarendon Press, Oxford UK, p. 372.

Robins, A., Apsley, D., Cambridge Environmental Research Consultants, 2013. Modelling of Building Effects in ADMS. http://www.cerc.co.uk/environmental-software/assets/data/doc_techspec/CERC_ADMS5_P16_01.pdf (accessed 22.09.15).

Schewe, G., Colebrook, J., 2013. Use of the urban option in AERMOD for a large industrial facility. In: Control #21, Air & Waste Management Association Specialty Conference, Guideline on Air Quality Models: the Path Forward, Raleigh, NC. March.

Scire, J.S., Strimaitis, D.G., Yamartino, R.J., 2000. A User's Guide for the CALPUFF Dispersion Model (Version 5). Tech. Rep. Earth Tech, Inc., Concord, MA, p. 521. http://www.src.com/calpuff/download/CALPUFF_UsersGuide.pdf (accessed 01.12.15).

Schulman, L.L., Strimaitis, D.G., Scire, J.S., 2000. Development and evaluation of the PRIME plume rise and building downwash model. J. Air Waste Manag. Assoc. 50, 378–390.

Sykes, R.I., Cerasoli, C.P., Henn, D.S., 1999. The representation of dynamic flow effects in a Lagrangian puff dispersion model. J. Hazard. Mater. 64, 223–247.

Szembek, C., Paine, R., Gossett, S., 2013. Resolution of 1-hour SO_2 non-attainment area in Kingsport, TN: model evaluation analysis results to date. In: Control #8, Air & Waste Management Association Specialty Conference, Guideline on Air Quality Models: the Path Forward, Raleigh, NC. March.

U.S. Environmental Protection Agency, 1995. SCREEN3 Model User's Guide. http://www.epa.gov/scram001/userg/screen/screen3d.pdf (accessed 09.03.15).

U.S. Environmental Protection Agency, 2003. AERMOD: Latest Features and Evaluation Results. http://www.epa.gov/ttn/scram/7thconf/aermod/aermod_mep.pdf (accessed 05.03.15).

U.S. Environmental Protection Agency, 2004a. AERMOD: Description of Model

Formulation. http://www.epa.gov/scram001/7thconf/aermod/aermod_mfd.pdf (accessed 13.03.15).
U.S. Environmental Protection Agency, 2004b. User's Guide to the Building Profile Input Program. http://www3.epa.gov/scram001/userg/relat/bpipdup.pdf (accessed 22.11.15).
U.S. Environmental Protection Agency, 2005. Guideline on Air Quality Models (Appendix W); 40 FR 68218. http://www.epa.gov/ttn/scram/guidance/guide/appw_05.pdf (accessed 14.12.15).
U.S. Environmental Protection Agency, 2012. AERMIC Update. http://www3.epa.gov/ttn/scram/10thmodconf/presentations/1-9-Brode_10thMC_AERMIC_Update_03-13-2012.pdf (accessed 14.12.15).
U.S. Environmental Protection Agency, 2015. AERMOD Implementation Guide. http://www.epa.gov/ttn/scram/7thconf/aermod/aermod_implmtn_guide_3August2015.pdf (accessed 27.08.15).
U. S. Geological Survey, 2015. Landsat Missions: Landsat 8. http://landsat.usgs.gov/landsat8.php (accessed 14.12.15).
Voogt, J.A., Oke, T.R., 2003. Thermal remote sensing of urban climates. Remote Sens. Environ. 86, 370–384.

Appendix E

Communication from EPA Region 4 Regarding Eastman Modeling Approaches

EPA Region 4 Response to Eastman's Additional EASTMOD Information submitted via email from Stephen Gossett on March 3, 2015

EPA Region 4 has completed our review of Eastman's proposal to use an alternative model (EASTMOD) for air modeling required for the Sullivan County, Tennessee, Sulfur Dioxide (SO2) Attainment Demonstration State Implementation Plan (SIP). Based upon a review of all of the information that has been provided by Eastman since the original proposal in 2014, EPA is in a position to approve portions of the proposed changes to the AERMOD Modeling System that are incorporated into the EASTMOD proposal and not allow other portions of the proposal. In order for an alternative to EPA's recommended AERMOD Modeling System to be approved for use in the SO2 Attainment Demonstration SIP, a formal approval from EPA Region 4 pursuant to Section 3.2.2 of 40 CFR Part 51, Appendix W, is needed. The following discussion identifies the portions of EASTMOD which we are in a position to approve and provides our rationale for not allowing other portions of the proposal.

We have determined that the following modifications to the regulatory AERMOD modeling system are acceptable for the Eastman SO2 Attainment Modeling:

- Beta ADJ_U* option in AERMET
- LOWWIND2 beta option in AERMOD (with a single 0.4 m/s minimum sigma-v value)
- AERLIFT for the five closely-spaced B-253 powerhouse stacks that are approximately 15 meters apart.

We have determined that the following modifications requested by Eastman are not acceptable:

- Proposed modifications to the LOWWIND2 beta option to allow use of split minimum sigma-v values for stable and unstable atmospheric conditions
- Proposed use of AERLIFT for the two widely-spaced B-83 powerhouse stacks that are approximately 50 meters apart.

EPA has performed considerable testing of both the beta ADJ_U* option in AERMET and the LOWWIND2 beta option in AERMOD using multiple tracer-studies. Since Eastman has shown that the combination of these beta options has improved model performance for their site-specific case, EPA believes that these alternative model options are appropriate for their SO2 Attainment Demonstration SIP modeling. As has been stated in the past, EPA continues to have concerns about Eastman's proposal to use split minimum sigma-v values for unstable (0.4 m/s) and stable (0.6 m/s) atmospheric conditions, due in part to the fact that the AERMOD model formulation incorporates a horizontal plume meander component that effectively increases lateral plume spread, especially under low wind stable conditions. As a result of these concerns, EPA does not believe that the additional information provided by Eastman on March 3, 2015, justifies use of this proposed change to the model.

Based upon the site-specific model performance information provided by Eastman, it appears that use of the LOWWIND2 beta option with a single minimum sigma-v value of 0.4 m/s significantly improves model performance for the Ross N. Robinson, Meadowview, Skyland Drive and B-267 monitors when compared to the regulatory default version of AERMOD. We are open to approving a minimum sigma-v value of 0.4 m/s (versus the current default value of

0.3 m/s associated with the beta LOWWIND2 option) for the Eastman specific case due to the complex dispersion environment associated with very low wind speeds and nearby complex terrain. These influences are likely to result in significant vertical wind shear that could contribute to increased lateral plume dispersion.

As indicated in our Technical Review Comments dated September 5, 2014, EPA Region 4 has determined that the proposed AERLIFT component of EASTMOD is a source characterization procedure and is not an integral part of the AERMOD Modeling System. Therefore, it is not subject to the Appendix W, Section 3.2.2 alternative model evaluation criteria. EPA Region 4 has considered the AERLIFT procedure separately from the modifications proposed to be made to the actual AERMOD Modeling System. Based upon the entirety of information provided by Eastman regarding AERLIFT, EPA believes that the AERLIFT procedure is acceptable for use in modeling the five closely-spaced stacks at the B-253 powerhouse, but is not acceptable for the two B-83 stacks.

The additional information provided by Eastman in the March 3, 2015, submittal clearly indicates that use of AERLIFT for the five closely spaced B-253 stacks improves model performance at the Ross N. Robinson, Skyland Drive and Meadowview monitor locations and shows a small improvement for the B-267 monitor location when compared to the no-AERLIFT cases. The studies in the references cited by both EPA and Eastman in previous correspondence provide supporting information for use of AERLIFT for the five closely-spaced (approx. 15 meters apart) B-253 stacks. Conversely, the use of AERLIFT for the two B-83 stacks that are relatively far apart (approx. 50 meter or 11 stack diameters apart) results in very little change to the model performance at the Ross N. Robinson, Skyland Drive, Meadowview and B-267 monitor locations when compared to the no-AERLIFT cases. As has been pointed out in previous EPA comments, the literature appears to be consistent regarding the lack of any plume rise enhancement for two stacks spaced far apart like the B-83 stacks. The lack of performance improvement with AERLIFT for the B-83 stacks is consistent with the studies which question plume rise enhancement for two far apart stacks. Therefore, EPA does not believe it is appropriate to approve the use of AERLIFT for the B-83 stacks.

EPA also notes that the additional information provided by Eastman indicates that importance of the AERLIFT procedure will be greatly reduced for the future attainment year modeling case, in which the B-253 SO_2 emissions will be mostly eliminated by the fuel switch from coal to natural gas for the B-253 boilers.